The Design, Synthesis, Characterization, and Mechanical Testing of a Novel Degradable Polymeric Biomaterial for Use as a Bone Substitute

by

Michael Jerome Yaszemski, M.D.

Submitted to the Department of Chemical Engineering
in Partial Fulfillment of the Requirements for the Degree of

Doctor of Philosophy in Chemical Engineering

at the
Massachusetts Institute of Technology

June 1995

Signature of Author . . . . . .
Department of Chemical Engineering
April 27, 1995

Certified by . . . . . .
Robert S. Langer
Germeshausen Professor of Chemical and Biochemical Engineering
Thesis Supervisor

Certified by . . . . . .
Wilson C. Hayes
Maurice Muller Professor of Biomechanics, Harvard Medical School
Thesis Supervisor

Accepted by . . . . . .
Robert E. Cohen
Chairman, Committee for Graduate Students

THE DESIGN, SYNTHESIS, CHARACTERIZATION, AND MECHANICAL TESTING OF A NOVEL DEGRADABLE POLYMERIC BIOMATERIAL FOR USE AS A BONE SUBSTITUTE

by

MICHAEL JEROME YASZEMSKI, M.D.

Submitted to the Department of Chemical Engineering
on 27 April 1995 in partial fulfillment of the
requirements for the Degree of Doctor of Philosophy in
Chemical Engineering

ABSTRACT

This work focuses on the development of a candidate material for temporary synthetic bone. The material is a particulate filled composite based on an unsaturated linear polyester. The components are mixed with a monomer that cross links the double bonds of the unsaturated polyester. Degradation occurs via hydrolytic degradation of backbone polymer's ester linkages. This strategy of prepolymer synthesis via condensation polymerization in the laboratory followed by cross linking the unsaturated prepolymer via radical polymerization at surgery offers design flexibility. The radical polymerization allows curing during surgery to facilitate reconstruction of various shaped bone defects. The laboratory synthesis of the prepolymer allows alterations of its composition and physical properties to effect desired properties in the resulting composite material. The effects of several composite material formulation recipes on the in vitro mechanical properties and in vivo histologic characteristics of the resulting material are presented. The prepolymer molecular weight, presence of a leachable salt, and amount of cross linking monomer had strong effects on the resulting strength and modulus of the composite. These strengths were of a magnitude appropriate for consideration of the material as a temporary trabecular bone substitute. The in vivo studies in a rat proximal tibia model demonstrated progressive growth of new bone against the receding surface of the degrading material, and insinuation of new bone trabeculae into the interior of the degrading specimen. There was an absence of a foreign body inflammatory response to the presence of this material over a five week time span. The material is an attractive candidate for temporary replacement of trabecular bone.

Thesis Supervisor: Dr. Robert S. Langer

Title: Germeshausen Professor of Chemical and Biochemical Engineering

This work is dedicated to my family. They are the motivation for this and all other work that I do.

To my grandparents, Mr. and Mrs. Andrew Yaszczemski, and Mr. and Mrs. Mario Ascani, now all deceased, for wonderful childhood memories.

To my parents, Mr. and Mrs. Chester Yaszczemski, for their love and guidance into adulthood, and insistence on a quality education.

To my wife, Karen Adamec Yaszemski, for her love and friendship over the fifteen years of our marriage, and her constant support of my academic endeavors at the expense of her own.

To our children, Andrew John and Alexandra Katherine, whose unconditional love makes us proud to be their parents.

TABLE OF CONTENTS

List of Figures

List of Tables

CHAPTER 1

The Evolution of Bone Transplantation: Molecular, Cellular, and Tissue Strategies to Engineer Human Bone

Introduction

The need to transplant bone to a deficient skeletal location has been recognized for centuries[1,2]. Bone occurs in two forms, trabecular and compact, and it performs several functions. First, bone is the primary reservoir of calcium in the body, and exchanges this mineral readily with the extracellular fluid environment. The concentration of calcium in the body fluids is tightly regulated, and the supply of calcium in bone is critical to this control. Second, the hematopoietic marrow that is located in trabecular bone supplies the body's cells, tissues, and organs with their nutrient carrying red blood cells and infection fighting white blood cells. Neither of these two functions, however, drives the need for bone transplantation to a deficient skeletal site. Bone elsewhere in the skeleton can satisfy these requirements. The third function of bone is its mechanical role in supporting the body's tissues, and in providing sites of attachment for the muscles that effect body movement and locomotion. Bone at a distant location cannot perform this function for a skeletal region that is deficient in either compact or trabecular bone. The mechanical function of bone, once lost by injury or other means, can only be regained by restoring skeletal continuity at

the location of interest.

The restoration of skeletal continuity often involves bone transplantation. The biologic process that begins with bone transplantation and results in normal bone structurally and mechanically exploits a unique property of bone. When it is injured, bone does not heal with a fibrous scar as do virtually all other tissues. The response of bone to injury is to regenerate bone tissue and then remodel that newly formed bone in the direction of local stresses. The sequence of bone regeneration after fracture is similar to the incorporation of transplanted bone at the recipient site and to the growth of children's bone at the physis (also called the growth plate). The development of strategies to engineer human bone requires an understanding of these three processes, because each of them is a manifestation of the body's evolutionary solution to maintain skeletal integrity. Transplant incorporation, physeal growth, and fracture healing all result in the formation of new bone that can then remodel itself to optimize its mechanical function for it's particular skeletal location. This should be the ideal goal of tissue engineering strategies to engineer human bone. The initial biomaterial or biomaterial - cell construct should provide temporary mechanical strength to the reconstructed region, allow or induce the region to reconstitute itself with new bone, degrade in a controlled fashion into nontoxic molecules that the body can metabolize or excrete, and then allow the usual process of remodelling to optimize the mechanical properties of the newly formed bone.

The final common pathway, that is, the remodelling of newly formed bone along lines of the local stress field, has a complex mechanism that is only partially understood more than one hundred years after its discovery[3]. The goal of remodelling is to transform newly formed bone into a mechanically competent support structure.

After a brief review of the history of bone transplantation, we will describe the gross and microscopic anatomy of the two types of bone, compact and trabecular. These two bone types occur in different body locations, and serve different functions that must be considered when designing systems to regenerate

bone. We will then discuss several of these systems, which include biodegradable polymers, cell-polymer constructs, ceramics, glasses, and bone components. Bioactive molecules are sometimes incorporated into these materials, and the materials then serve an additional function as delivery systems for the active molecules.

History of Bone Transplantation

There are several references in the literature to the first recorded bone graft attempt. Lane[4] cites a reference by a Dutch surgeon, Job Van Meek'ren[2] in 1668. Chase and Herndon[5] and Gross et al[6] mention experiments on periosteal new bone formation by Duhamel in 1742; their citation for the earliest autograft is Phillip von Walther in 1820, and their citation for the first allograft is Macewen in 1878. These authors also give the following chronology: Ollier concluded in 1867 that transplanted periosteum and bone remained alive and could become osteogenic. Prolo and Rodrigo[7] place the date of Duhamel's experiments at 1739, and mention that he implanted subperiosteal silver wires to demonstrate osteogenesis. Axhausen, in 1909, demonstrated that transplanted bone dies, but that most periosteum survives and is osteogenic. Senn[1], in 1889, implanted hydrochloric acid treated decalcified allograft bone into chronic osteomyelitis cavities, with the goal of promoting antisepsis within them. He observed ossification of this tissue from the walls of the defects. Barth[8], in 1898, stated that transplanted bone, marrow, and periosteum die and are replaced by new bone from the surrounding tissue without prior resorption of the transplanted graft. He coined the term "schleichender ersatz", which translates from German to English as "creeping substitution". Axhausen's description in 1909 (see above) was a correct revision of Barth's initial proposition, and the term *schleichender ersatz* was applied to this description. Phemister[9], in 1914, described the process of new bone forming from elements present in bone and utilizing the dead mineralized framework of bone as a scaffold upon which to grow. This is the process initially

proposed by Axhausen; Phemister expanded upon it, presented it to the English language literature, and introduced the English term "creeping substitution". This application of the term *creeping substitution* to the process of transplant resorption and new bone regeneration as described by Axhausen and Phemister is different than its original meaning as proposed by Barth. Nevertheless, the Axhausen-Phemister description of the biologic process, and the term *creeping substitution* have both persisted to the present time.

Levander[10] injected extracts of bone into muscle and demonstrated the formation of new bone in the heterotopic muscle site. This report, from the 1930's, demonstrates early thoughts on the induction of osteogenesis by some factor present in the bone transplant. It was approximately three decades from his publication until the demonstration in 1965 by Urist[11] that an extract of demineralized bone matrix could cause invading mesenchymal cells from the host to become osteoblasts and make new bone in a heterotopic site. The quest to identify this putative bone morphogenetic protein (BMP) lasted more than another two decades. The isolation and biochemical sequencing of BMP occurred in 1989[12], and its production by recombinant DNA technology became a reality soon afterwards[13]. There are seven different BMP's that have been identified, and they are called BMP-1 through BMP-7. The activity associated with Urist's observations in 1965 is possessed by BMP-2.

The historical trail of bone transplantation has led us to this point: the successful regeneration of bone requires cells that will produce osteoid (bone matrix) , an appropriate scaffold upon which the new bone can grow, and bioactive molecules to direct the process. The host must, of course, provide a vascular supply and nutrients. The transplanted construct must usually impart some mechanical properties to the reconstructed region, and these can be approximated by the mechanical properties of the bone being replaced. The exact mechanical requirements are dictated by the anatomy, functional loading, and clinical circumstances of a particular reconstruction. The technology now exists to address each of the required bone regeneration components separately[14,15]. The

evolution of bone transplantation is now entering an era where novel combinations of the required constituents and equally novel processes to deliver them are undergoing experimentation.

Bone Anatomy

Mature bone exists as compact bone or as trabecular bone. Compact bone is also called cortical bone, and trabecular bone is also called cancellous or spongy bone. Compact bone is distinguished from trabecular bone by the spatial orientation of its mineral and organic elements, and by its characteristic locations in the skeleton. Compact bone comprises the outer tubular shell of the long bones, and the outer surface of the small bones and flat bones. It is much more dense than trabecular bone, and it consists of parallel cylindrical units called osteons (or Haversian systems). Compact bone is anisotropic, and the orientation of the osteons determines, to a great extent, the directionality of its mechanical properties. Trabecular bone is less dense than compact bone, and occurs near the ends of long bones, as the interior of small bones, and between the surfaces of flat bones. Trabecular bone is comprised of an array of plates and rods of bone tissue, and forms an open celled foam[16]. The orientation of the plates and rods is such that the trabecular bone is also anisotropic. It optimizes resistance to the usual stresses that occur in its particular location. Long bones are described by regions: diaphysis, metaphysis, and epiphysis. These descriptive terms use the *physis*, or growth plate, as their reference point. The physis is the specialized region near each end of a long bone from which longitudinal and appositional growth of the bone occur. The *epiphysis* ("upon the physis") is the portion of the long bone between the physis and the end of the bone. It is covered with the articular cartilage that allows the joint to move with low friction. The *metaphysis* ("next to the physis") is the transition from the wide part of the bone near the joint to the tubular part of the bone near the bone's center. The *diaphysis* ("far from the physis" or "between the physes") is the tubular center region of a long bone that

lies between the expansions at either end. After skeletal maturity, the physis no longer exists, but these three terms are still used to identify the region of interest in a long bone. These terms are not used in the discussion of either flat or small non-tubular bones.

Mature bone is *lamellar* bone. New bone, whether formed at the physis, during fracture repair, in neoplasia, in embryonic life, or as a result of bone graft incorporation, is *woven* bone. Woven bone becomes lamellar bone through the process of remodelling. The randomly oriented collagen fibers of woven bone become parallel fibers in lamellar bone. The mineral phase that accompanies these collagen fibers is directional: this organized, remodelled mineral phase gives lamellar bone its anisotropic properties. This is true in the organized lamellar osteons of compact bone and in the organized plates and rods that constitute the open cellular foam structure of trabecular bone.

Newly formed bone is also described by its developmental origin: it has formed via either *intramembranous ossification* or *endochondral ossification*. Intramembranous ossification is the formation of woven bone directly from condensed mesenchymal tissue without the intermediate formation of a cartilaginous framework of the future bone. Endochondral ossification involves a cartilaginous intermediate formed from mesenchymal tissue. This cartilage framework is then ossified to form the new bone. Intramembranous ossification occurs primarily in the embryonic formation of the flat bones (e.g. skull), and, in part, the clavicle. Endochondral ossification occurs in the embryonic formation of the long bones, in fracture repair, in physeal growth of the immature skeleton, and in the incorporation of bone grafts. Note that the term *ossification* imparts a special meaning that is not conveyed by the two related terms *calcification* and *mineralization*. Calcification is a term that indicates deposition of calcium salts in tissues. This deposition is not in any particular pattern, and occurs because the tissue concentration of the calcium salt has exceeded the solubility limit for that salt. It can continue unabated, limited only by the supply of calcium in excess of the solubility limit and the density that the deposited salts can attain. Ossification

is the orderly deposition of calcium salts into predetermined locations on a collagenous framework called osteoid. The osteoid is laid down by the bone forming osteoblast cells. The calcium salts deposited in this fashion form hydroxyapatite, the mineral phase of bone. Mineralization is the most general of the three terms, and refers to the deposition of mineral salts in tissue via either calcification or ossification. The outer surface of bones is covered by a connective tissue called periosteum. This tissue is thicker in children, and is less prominent in adults. Its inner layer, the cambium layer, contains cells that can become osteoblasts and make bone[17].

The normal anatomy of bone is a result of evolutionary functional optimization via structural adaptation. When we describe various tissue engineering strategies to regenerate bone, it will be productive to frequently return to and review this anatomy. We can consider the contributions of each of these natural components to the function of bone as we attempt to discover acceptable substitutes for those functions.

Normal Fracture Healing

A bone fracture disrupts skeletal continuity and mechanical function, injures local blood vessels, and initiates the process of fracture repair. This process can be described by a combination of its three biologic stages[18] and its four biomechanical stages[19]. The biologic stages are inflammation, repair, and remodelling. They recapitulate the endochondral ossification that occurs during intrauterine growth. The first event that occurs after a fracture is the escape of blood from damaged vessels, and the formation of a hematoma at the fracture site. This hematoma organizes; that is, the body's coagulation cascade becomes activated, and it attempts to stop the hemorrhage by clotting the blood. A fibrin clot forms, platelets in the blood attach to it, and they release vasoactive mediators and growth factors. Acute inflammatory cells arrive at the site and remove necrotic tissue. Polymorphonuclear leucocytes are the first inflammatory

cells to arrive, and are followed by macrophages. Inflammation is the shortest phase in the repair process, and is followed by repair. The process of repair consists of the cellular synthesis of new bone organic matrix, and the ossification of that matrix to form new woven bone. The osteoblasts that make the new matrix originate in pluripotential mesenchymal cells. These cells are derived from both the site of injury and from distant sites via the bloodstream. The inner layer of the periosteum, called the cambium layer, likely contributes the first cells to the repair process. The combination of osteoblasts, cartilaginous matrix, and woven bone is called fracture callus. This callus is the product of fracture repair, and is the new raw material for fracture remodelling. Remodelling is the third and longest biologic stage of fracture healing. During this phase, the woven bone undergoes sequential resorption and deposition to become more organized lamellar bone. This results in bone whose organic and mineral phases are better aligned to resist local stresses.

The four biomechanical stages of fracture healing were determined by testing healing fractures to failure in torsion[19]. The types of failure that were observed reflected increasing strength of the healing fracture site as it passed through the three biologic stages of healing. In the first biomechanical stage, refracture of the healing fracture under torsional load occurs through the original fracture site with low stiffness compared to the characteristic stiffness of the uninjured bone. In the second stage, the refracture still occurs through the original fracture site, but the stiffness has increased to a range characteristic of hard tissue. In biomechanical stage three of healing, the refracture occurs partly through the original fracture site, and partly through previously intact bone. The stiffness is of the order of magnitude of hard tissue, as it was in stage two. In stage four, the location of the fracture is not related to the site of the original injury. A stage four refracture pattern indicates that remodelling has restored the original mechanical properties to the injured tissues. In clinical practice, many injury variables, patient variables, and treatment variables influence the time that each of these stages requires. In general, remodelling of a major long bone fracture will take a time

interval on the order of a year to return the bone to its prefracture strength. We will now see that the fracture healing process bears striking similarities to the endochondral ossification that occurs at the physis of skeletally immature bones.

Skeletal Growth at the Physis

Long bones in a child increase both their length and diameter via growth at a specialized cartilaginous region near their ends called the *physis* or *growth plate*. The formation of new woven bone at the physis occurs via endochondral ossification. Appositional remodelling of the diaphysis occurs via intramembranous ossification. We now discuss the physeal growth and its similarities to fracture healing and incorporation of bone transplants.

The physis can be described by functional and anatomic zones[20]. The functional zones, beginning at the epiphyseal end, are the zones of growth, maturation, transformation, and remodelling. The functional zones can be further described by anatomic regions. The growth zone contains cells that are in germinal, proliferative, and columnation regions. The maturation zone contains the cellular hypertrophy and calcification regions. The transformation zone contains the vascular penetration and ossification regions. The remodelling zone is the junction between physis and metaphysis, and consists of the primary and secondary spongiosa.

The cells in the growth zone begin to divide, secrete extracellular cartilage matrix, and line up in columns. This increases the length of the bone by a combination of increased number of cartilage cells and an increased amount of intercellular matrix. This increased length of cartilage is the framework for subsequent endochondral ossification. The bone widens at the physis by a contribution of cells from a specialized area of the growth zone called the groove of Ranvier. The columns of cartilage cells are separated from each other by longitudinal bars of cartilage matrix; cells in each column are similarly separated by transverse bars of cartilage matrix. As newly divided cells are added to the top

of each lengthening column, the cells further down the column begin to enlarge (hypertrophy), and secrete matrix vesicles. These vesicles are the sites of initial calcification of the cartilage matrix. The calcified cartilage matrix furthest from the zone of growth is invaded by the ingrowth of blood vessels from the metaphysis. This vascular invasion brings cells and biomolecules that remove the last transverse cartilage bar which separates physis from metaphysis. This area now becomes metaphysis, and osteoblasts deposit bone matrix (osteoid) on the calcified cartilage bars. This region has ossified, and consists of woven bone called the primary spongiosa. This woven bone is remodelled, just as the initial woven bone in fracture healing is remodelled. The remodelled woven bone is termed the secondary spongiosa. A rather striking exhibition of remodelling occurs during physeal growth. The physis, and hence the ends of long bones, are wider than the diaphysis, or shaft of those bones. The narrow, tubular shaft is a mechanically optimized structure for bearing the loads that it experiences. The newly formed metaphyseal bone is the same diameter as the physis that made it and that is growing away from it. Sequential resorption of woven bone from the metaphysis' outer surface and deposition of lamellar bone on its inner surface decreases its diameter as it becomes diaphysis.

The above description is an intentionally brief narrative of a complex process. The pertinent points for this discussion are that remodelled bone occurs through a process that begins with a source of committed cells that form a cartilaginous precursor of the eventual bony region. The cells then die, and an ingrowing vascular supply brings cells and biomolecules that cause bone extracellular matrix to occur throughout the cartilaginous framework. This matrix ossifies, and is then woven bone which, via a process of resorption and reossification, becomes remodelled lamellar bone. We now discuss bone transplant incorporation, and its similarities to both fracture healing and physeal growth.

The Biology of Bone Graft Incorporation

The clinical "gold standard" for bone transplantation is the autogenous trabecular graft. Allografts and autogenous compact grafts incorporate via the same general scheme as autogenous trabecular grafts, but they have some important differences. We begin with a description of autogenous trabecular graft incorporation. The transplantation of the graft invariably injures local vessels, and leaves bleeding host trabecular bone at the recipient site. This activates the blood clotting cascade, and a fibrin clot forms. The clot organizes into fibrous granulation tissue, and attracts both inflammatory cells and new vascular tissue. The elements of the trabecular graft undergo necrosis. There is controversy over whether the cellular elements live and contribute to osteogenesis, but their contribution, if present, is likely small compared to that of the host tissues[17]. The trabecular graft begins to revascularize within hours of transplantation, and revascularization is usually complete in two weeks. New fibrovascular granulation tissue moves through the porous trabecular network and occupies the graft. Osteoblasts, the bone forming cells, appear with the vascular tissue. Mesenchymal osteoprogenitor cells differentiate to become the osteoblasts. There are several candidates for the mesenchymal cells that become osteoblasts[17]. These include vascular endothelial cells, circulating monocytes, reticuloendothelial system cells, and fibroblasts. The invasion of the graft by neovascularization, followed by the appearance of bone forming cells in the region, mimics the situation that was discussed above for physeal growth. Recall that, at the physis, vascular channels in the metaphysis broke through the last transverse cartilaginous septum which separated metaphysis from physis. This vascular invasion then brought osteoblasts that deposited osteoid on the calcified cartilage bars of the physis. The trabecular graft has an open porous structure that permits the deposition of new bone directly on necrotic trabeculae. The transplanted trabeculae do not lose their mechanical strength when they die. Therefore, a trabecular graft undergoes an initial increase in mechanical strength

as new bone is deposited on existing necrotic trabeculae. Then, as the necrotic trabeculae are later remodelled, the strength of the incorporated transplant decreases toward that of normal trabecular bone. This sequence is one of three differences between the incorporation of trabecular and compact grafts. Heiple[21] has reported 25 years experience with the dog ulna model for investigation of trabecular transplant biology. This model is a segmental defect in the ulna, uses the contralateral ulna as a control, and does not use internal fixation. Heiple states that, in this model, trabecular autograft transplants are revascularized completely and have fibrous tissue continuity two weeks post transplantation. They are completely filled with new bone or a bone-cartilage combination by two months, and are already remodelling the new woven bone to lamellar bone at that time.

The three important differences in the sequence of incorporation between trabecular and compact bone transplants have implications for the clinical management of patients after transplantation of compact or trabecular bone. The differences lie in the rate of transplant revascularization, the osteoblastic vs. osteoclastic response, and the completeness of the repair. They must be considered when designing materials and strategies to replace bone.

The sequence of graft incorporation is similar for compact and trabecular transplants during the first two weeks. The formation of the hematoma, and its organization into a fibrin clot are identical in the compact and trabecular cases. The trabecular transplant is revascularized much more rapidly than the compact bone transplant. Revascularization of the trabecular graft occurs through the open marrow spaces. The same process in the compact graft must occur through existing haversian canals. The porosity that these haversian systems (osteons) confer upon compact bone is low compared to the porosity of trabecular bone. The ingrowth of new blood vessels through the haversian canals takes much longer than the ingrowth of new vessels through the open pores of trabecular bone. Compact autogenous grafts may require two months to revascularize[7]

compared to two weeks for trabecular grafts.

The second difference between the processes of compact and trabecular transplant incorporation lies in the sequence of new bone substitution for the necrotic transplant. We mentioned above that the host response to a trabecular graft is osteoblastic. That is, the trabecular graft has new woven bone form on its necrotic trabeculae without prior resorption of those trabeculae. The necrotic compact graft, however, causes the host to resorb parts of it before any new bone is laid down. Therefore, osteoclasts, which resorb bone, act before osteoblasts make new woven bone in the presence of a compact bone transplant. The importance of this difference is that compact transplants, often used to treat large segmental bone defects, undergo a stage of decreased mechanical strength. This occurs between approximately six weeks and six months post-transplantation, when the initial resorptive (osteoclastic) phase has outstripped the appositional (osteoblastic) phase of compact transplant incorporation[17]. Compact transplants can lose 50% of their strength in six months, and this loss is reversed over one to two years[7].

The third difference between the two incorporation processes is the completeness of the repair. The transplanted trabeculae of trabecular grafts are completely resorbed during remodelling, and the entire repaired region becomes remodelled lamellar bone. Compact grafts remain an admixture of necrotic and viable bone for years, and may never completely become new bone[17]. The residual necrotic bone in a compact transplant may be 50-90% of the original graft many years after transplantation[7]. The significance is that, although the necrotic graft retains its strength, the region of space that it occupies cannot undergo complete remodelling, and therefore may not contain optimally oriented bone for its mechanical needs.

Biomechanics of Trabecular and Compact Bone

Bone needs to resist the loads placed on the skeleton during the activities of living. Many such loads have been estimated, and they place compressive, tensile, and shear forces on the bone[22,23]. Trabecular bone functions mostly in compression, but its strength and modulus are approximately the same in both tensile and compressive loading. Compact bone functions in compression, tension, and shear. The mineral phase of compact bone imparts strength in compression and shear, and its collagen fibers provide tensile strength. Compact bone, in the form of oriented remodelled haversian systems (osteons), forms the tubular cortices of long bones. These bones are loaded primarily by compressive forces at their ends. This loading configuration, however, imparts both bending and torsional moments to the long bones. When we consider strategies to replace the mechanical function of bone, it behooves us to consider the forces that any replacement material will experience. The experimentally determined strengths and moduli of compact and trabecular bone provide a useful measure of appropriate strengths and moduli for replacement materials. These values appear below, and have been collected from several sources[22-25].

Compact bone is anisotropic. The measured strength depends on the orientation of the applied test loads with respect to the direction of the osteons. The ranges of reported strengths of compact bone, when tested in a longitudinal direction (parallel to the long axis of the osteons) are: 78.8-151 MegaPascals (MPa) in tension, and 131-224 MPa in compression. Compact bone strength ranges, when tested in a transverse direction (perpendicular to the long axis of the osteons) are: 51-56 MPa in tension, and 106-133 MPa in compression. The range of reported shear strengths of compact bone (tested in torsion) is 53.1-70 MPa. The reported ranges of moduli (Young's modulus) for compact bone are as follows. The longitudinal modulus range (both tension and compression) is 17-20

GigaPascals (GPa). The transverse modulus range is 6-13 GPa. The reported shear modulus is 3.3 GPa.

The strengths and moduli for trabecular bone are related to the apparent density of trabecular bone by a power law function[22]. The density of human trabecular bone varies from approximately 0.1 grams per cubic centimeter up to 1.0 grams per cubic centimeter. For comparison, compact bone has a density of approximately 1.8 grams per cubic centimeter. A trabecular bone specimen with a density of 0.2 grams per cubic centimeter has a porosity of about 90%. The strength of trabecular bone varies widely over the range of observed densities. The strength varies as the square of the apparent density, and the modulus varies as either the square or cube of the apparent density. The strength and modulus are both sensitive to the rate of loading. This is a manifestation of the viscoelastic nature of bone. Midrange values for trabecular bone strength and modulus that can serve as design goals for replacement materials are 5-10 MPa strength and 50-100 MPa modulus[26].

We have discussed the mechanisms that the body uses to produce remodelled, structurally competent bone. We have also reviewed the mechanical properties of compact and trabecular bone that are representative of that structural competence. We now discuss several strategies that are alternatives to compact and trabecular bone transplantation. The techniques reviewed here will be geared toward orthopaedic applications, although they can also be considered in the context of craniomaxillofacial applications. The biologic principles are identical in the two classes of applications, but the load bearing requirements are somewhat different[14].

Strategies for Bone Regeneration

The variety of reported novel techniques to regenerate bone make use of polymers, ceramics, transplanted cells, and bioactive molecules. These components have been used in different combinations with each other and with transplanted bone. Lane's review[4] states that "it is crucial that potential graft substances be experimentally characterized in terms of their precise contributions to the bone-forming mechanisms." We will now discuss several potential solutions to the problem of bone regeneration, and how each of them addresses this statement.

There have been a variety of animal models used for the evaluation of bone replacement materials, and have included rodents[26,27], rabbits[27,28,29], dogs[4,21,30], and non-human primates[31,32]. The choice of model involves decisions concerning cost, stage of development of the particular material, and the intended application for the material. There have been models proposed and used that are specific for craniomaxillofacial applications[33], orthopaedic trabecular bone applications[21,27], and orthopaedic cortical (compact) bone applications[4]. Preliminary investigations of a novel material might typically begin in a rodent model. After initial demonstration of a promising material, the evaluation progresses to a higher animal model. This allows data collection in a skeletal system whose bone physiology and mechanical loading characteristics (for orthopaedic applications and some craniofacial applications) more closely mimics those of humans. Ripamonti has suggested that a material should ultimately undergo nonhuman primate evaluation prior to any human use[32]. The common theme in all the models is that they include a skeletal defect that will predictably not heal, in the majority of cases, in the lifetime of the animal[33]. The exceptions to this rule are some of the rodent models used for early feasibility and biocompatibility testing of a new material[26,27].

Polymers

The strategies that include polymers exploit two of their attractive properties. First, there is great design flexibility, because the polymer composition and structure can be tailored to the specific need. Novel polymer synthesis is often the first step in material selection and formulation. The second useful polymer property is biodegradation. Polymers can include chemical bonds that undergo hydrolysis upon exposure to the body's aqueous environment, and they can also degrade by cellular or enzymatic pathways. The degradation rate is amenable to control by alterations in polymer properties such as hydrophobicity and crystallinity. Polymeric systems that have been investigated for bone regeneration include the poly (α-hydroxy esters)[29,34,35,36], polydioxanone[37], poly(propylene fumarate)[26], poly (ethylene glycol) (PEG)[29], poly (orthoesters)[38], polyanhydrides[39], and polyurethanes[40]. The most frequently investigated poly (α-hydroxy esters) have been poly (L-lactic acid) (PLLA), poly (glycolic acid) (PGA), and poly (lactic-co-glycolic acid) (PLGA). These three materials, along with polydioxanone, have a long history of use as degradable surgical sutures, are approved for human use by the Food and Drug Administration, and are reasonably biocompatible.

Polydioxanone has been combined in semi-rigid sheet form with demineralized bone matrix (DBM) in rat calvarial defects. It functioned as a restraining agent for the particulate DBM, and provided shape control[37]. Polyurethane, in membrane form, was used to form a tube around a rabbit radius defect[40]. Ten of ten defects healed, compared to one of ten untreated contralateral controls. This is an example of the "guided tissue regeneration" principle, in which the tube of polymer is purported to prevent the ingress and ingrowth of tissues different from the injured tissue during healing. Polymers of silicon (glasses) have been combined with DBM, and demonstrated faster bone

regeneration than DBM alone[41]. PLLA has been copolymerized with PEG to yield a low viscosity material that can be injected through a syringe. The addition of PLGA to make a PLLA-PEG-PLGA terpolymer results in a firmer, moldable material. These polymers have been used as delivery systems for bioactive molecules[29]. Poly (propylene fumarate) (PPF) has been incorporated into composite materials to replace trabecular bone[26,42], and to deliver antibiotics to bone in high local concentration[43]. The fumaric acid double bond of the polymer chain has been used to secondarily cross link the PPF during formulation of the composite material. This material has demonstrated adequate mechanical properties in vitro to function as a temporary trabecular bone replacement[44,45].

Ceramics

The use of ceramics in bone regeneration applications is based upon their structural similarity to hydroxyapatite, the mineral phase of bone. The two most commonly investigated ceramics have been β-tricalcium phosphate (β-TCP) and synthetic hydroxyapatite (HA)[46]. These materials are osteoconductive: they provide an appropriate open cell porous structure onto which osteoblasts can deposit bone[47]. They are biocompatible[48]. They differ in several aspects, one of which is the rate of resorption. HA resorbs very slowly compared to β-TCP[30.49]. In a proximal tibial and distal femoral model, only 5.4% of HA had resorbed at three months compared to 85% resorption of β-TCP during the same time period[49]. Various authors have considered HA, and hence its slow resorption relative to the characteristic time span for bone regeneration, to be both an asset[50] and a liability[51]. The argument against HA is that the new bone, once formed in the porous network of the HA scaffold, cannot experience the mechanical loading that it needs to remodel if the HA remains strong. Long term persistence of remodeled bone would be more likely to occur if the initial scaffold would

degrade and allow the bone to be loaded. The argument in favor of HA is that its structure more closely resembles natural bone hydroxyapatite than does that of β-TCP, and therefore it represents a better scaffold for bone ingrowth. β-TCP is a multicrystalline, porous ceramic, and is not identical to tribasic calcium phosphate[48]. A natural source of HA from coral (Porites species) has been used in bone regeneration studies[30,51]. This coralline HA has also been used as a mold to synthesize HA by a technique called the replamineform process.

Coralline HA was used as a delivery vehicle for osteogenin, one of the family of bone morphogenetic proteins (BMP's), in a rat calvarial study [51]. There were four experimental groups: HA plus osteogenin, HA alone, empty control defects, and collagen plus osteogenin. Only the collagen plus osteogenin group formed significant bone in the defect, and the authors hypothesized that perhaps the relatively nonresorbable HA released osteogenin less well than did β-TCP. The use of coralline HA in a dog radius model resulted in complete filling of the HA pores with new bone at three months. There was no degradation of the original quantity of HA at the three month time point[30].

Bioactive Molecules

The identification of human bone morphogenetic protein[12] and its production by recombinant DNA technology[13] has ushered in the development of novel systems to deliver it to bone repair sites in an effective manner. BMP has been delivered to a segmental rabbit tibial defect via a polymer containing PLLA, PEG, and PLGA[29]. There was complete restoration of the defect in twelve weeks. Mechanical strength in this model was supplied by an HA rod spanning the defect and an external skeletal fixator. The polymeric material was used solely as a BMP delivery system. Two dosages of BMP-2 (1.4 μg and 11 μg) were tested in a rat femoral defect model[52]. The carrier was rat DBM, and contralateral control

defects contained DBM without BMP. The high dose group had ten of ten segmental defects heal. None of the defects healed in either the low dose group or the DBM controls. Other carriers have included a PLGA-TCP composite[53], collagen[54], plaster of paris[55], and HA impregnated with collagen[56]. These systems produced new bone in heterotopic sites, and demonstrated more bone with increasing BMP doses.

In a study of BMP delivery to treat nonunions[57], four patients with distal tibial metaphyseal nonunions who were at the point of amputation as their next step in management were treated with human allogenous BMP in a PLLA-PLGA delivery system. BMP represented 0.001% of the fresh weight of donor bone, and was extracted with other noncollagenous proteins. All four patients healed their nonunions within five months after this treatment.

Cellular Transplantation

The delivery of bioactive molecules to the site of bone repair assumes that those molecules will act upon mesenchymal cells, cause those cells to migrate to the site, differentiate, and express bone forming function. Several approaches to bone regeneration envision the delivery of the cells themselves to the repair site. Osteoblasts have grown on poly (α- hydroxy esters) and expressed their phenotype, as measured by production of alkaline phosphatase and type 1 collagen[58]. An osteoblast like cell line (MC3T3-E1) was grown on both the poly (α- hydroxy esters) and the polyphosphazines, and the cells retained their phenotypic expression[59]. One strategy used harvested autologous chondrocytes, and expanded their numbers by cell culture into porous HA. The composite of HA plus cells was then implanted into a rabbit ulna defect[28]. The rabbit has a synostotic radius and ulna, and therefore required no internal fixation of the defect. The study demonstrated bone formation at twelve weeks. There was no

bone in the contralateral defect, which contained HA as a control. The rationale for this approach is that chondrocytes are easier to culture than osteoblasts. Cartilage is aneural, alymphatic, and avascular. The nutrition of cartilage occurs by diffusion. These cells, once transplanted into the bone repair site, must make the cartilage matrix that forms the scaffold for endochondral ossification.

Summary

The need to replace bone when the body's repair mechanism fails has existed for a long time, and will, in all probability, continue to do so. The eventual solution to this problem will likely contain some of the concepts that have been reviewed here. The necessary elements of the solution should, we believe, include the following items. First, the material that initially re-establishes the injured skeleton's mechanical integrity should be a temporary material. This is necessary because the bone that forms must be allowed to bear load, and remodel in response to that load. An integral part of this requirement, for Orthopaedic applications, is that the mechanical properties of the material be adequate to perform the function of the type of bone it replaces. Second, the material must degrade in a controlled fashion into nontoxic products that the body can metabolize or excrete via normal physiologic mechanisms. Third, a vascular supply must be re-established into the reconstructed region to bring nutrients, cellular precursors, and bioactive molecules to the region, and to remove metabolic wastes and necrotic debris. Note that some of the potential solutions include cells and bioactive molecules, but the nutritional and waste removal functions of the vasculature are still necessary. Finally, consideration should be given to the intended clinical use of the materials. This will insure that material variables such as shelf life, time period between identified need and availability, and handling properties receive due thought during the design phase. Similarly,

the design phase should include surgical considerations such as the required operative exposure, alterations to existing surgical techniques that a new material may impose, and post-surgical rehabilitation differences that may be necessary. These will probably be easier to consider during the design than to retrofit at a later time.

CHAPTER 2

Two Stage Synthesis of Poly (Propylene Fumarate) via Initial Schotten-Baumann Reaction Followed by Transesterification of Trimer to Polymer.

Introduction

Poly (propylene fumarate) (PPF) has undergone development as a candidate polymer for use in a biodegradable composite material for Orthopaedic applications. Prior methods of synthesis employed harsh reaction conditions that made it difficult to obtain reproducible product. This work involves a novel synthesis technique to produce PPF. The process is an initial Schotten-Baumann reaction between the diacid chloride of fumaric acid and propylene glycol to produce a trimer. The trimer, bis-(hydroxypropyl) fumarate, then undergoes a self transesterification to form the polymer. The reaction is reproducible, simple to carry out, and avoids the previous severe reaction conditions that led to undesirable side products. We suggest that it represents an attractive method to synthesize this polymer for subsequent use in composite materials for Orthopaedic applications.

Bone is a unique tissue in its response to injury. Tissues in the body, when injured, progress through a process of inflammation and repair that results in scar tissue at the site of injury. An injury to bone (that is, a fracture) initially responds in a manner similar to that of other tissues, but an important difference in the healing process occurs: the evolving repair tissue becomes bone instead of scar.

The motivation for this work is to exploit bone's inherent self healing ability by developing a material that can provide structural support to a region of the skeleton and be biocompatible, degrading in a controlled fashion into non-toxic substances that the body can eliminate via normal metabolic pathways. Poly (propylene fumarate) (PPF) has been investigated[60,61,62,42,63,44,45] as a backbone polymer for use in a composite material to address the need for a temporary bone substitute. PPF is an alternating copolymer of propylene glycol and fumaric acid. The attractive features of PPF for this application include the double bond that is present in each fumarate structural unit, the ester linkage between each structural unit, and the nature of the two monomers that comprise the repeating unit. The double bond makes the polymer amenable to crosslinking via radical polymerization at the time of composite material formation. This offers the capability to mix the sterilized components of the composite material during an operation, and have the material pass through a moldable putty stage. The putty stage is quite useful for filling irregularly shaped defects in bone. The second property mentioned above, the ester linkage, is the basis for *in vivo* degradation of the polymer. The equilibrium nature of stepwise condensation polymerization results in ester hydrolysis upon exposure to the body's aqueous environment[45]. The rate of degradation of the composite material can be controlled by varying the PPF molecular weight and the hydrophilicity of its immediate environment (determined by other ingredients of the composite formulation). The third attractive property of PPF, i.e. the nature of its monomers, is related to biocompatibility. If the assumption is made that the polymer will degrade *in vivo* to its constituent monomers (an assumption that will need to be checked later), then those monomers must be compatible with the human body. They must not be toxic, and the body must be able to metabolize or excrete them via normal physiologic pathways. The two monomers that comprise PPF are propylene glycol and fumaric acid. Propylene glycol is widely used as a diluent in

intravenous fluids, and fumaric acid is a component of the physiologic Krebs cycle of human metabolism.

Poly (propylene fumarate) has been synthesized by several methods[44,60,62]. Each method has had drawbacks, including long reaction times, exacting polymerization conditions, and the presence of side reactions. The motivation for this work was to devise a quicker, more reproducible method of synthesizing PPF.

Materials and Methods

The synthesis strategy involves an initial Schotten-Baumann reaction between a diacid chloride (fumaryl chloride, Cl-CO-CH=CH-CO-Cl) and a dialcohol (propylene glycol, HO-CH_2-CHOH-CH_3). This is a rapid, irreversible reaction that is performed at room temperature and atmospheric pressure. There is no catalyst, and the HCl that is produced is trapped by bubbling it through aqueous NaOH. The reaction is run with an excess of propylene glycol (Aldrich Chemical Company, St. Louis, MO), and produces the trimer, bis-(hydroxypropyl) fumarate. Figure 2-1 demonstrates the reaction sequence. The fumaryl chloride (Aldrich Chemical Company, St. Louis, MO) and propylene glycol (Fisher Scientific, Pittsburgh, PA) were reagent grade and were distilled prior to use. First, 5.6 moles (426 gm) of propylene glycol was added to a 1 liter, 3 neck flask and stirred with a magnetic stirrer. Then, approximately 1.9 moles (284 gm) of fumaryl chloride was placed in a separatory funnel and added dropwise to the beaker containing propylene glycol. The addition rate was adjusted to control the rate of HCl production, which would become violent if the fumaryl chloride addition rate was too fast. The total volume of fumaryl chloride was added over 4 hours, and the reaction mixture was stirred for an additional 1 hour. The product of this reaction is bis-(hydroxypropyl) fumarate trimer and unreacted propylene glycol. This product is the starting mixture for the second

reaction.

The second reaction is a transesterification of bis- (hydroxypropyl fumarate) to produce poly (propylene fumarate). The proposed reaction mechanism appears in Figure 2-2. The transesterification produces one molecule of propylene glycol for every ester linkage made. The condensate thus contains the excess unreacted propylene glycol from the first reaction and propylene glycol formed as the second reaction proceeds. The mixture of bis-(hydroxypropyl) fumarate trimer and unreacted propylene glycol from the first reaction was placed in a one liter glass reaction vessel (Ace Glass, Vineland, NJ). The reactor setup appears in Figures 2-3 and 2-4. Figure 2-3 is a drawing of the entire system, and Figure 2-4 is an enlargement of the reaction vessel, oil bath, and nitrogen inlet. The reaction vessel was fitted with an electric mechanical stirrer, distillation head, nitrogen inlet, and thermometer at the level of the condensation side arm of the distillation head. A water cooled condenser, 30 cm long, was fitted to the distillation head, and a graduated collector was placed at the outlet of the condenser. The nitrogen inlet was connected to a Teflon bubble plate at the bottom of the reaction vessel . The bubble plate was custom made in our laboratory to fit the bottom of the 1 liter reaction vessel, and provided a constant upward flow of nitrogen through the entire volume of the reaction mixture. This helped to maintain uniform mixing as the polymerization progressed and the viscosity increased. The nitrogen was supplied from a cylinder via a two stage regulator. The nitrogen flow was adjusted so that steady streams of bubbles rose through the polymerization mixture without spattering the reaction contents throughout the 1 liter vessel. The polymerization temperature was controlled by raising a heated oil bath (Instatherm, Ace Glass, Vineland, NJ) around the reaction vessel. The reaction vessel and associated glassware were affixed to a metal grid support system inside a fume hood. The oil bath was placed on a scissor-type jack stand (Ace Glass, Vineland, NJ), heated to the desired reaction

POLY(PROPYLENE FUMARATE) SYNTHESIS

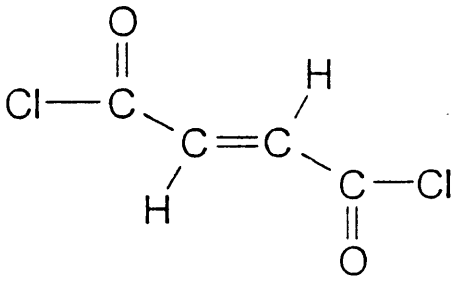

FUMARYL CHLORIDE

"A"

+

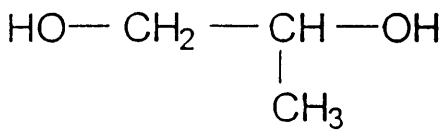

PROPYLENE GLYCOL
(Large Excess)

"B"

SCHOTTEN-BAUMANN REACTION

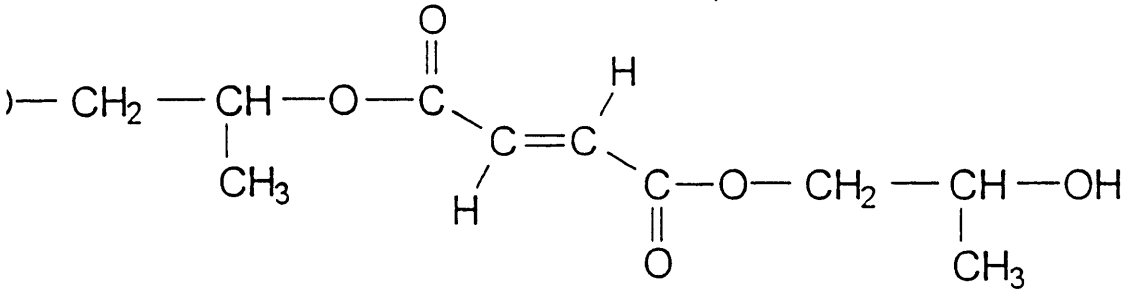

"B-A-B" TRIMER

BIS(HYDROXYPROPYL FUMARATE)

+

HCl
(REMOVED AS A GAS)

Schotten-Baumann Reaction Sequence

Figure 2-1

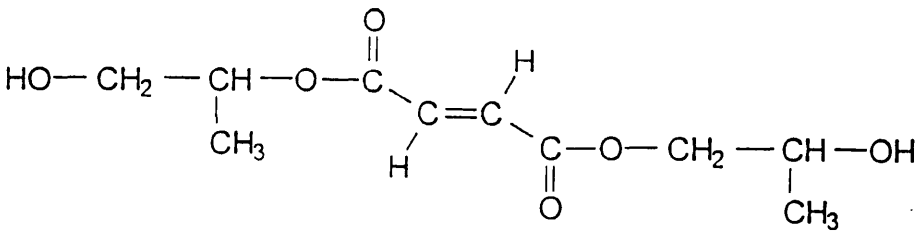

"B-A-B" TRIMER

BIS(HYDROXYPROPYL FUMARATE)

TRANSESTERIFICATION

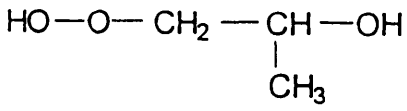

PROPYLENE GLYCOL

+

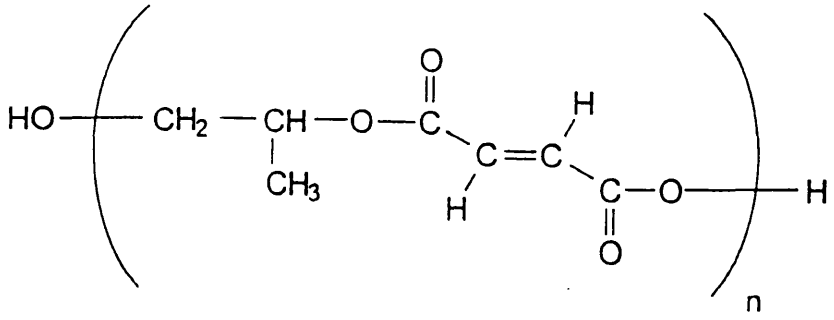

POLY(PROPYLENE FUMARATE)

Transesterification Reaction Scheme

Figure 2-2

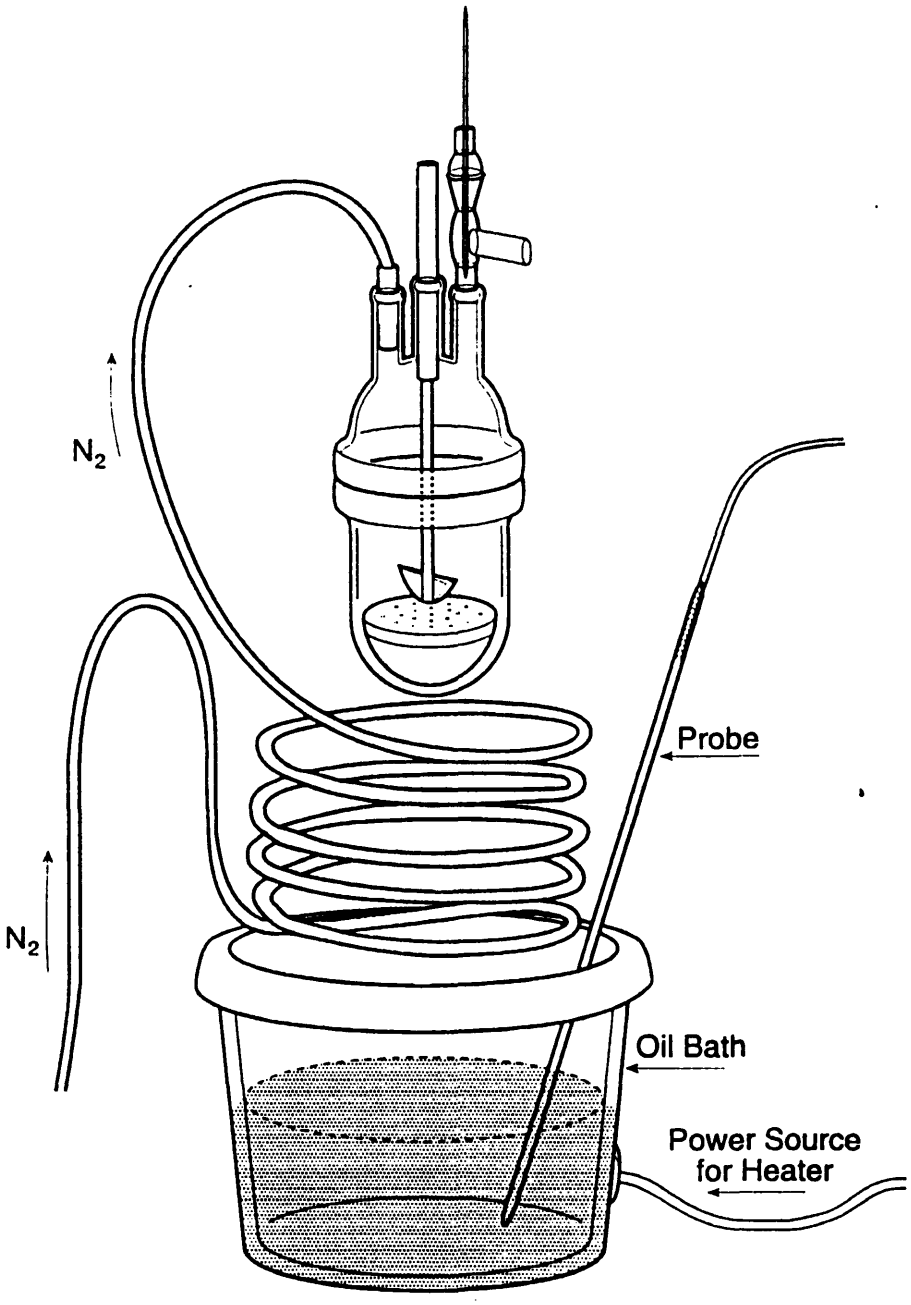

Reaction Apparatus

Figure 2-3

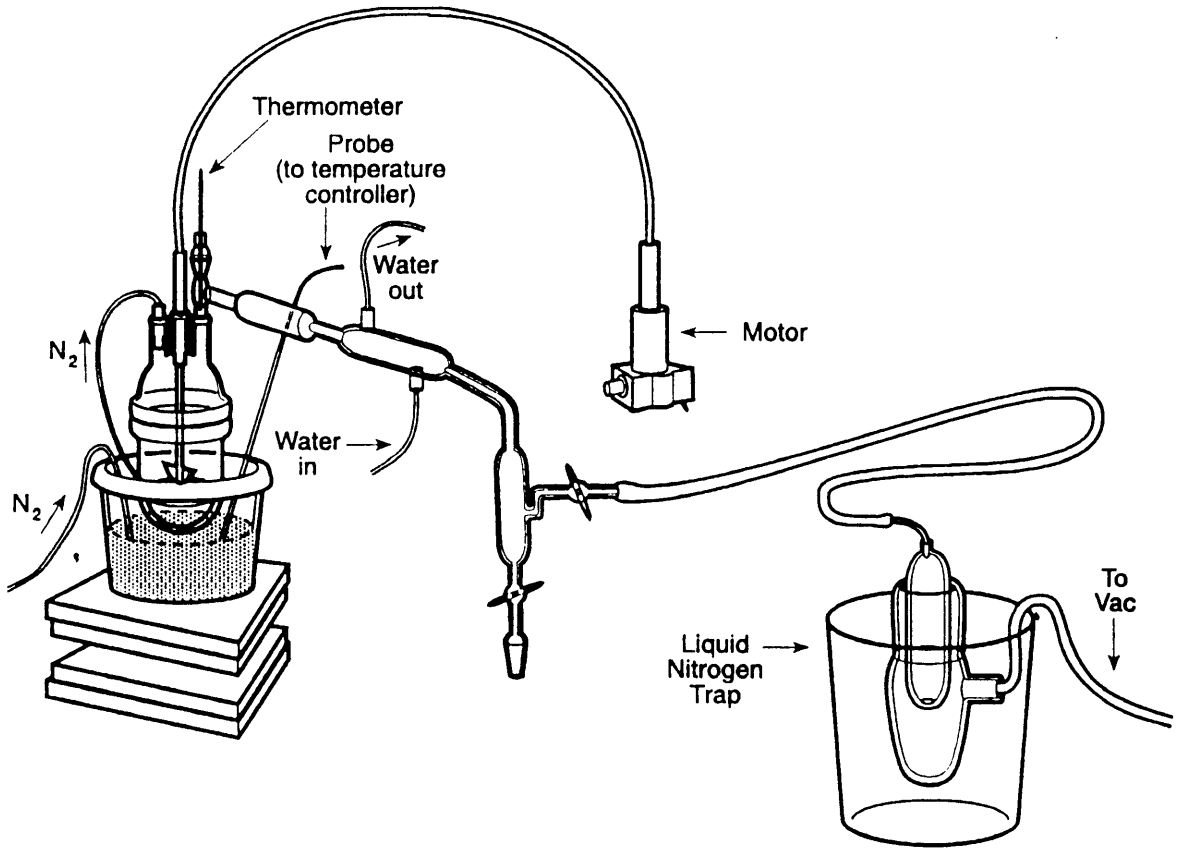

Reaction Apparatus: Close Up View of Reaction Vessel,

Nitrogen Heat Exchanger, and Constant Temperature Bath

Figure 2-4

temperature, and raised onto the reaction vessel. The oil temperature was controlled by a time proportional, digital temperature controller (Model 12106, Ace Glass, Vineland, NJ) that used a platinum resistive temperature device (RTD) sensor. The sensor was placed in the oil bath, not in the reaction vessel. Experience with prior attempts to position the platinum RTD sensor inside the reaction vessel demonstrated that rapid increases in polymer viscosity near the end of the reaction occasionally damaged the stirrer and the RTD sensor. Hence, reaction temperature was controlled by sensing the temperature of the oil bath that surrounded the reaction vessel, and controlling the oil bath temperature to ±0.1°C. The polymerization was performed in an inert nitrogen atmosphere to exclude oxygen and water vapor. The nitrogen was preheated to the reaction temperature by passing it through a ten foot length of coiled 0.25" copper tubing. The tubing was immersed in the oil bath in the space between the reaction vessel and the glass wall of the bath. The reaction pressure was controlled by a vacuum pump (General Electric, Fort Wayne, IN) connected to the condensate receiver. The pressure was monitored by a closed tube mercury manometer that was connected to the line between the receiver and the vacuum pump. An adjustable bleeder valve (a hose clamp on tubing that was open to atmospheric pressure and connected to the vacuum line with a three way adapter) was used to control the system pressure. Simultaneous adjustment of the bleeder valve and the nitrogen flow rate allowed the attainment of reaction pressures down to 30 mmHg while maintaining a steady flow of nitrogen bubbles through the reactants. A cold finger vapor trap was immersed in liquid nitrogen between the condensate receiver and the vacuum pump to protect the pump. The polymerization reaction will proceed in the absence of catalyst, but it occurs much more rapidly with the addition of 2 to 3 weight percent antimony trioxide (Sb_2O_3) as a basic transesterification catalyst. Transesterification reaction times to reach an equivalent molecular weight polymer with and without catalyst are 8 hours and 76 hours respectively.

The ability to polymerize in the absence of catalyst is attractive in view of this polymer's intended biologic use, in that catalyst removal need not be verified in a subsequent purification step.

The reaction began at 160°C and atmospheric pressure. When the rate of condensate production decreased, the pressure was lowered to 30 mmHg. When condensate production ceased at these conditions, the reaction was stopped by lowering the oil bath and turning off the temperature controller. Prior experience showed that further increases in temperature would effect gelation of the polymer. The pressure was gradually returned to atmospheric while maintaining a positive flow of nitrogen through the reaction vessel. The product, a yellow viscous semisolid at room temperature, was removed from the reaction vessel, placed in a sealed glass jar, and kept in a vacuum desiccator until needed for analysis. The condensate from the reaction was distilled, and it boiled uniformly at 186°C and atmospheric pressure. This is the boiling point of propylene glycol. The polymer was purified by solution in THF and subsequent precipitation from petroleum ether. This solution-precipitation sequence was performed three times. The PPF is readily soluble in THF, and the antimony trioxide catalyst is not. The polymer - THF solution is separated from the catalyst by decanting and filtering it, and the polymer is recovered by precipitation from a nonsolvent (petroleum ether). The precipitation is done by adding the available volume of polymer solution slowly to a vigorously stirred beaker that contains approximately four times that volume of petroleum ether.

The polymer was analyzed by multi-angle light scattering and size exclusion chromatography (SEC) for determination of number average molecular weight (M_n), weight average molecular weight (M_w), and polydispersity index (PDI). The light scattering data were collected on a MiniDawn multi-angle detector (Wyatt Technology, Santa Barbara, CA), and gave an absolute estimate of M_w, which was used to calibrate the SEC instrument (Waters/Millipore,

Milford, MA) using narrow band polystyrene standards. The Waters instrument consisted of a Model 700 autoinjector, Model 600E pump, Model 996 photodiode array detector, Model 410 refractive index detector, Ultrastyragel 7.8 mm x 300 mm column with and 10^3 Å pore size (Waters/Millipore, Part #10572), a second, linear Phenogel 7.8 mm x 300 mm column in series (Phenomenex, Part# 26973, Torrance, CA), and a Millenium™ 2010 control software system. The mobile phase was tetrahydrofuran (THF), and data were gathered at a flow rate of 1 ml/min. The polymer was diluted to 0.5% in THF (w/v), passed through a 0.45μ filter, and injected into the mobile phase in 50-100 μl aliquots for molecular weight analysis.

Polymer analysis also included ^{1}H -NMR and ^{13}C-NMR, elemental analysis, gas chromatography/mass spectrometry (GC/MS), and Fourier transform infrared spectroscopy (FTIR). The FTIR spectroscopy was performed on a Beckman 1000 spectrophotometer using sodium chloride plates or silver chloride plates. Fourier transform proton nuclear magnetic resonance (FT/^{1}H-NMR) spectroscopy was performed on a Hitachi R-1500 spectrophotometer (60 mHz) using 3% volume/volume concentrations with tetramethoxysilane (TMS) as a standard in either deuterated chloroform ($CDCl_3$) or dimethylsulfoxide (d^6-DMSO). Carbon-13 nuclear magnetic resonance (^{13}C-NMR) were performed on a JEOL FX270 convertible NMR spectrometer using $CDCl_3$ in concentrations of 1% for the proton NMR (270 MHz absorption frequency) and 10% for the ^{13}C-NMR (68.7 MHz absorption frequency) with TMS as a standard. Elemental analyses and mass spectral data using a Perkin-Elmer 2400 Series 2 Elemental Analyser and a Finnegan Model 4121C Gas Chromatogaph/Mass Spectrophotometer (GC/MS) respectively.

Results

The results of the two step reaction are presented separately for the Schotten-Baumann reaction to form trimer, and the transesterification of trimer to polymer. The trimer is a clear viscous liquid at room temperature and atmospheric pressure. Elemental analysis revealed 40% carbon, 8.1% hydrogen, 8% chlorine, and 43.9% oxygen. The theoretical values for elemental analysis are 51.7% carbon, 7% hydrogen, 0% chlorine, and 41.3% oxygen. The difference between the theoretical and calculated elemental analyses is explained by incomplete conversion of fumaryl chloride to the diol trimer. The trimer is soluble in THF, diethyl ether, and dichloromethane. The C-13 NMR data demonstrate the presence of both diol trimer and half-product (δ=19.2, 68.4, 76.6, 134.2, and 165 ppm). The half product (Figure 2-5) results from the reaction of a fumaryl chloride molecule with one molecule of propylene glycol, leaving the second chloride of the fumaryl chloride unreacted. The GC/MS data are consistent with the presence of both trimer and half-product. Table 2-1 contains the GC/MS values for the observed mass/charge ratios, and the proposed molecular fragments that correspond to these data. These fragments are identified either as the diol trimer molecule (T) minus a fragment (e.g. "T - C_3H_5O"), or as the fragment itself.

The product of the second reaction is a dark yellow to light brown polymer that is nearly, but not quite, a solid at room temperature. The polymer can be drawn into fibers as it is cooling from the reaction melt of 160°C to room temperature. The molecular weight attained by stopping the reaction just prior to gelation is M_n = 1534, M_b = 2714, with a polydispersity of 1.77. This point is reached after 78 hours reaction time without catalyst. The same product is attained after 23 hours reaction time in the presence of 2% Sb_2O_3 as catalyst. The catalyst weight is calculated based on initial weight of trimer charged to the reactor. Polymer molecular weight as a function of reaction time appears in

FORMATION OF HALF PRODUCT

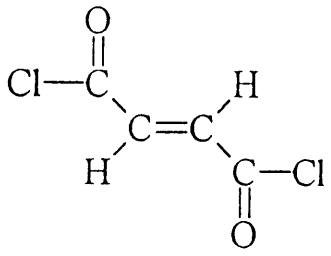

+

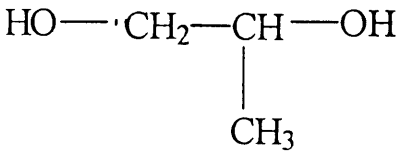

FUMARYL CHLORIDE
"A"

PROPYLENE GLYCOL
"B"

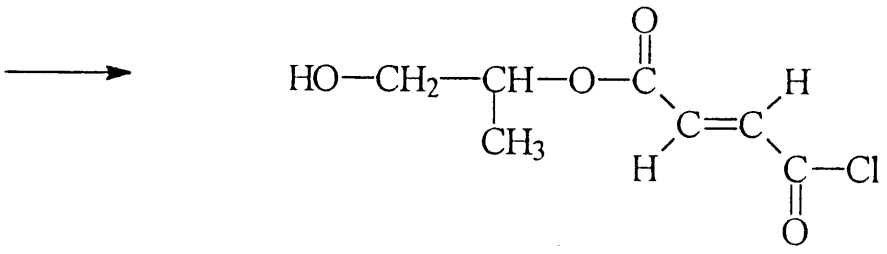

HALF PRODUCT

Reaction Sequence to Form Half-Product

Figure 2-5

Figure 2-6 for the catalyzed reaction. The SEC data that were used to construct Figure 2-6 appear as Figures 2-7a, 2-7b, 2-7c, and 2-7d. Thermal analysis via differential scanning calorimetry (Perkin Elmer Corp., heating rate = 10°C/min, calibration with indium standards) demonstrates a glass transition temperature at -8°C.

Table 2-1: GC/MS Data for Trimer

M/Z	Fragment Structure
215	T - (OH)
193	Half Product (see Fig. 4)
175	T - (C_3H_5O)
157	T - (OC_3H_6OH)
99	T - (OC_3H_6OH) - (C_3H_6O)
85	($C_2H_2COOCH_3$)
71	(C_2H_2COOH)
59	(C_3H_6OH)
45	(C_2H_4OH)

Elemental analysis (Wright Laboratories, Wright-Patterson AFB, OH) revealed the following composition: 51.3%C, 43.3%O, and 5.4%H (theoretical: 53.9% C, 40.8% O, and 5.3% H). The FTIR spectrum (Figure 2-8) demonstrated the expected absorbances (1000, 1200, 1250, 1650, 1720 and 3000 cm^{-1}) for the C-H stretch of the carbon-carbon double bond hydrogens, the C-O stretch, the ester linkages, the trans carbon-carbon double bond at the α carbon to the ester linkage, the carbonyl C-O stretch, and the C-H stretch. The polymer is soluble in

THF. The mass spectral data for the PPF appear in Figure 2-9 and Table 2-2. The actual spectrum is shown in Figure 2-9. Table 2-2 is constructed to show the fragmented species associated with the observed charge to mass ratios in the

Table 2-2: GC/MS Data for Polymer

M/Z	Fragment Structure
527	$\{HO(C_3H_6OCOCH=CHOCO)_3C_3H_6\}^+$
469	$\{HO(C_3H_6OCOCH=CHOCO)_2C_3H_6OCOCH=CHC=O\}^+$
441	$\{HO(C_3H_6OCOCH=CHOCO)_2C_3H_6OCOCH=CH\}^+$
389	$\{HO(C_3H_6OCOCH=CHOCO)_2C_3H_6OH_2\}^+$
371	$\{HO(C_3H_6OCOCH=CHOCO)_2C_3H_6\}^+$
313	$(HOC_3H_6OCOCH=CHOCOC_3H_6OCOCH=CHC=O)^+$
285	$(HOC_3H_6OCOCH=CHOCOC_3H_6OCOCH=CH)^+$
233	$(HOC_3H_6OCOCH=CHOCOC_3H_6OH_2)^+$
215	$(HOC_3H_6OCOCH=CHOCOC_3H_6)^+$
173	$(HOC_3H_6OCOCH=CHOCOH_2)^+$
157	$(HOC_3H_6OCOCH=CHC=O)^+$
128	$(OC_3H_6OCOCH=CH)^+$
99	$(C_3H_6OCOCH)^+$
87	$(C_3H_6OCOH)^+$
82	$(O=CCH=CHC=O)^+$
71	$(COOC_2H_3)^+$
59	$(COOCH_3)^+$
44	$(CO_2)^+$

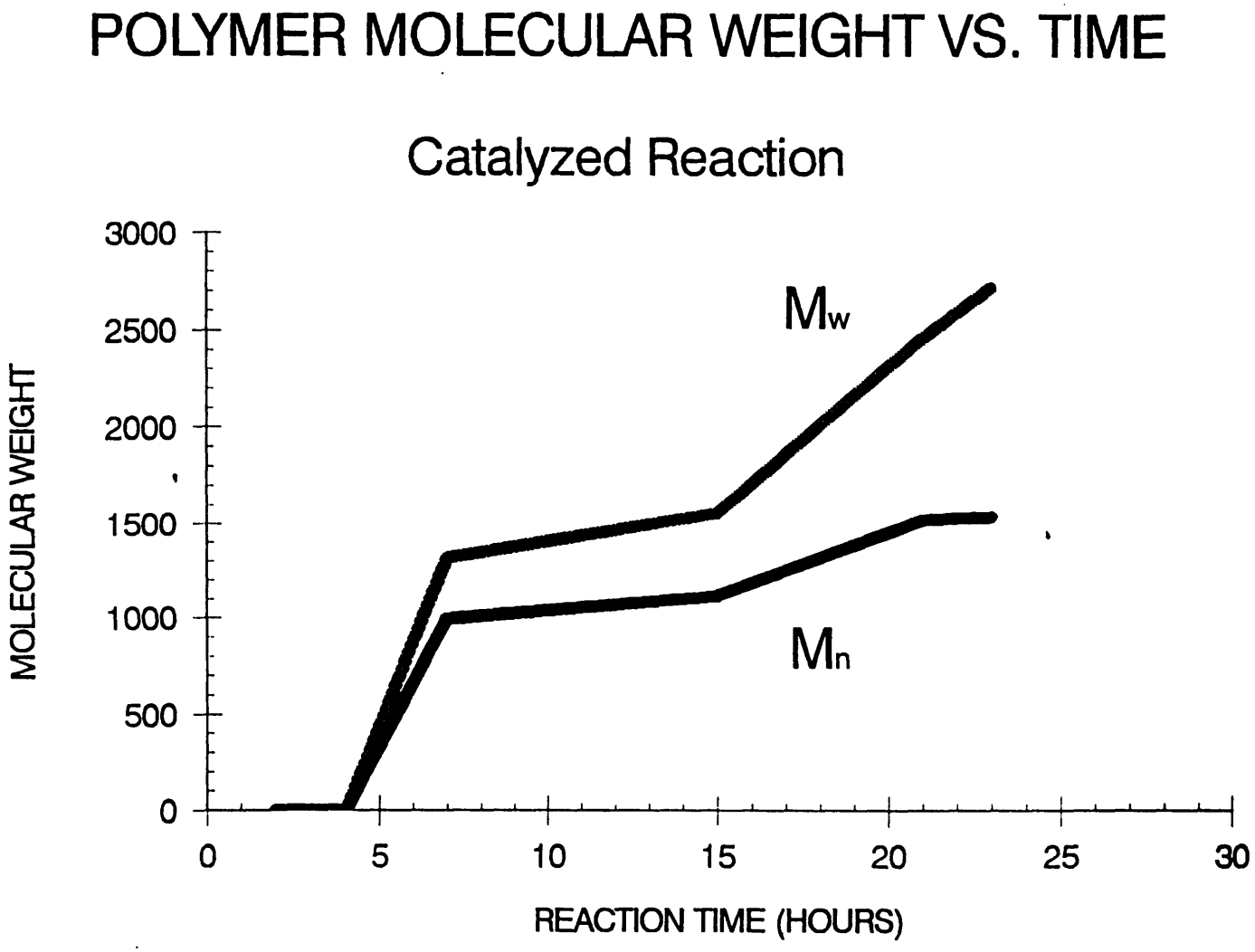

Polymer Molecular Weight as a Function of Reaction Time

Figure 2-6

Polymer Report

SampleName
202-12A

Date Acquired
09/13/94 12:29 PM

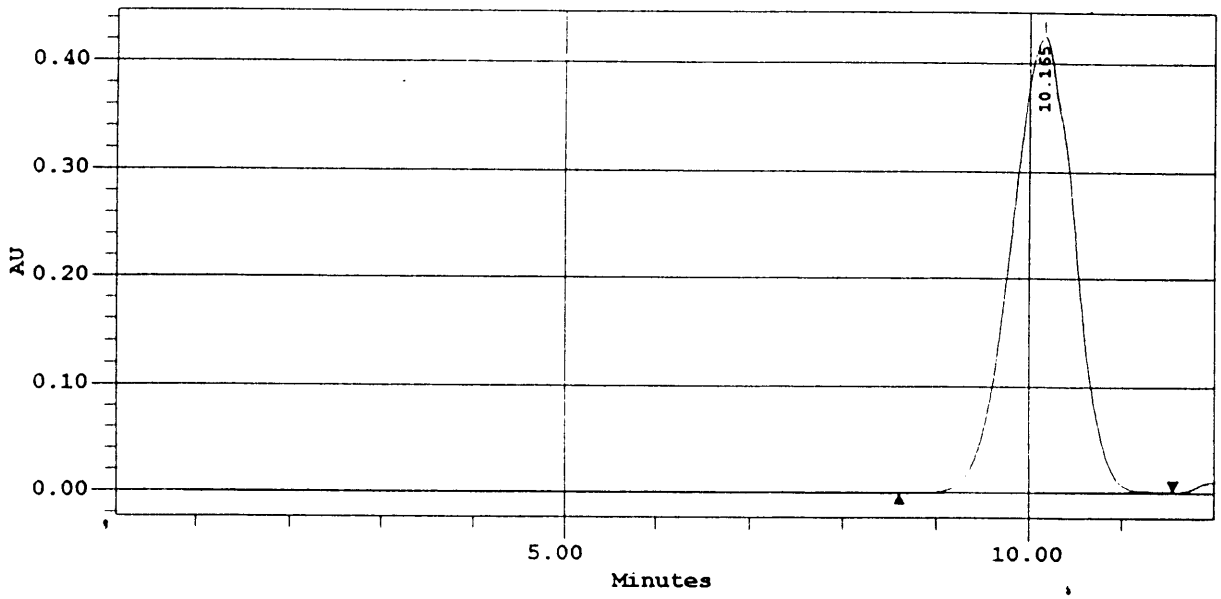

Polymer Results

#	SampleName	Mn	Mw	MP	Mz	Polydispersity
1	202-12A	992	1315	1075	1790	1.325583

Size Exclusion Chromatography Data Used to Construct Figure 2-6

Figure 2-7a

Polymer Report

SampleName
202-12B

Date Acquired
09/13/94 01:28 PM

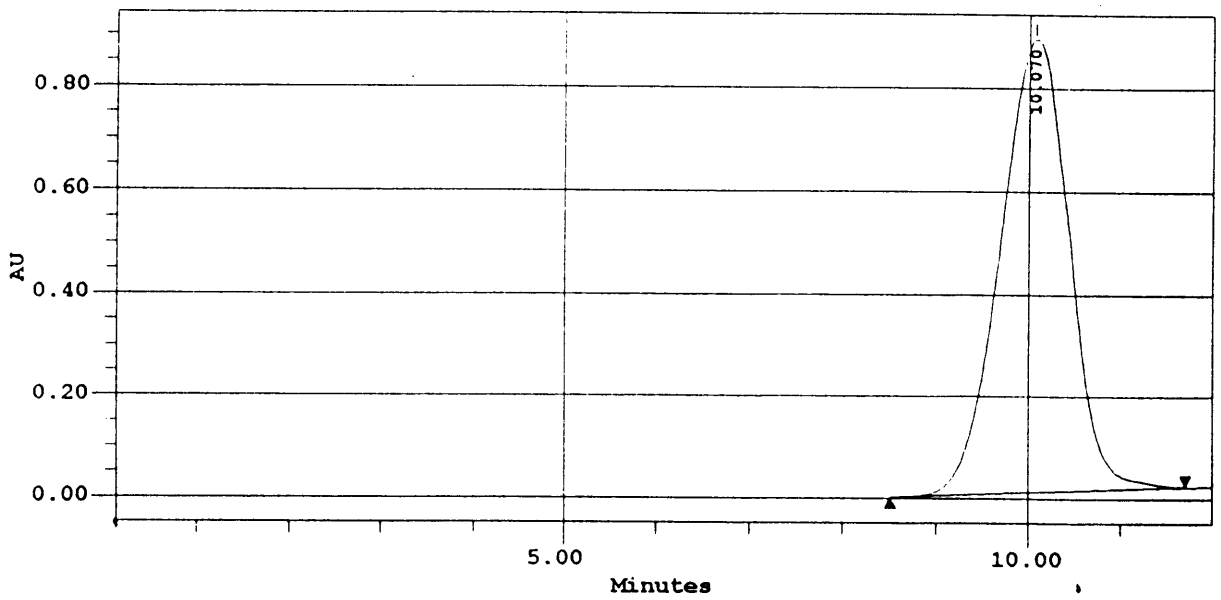

Polymer Results

#	SampleName	Mn	Mw	MP	Mz	Polydispersity
1	202-12B	1113	1553	1265	2212	1.394632

Size Exclusion Chromatography Data Used to Construct Figure 2-6

Figure 2-7b

Polymer Report

SampleName
202-12C

Date Acquired
09/13/94 02:09 PM

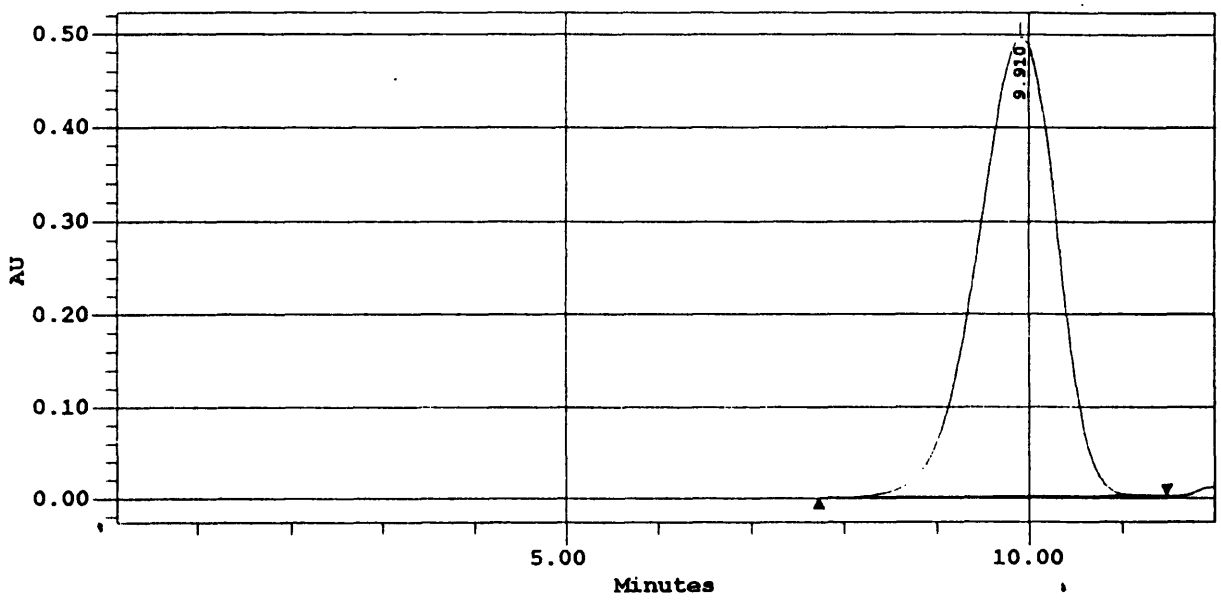

Polymer Results

#	SampleName	Mn	Mw	MP	Mz	Polydispersity
1	202-12C	1517	2457	1662	4726	1.619270

Size Exclusion Chromatography Data Used to Construct Figure 2-6

Figure 2-7c

Polymer Report

SampleName
202-12D

Date Acquired
09/14/94 11:21 AM

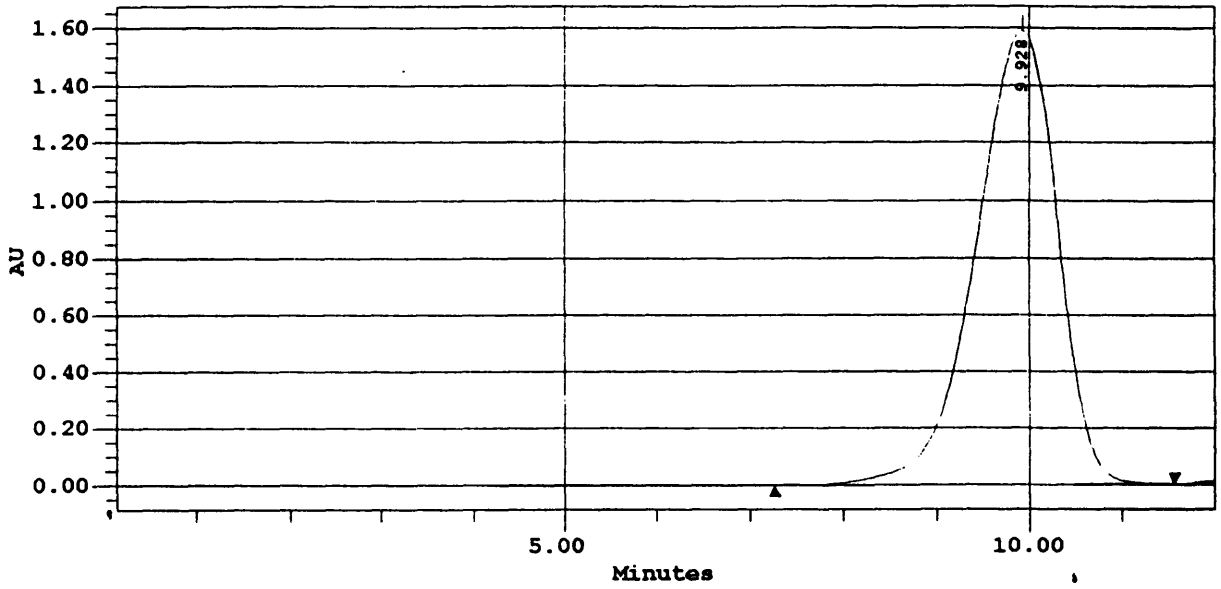

Polymer Results

#	SampleName	Mn	Mw	MP	Mz	Polydispersity
1	202-12D	1534	2714	1611	7504	1.769112

Size Exclusion Chromatography Data Used to Construct Figure 2-6

Figure 2-7d

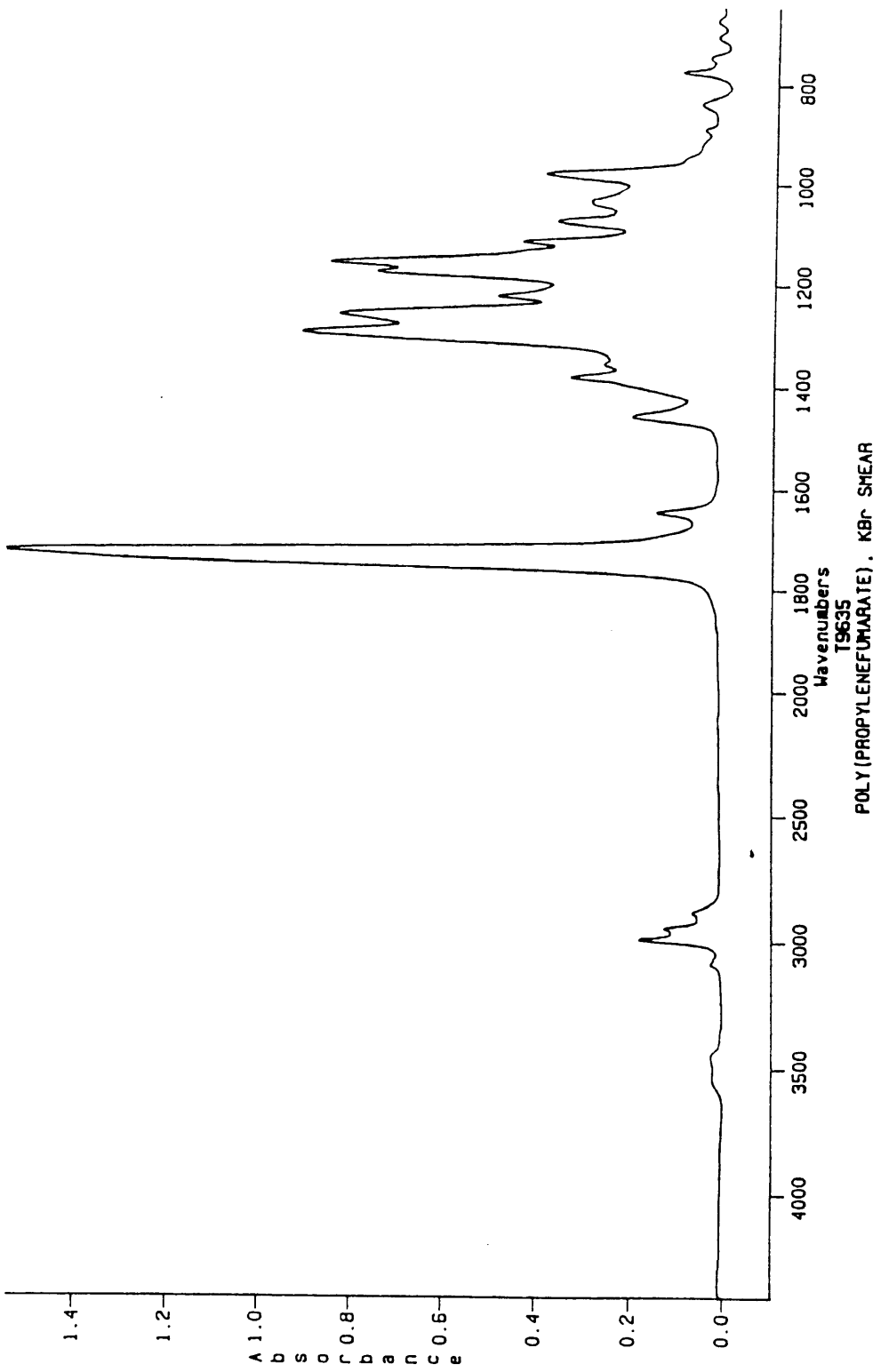

Fourier Transform Infrared Spectrum of PPF Polymer

Figure 2-8

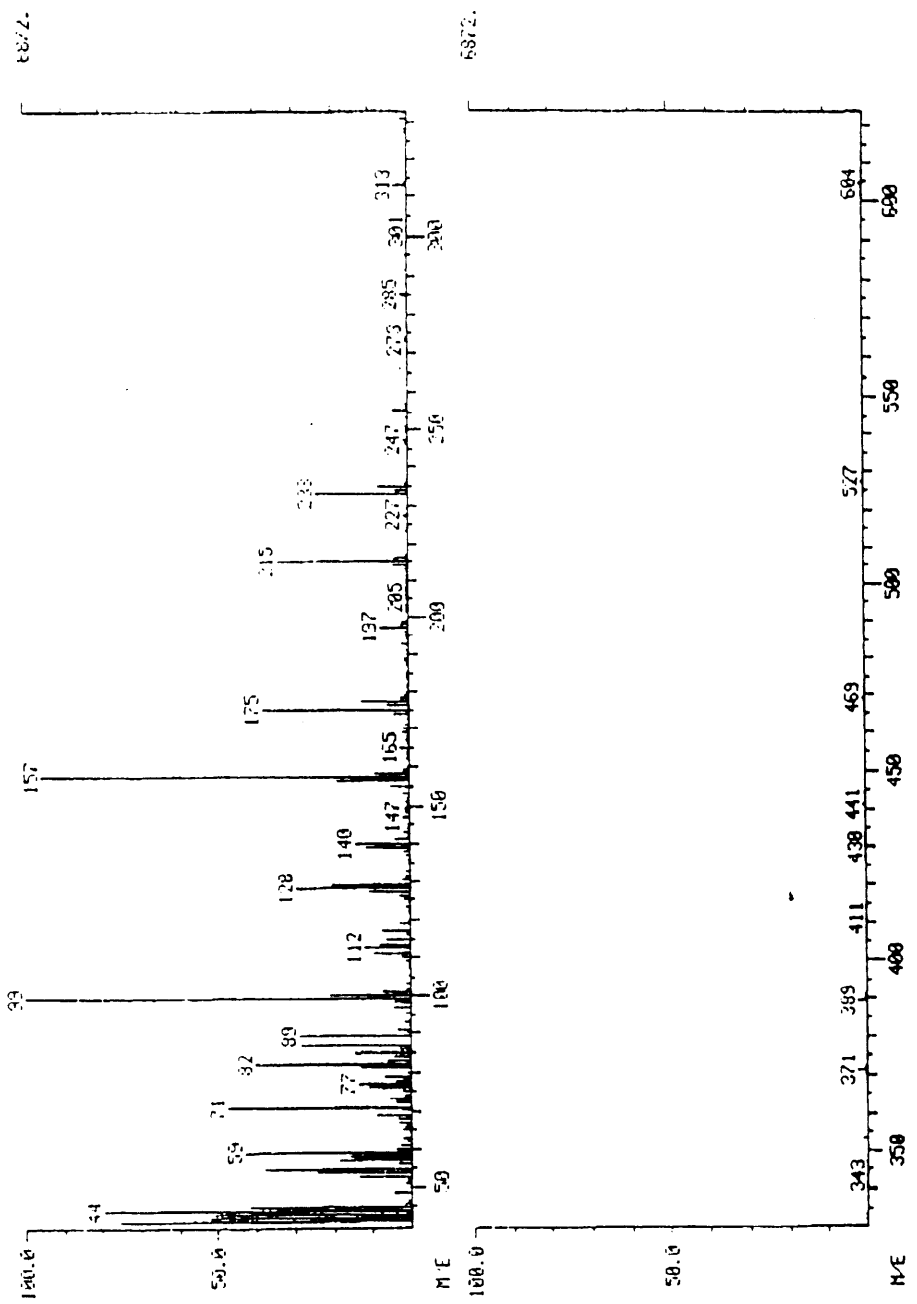

Mass Spectrum of PPF Polymer

Figure 2-9

spectrum. The GC/MS captures only those fragments that are volatile. The largest fragment observed was a heptamer ion at M/Z = 527. The GC/MS data are consistent with the proposed polymeric structure of PPF.

The proton nuclear magnetic resonance data for the polymer appear in Figure 2-10. The theoretical chemical shifts for the polymer repeating unit should be a singlet at δ = 6.8 ppm for the two trans hydrogens on the carbon - carbon double bond, and a multiplet at δ= 2.0 - 0.6 ppm for the six alkyl hydrogens from propylene glycol. The ratio of the two types of hydrogens in the polymer repeat unit is thus 1:3. The area integration of the NMR peaks that correspond to these hydrogens should bear the same ratio to each other. The observed spectrum demonstrates an area under the δ = 6.8 ppm peak of 0.327, and an area under the δ = 2.0 - 0.6 peak of 0.831. These areas are in the ratio of 1:3. The multiplet peak in the region δ = 3.0 - 5.6 is due to the THF solvent protons.

Discussion

The sequential Schotten-Baumann and transesterification reactions provide a simple, reproducible method to synthesize PPF. The analytical data indicate that the polymer and the intermediate trimer have the proposed structures. The FT-IR contains peaks that correspond to both the ester linkage and the carbon - carbon double bond at the α carbon to the carbonyl group. The possibility exists to prepare PPF without catalyst. This may be important should the presence of even small amounts of catalyst become an issue in the intended biologic use of PPF. The solid catalyst did precipitate out upon solution of PPF in THF during the purification of PPF. However, the trade off would be the increased reaction time necessary to synthesize PPF via the uncatalyzed route versus the increased time and effort necessary to demonstrate that the catalyst had been removed in syntheses that used it.

There is a small percentage of chlorine that remains in the polymer after reaction. The mass spectrometry data suggest that the chlorine is present as part of a fumaryl chloride molecule which reacts with propylene glycol through only one of its two chlorides. This was an unexpected finding, given the rapid nature of the Schotten-Baumann reaction and the excess of propylene glycol in the reactants. The presence of polymer that is terminated with a chloride may or may not be a problem in the proposed biologic use of PPF.

The polymer that is synthesized via a catalyzed route undergoes purification to remove the catalyst via solution in THF followed by precipitation of the polymer from a nonsolvent, petroleum ether. The H-NMR data show trace amounts of both THF and petroleum ether in product that is dried overnight in a vacuum desiccator. These trace impurities may pose a problem for biologic use, and experiments are underway to dry the product by rotary vaporization. . The PPF polymer is soluble in both vinyl pyrrolidone monomer and methyl methacrylate monomer. This is attractive, because vinyl pyrrolidone and methyl methacrylate are two candidate monomers to polymerize in the presence of PPF. Their chains can be crosslinked by the fumarate double bonds in PPF. This proposed crosslinking via radical polymerization of the PPF double bonds permits the formulation of a composite material based on PPF. The ability to make a liquid solution of PPF in monomer facilitates the handling of the composite material reactants. This is desirable for the intended polymerization of the composite during a surgical procedure.

Conclusions

The synthesis of poly (propylene fumarate) in two steps via sequential Schotten-Baumann and transesterification reactions is a straightforward, reproducible method to make this polymer. The ability to produce polymer

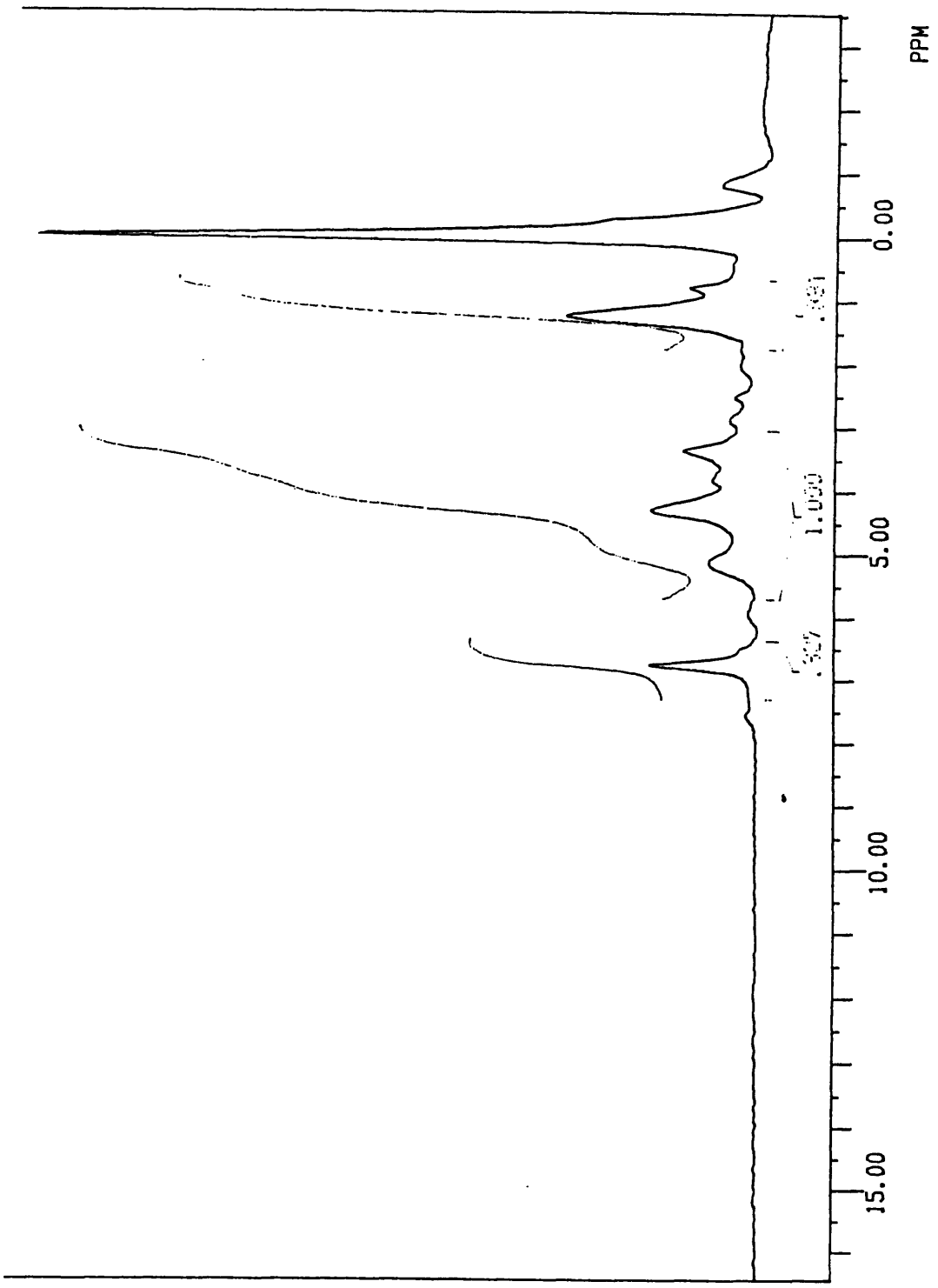

Proton Nuclear Magnetic Resonance Data for PPF Polymer

Figure 2-10

without the need for extremes of temperature is an advantage over several alternative synthesis routes. For example, prior stepwise polymerization methods that used the diethyl or dimethyl ester of fumaric acid and propylene glycol as monomers required temperatures up to 220°C to effect polymerization[42,63]. In addition, side reactions such as ether formation were common, and premature crosslinking often occurred throughout parts of the product polymer. The synthesis presented here produces PPF that has a polydispersity index which remains nearly constant over a range of molecular weights. This represents a more reproducible reaction than prior synthesis methods. The purity of the condensate collected in this two step scheme and the absence of other species upon analysis of the product polymer suggest that this scheme produces a pure product for subsequent inclusion in its intended composite material formulation.

The residual chlorine in both the trimer and polymer likely represents a terminal, unreacted fumaryl chloride endgroup. This may or may not be significant with respect to both biocompatibility and material property concerns in the material's intended biologic use. Nevertheless, attempts will be made to attain complete conversion of all fumaryl chloride to trimer in the first reaction step. These include alterations in the monomer ratios, the monomer addition rate, and the length of reaction.

The catalyzed second step allows the attainment of product that has M_w of 2714 g/mole after 23 hours of reaction. This is attractive, but brings the requirement of insuring complete catalyst removal for the intended biologic use. If in vitro and in vivo studies indicate promising mechanical and biologic properties, then it will be necessary to either demonstrate complete catalyst removal or revert to the longer, uncatalyzed transesterification reaction.

CHAPTER 3

The Physical Characterization of Poly (propylene fumarate) and Determination of its Mark - Houwink Constants.

Introduction

The chemical characterization of poly (propylene fumarate) (PPF) was presented in Chapter 2, and included size exclusion chromatography, elemental analysis, infrared spectroscopy, nuclear magnetic resonance spectroscopy, mass spectrometry, and light scattering analysis. The physical characterization of PPF, presented in this chapter, includes differential scanning calorimetry (DSC), thermogravimetric analysis (TGA), and dilute solution viscometry. The data from dilute solution viscometry will be combined with previously collected light scattering and size exclusion chromatography data to calculate the Mark-Houwink constants for PPF. These constants, **K** and **a**, relate the intrinsic viscosity of a dilute solution of the polymer to M_v, the polymer's viscosity average molecular weight.

Materials and Methods

Thermoanalytical data were obtained using a TA Instruments Model 2910 Differential Scanning Calorimeter (DSC) at a scanning rate of $\Delta T=10°C/min$ up

to 450°C in a nitrogen atmosphere. The cryogenic function of the DSC was used to start the data collection at a temperature below room temperature. The nitrogen source was purified, dried, and filtered. The nitrogen flow rate was 50 ml/min. Calibration was performed with Indium standards. A typical sample for analysis was approximately 12 mg of polymer in an aluminum specimen tray. A second, empty aluminum specimen tray served as a control for the thermal measurements.

Weight loss in helium was determined on a TA Instruments Model 2950 Thermogravimetric analyzer (TGA) at a scan rate of ΔT=10°C/min up to 900°C. The helium flow rate was 50 ml/min, and a typical sample size of polymer for analysis was 8 mg.

The viscosity measurements were performed with Ubbeholde Sizes 0 and 1 capillary viscometers (Fisher Scientific, Pittsburgh, PA). The data were collected for pure tetrahydrofuran (THF) solvent, and for various dilute solutions of PPF in THF. The solutions tested were 1%, 2%, and 3%. These were measured on a weight per volume (w/v) basis: grams of polymer per milliliters of solvent. For example, 0.25 grams of polymer dissolved in 25 ml of THF would be a 1% solution. The measurements were performed in a constant temperature bath. The bath was a ten gallon aquarium insulated on all four sides and on the top with one inch thick styrofoam insulation. The bath was filled with water, and the water was circulated through a heating-cooling unit which kept its temperature at 25° C ± 0.01° C. The surface of the water was further insulated with floating air-filled insulation spheres. The polymer solution to be tested was placed in the viscometer and immersed in the water bath by connecting the viscometer to a lab stand and clamp. The styrofoam insulation directly in front of the viscometer was removable to permit data collection by visual inspection. After allowing the test solution to equilibrate for thirty minutes in the constant temperature bath, the solution was drawn up past the upper mark of the viscometer, and allowed to flow through the capillary. The timer was started as the fluid meniscus passed the

upper viscometer mark, and the timer was stopped as the meniscus passed the lower mark. Each recorded data point, plus or minus its standard deviation, was the average of four readings. Data were collected for PPF that had three different molecular weights determined by size exclusion chromatography and light scattering. The first sample had M_n=1208 and M_w=1497, the second sample had M_n = 1224 and M_b = 1904, and the third sample had M_n = 1534 and M_w = 2714.

Results

The DSC demonstrated a glass transition temperature (T_g) of -8°C. The TGA showed a 4% weight loss due to solvent and propylene glycol (b.p.=187°C) over the temperature range of 0-200° C. Pyrolysis of the PPF occurred at 277 ° C. The DSC exotherm appears as Figure 3-1. The TGA data of temperature versus weight loss appear as Figure 3-2.

The dilute solution viscosity data appear in Table 3-1 for the PPF polymer having molecular weight M_w = 1497, in Table 3-2 for the polymer having M_w = 1904, and in Table 3-3 for the polymer having M_w = 2714. These data are the elution time, in seconds, for the dilute polymer solution to flow between the etch marks on the Ubbeholde viscometer versus the concentration, (C), of the dilute polymer solution in grams polymer per ml solvent. The pure solvent is identified as C= 0, and its elution time as t_0. The data were obtained for PPF in THF at 25° C. The relative viscosity of each dilute polymer solution is the ratio of the elution time of that solution to the elution time of pure solvent: $\eta_r = t/t_0$. The specific viscosity, η_{sp}, equals one minus the relative viscosity ($\eta_{sp} = 1 - \eta_r$). These are both dimensionless quantities. The reduced viscosity, η_{red}, equals the specific viscosity divided by the dilute solution concentration. The reduced viscosity has units of ml/g. The calculated values for these three viscosity parameters appear in Table 3-4 for the PPF having M_w = 1497, in Table 3-5 for the PPF having M_w =

Table 3-1

Ubbeholde Viscometer Elution Times for PPF in THF at 25° C

M_w=1497 g/mole

Concentration, C (g/ml)	Time , t (seconds)
0	t_0 = 582.1 ± 1.1
.01	600.6 ± 0.8
.02	626.2 ± 0.9
.03	651.2 ± 1.0

Table 3-2

Ubbeholde Viscometer Elution Times for PPF in THF at 25° C

M_w=1904 g/mole

Concentration, C (g/ml)	Time , t (seconds)
0	t_0 = 374.8 ± 0.7
.01	385.7 ± 0.1
.02	402.3 ± 1.0
.03	412.4 ± 0.8

Table 3-3

Ubbeholde Viscometer Elution Times for PPF in THF at 25° C

M_w = 2714 g/mole

Concentration, C (g/ml)	Time, t (seconds)
0	t_0 = 582.2 ± 1.1
.01	609.6 ± 1.0
.02	639.3 ± 0.9
.03	664.2 ± 1.9

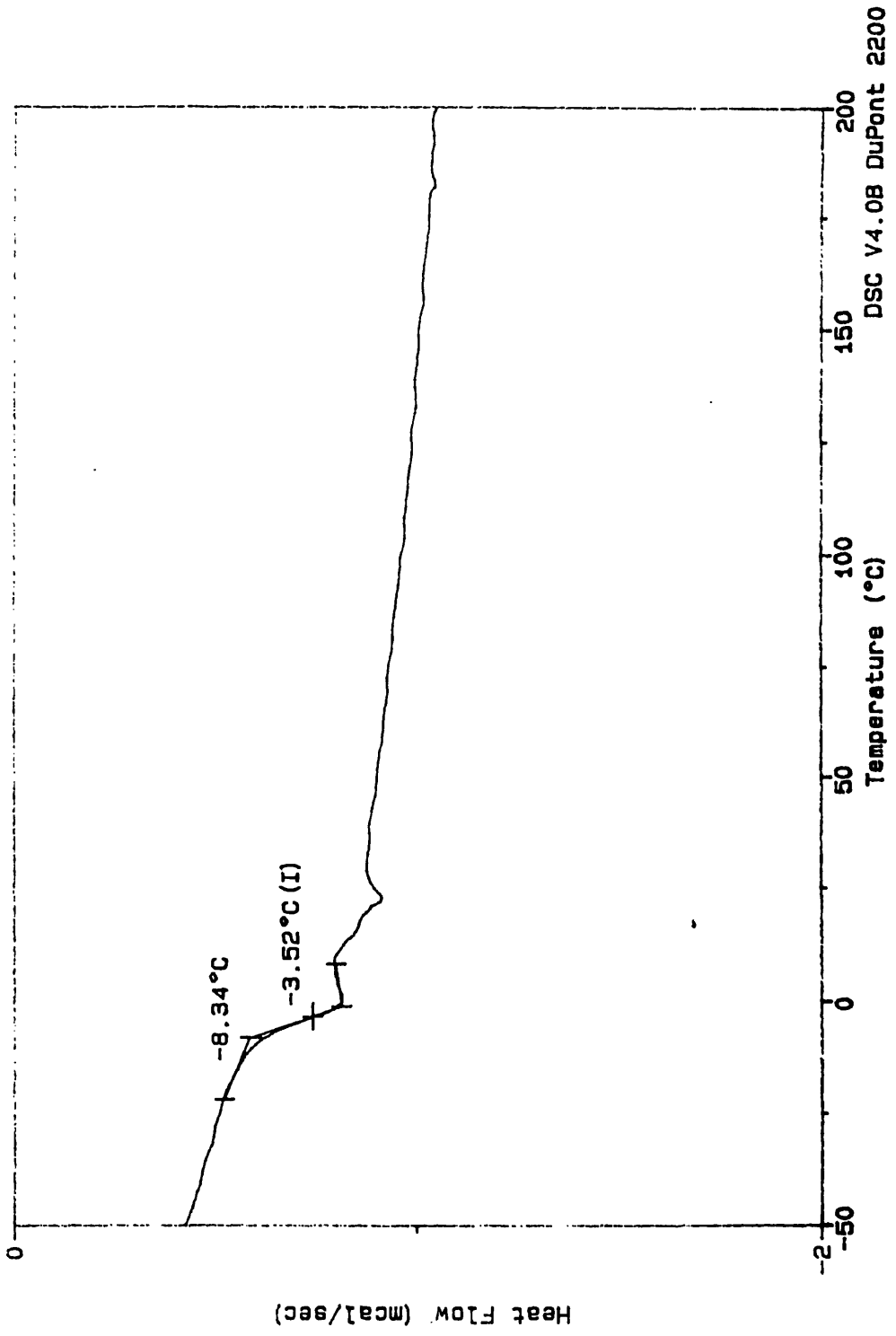

Differential Scanning Calorimetry Exotherm For PPF Polymer

Figure 3-1

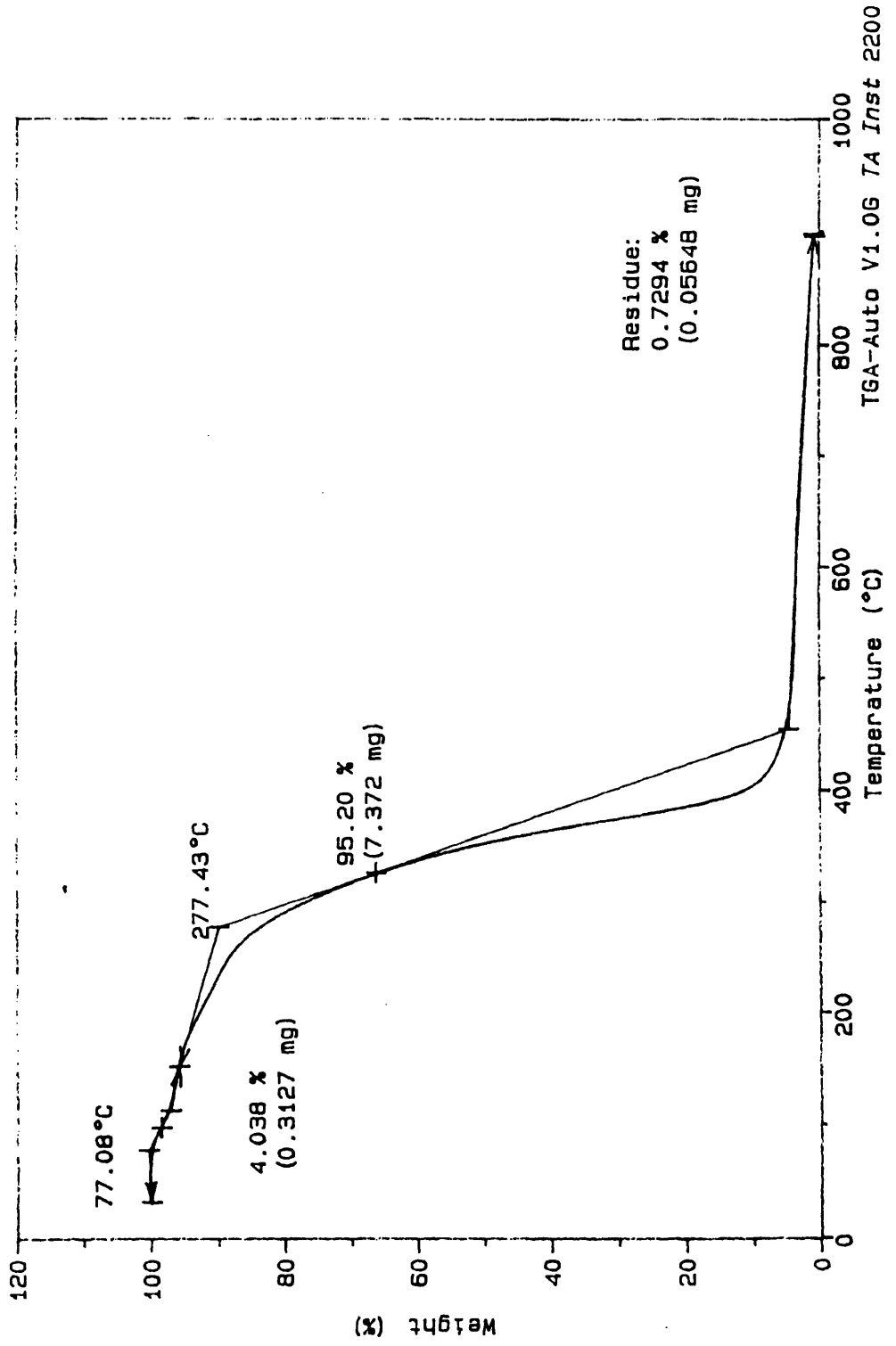

Thermogravimetric Analysis Graph of Weight Loss vs. Temperature for PPF

Figure 3-2

1904, and in Table 3-6 for the PPF having M_w = 2714. The intrinsic viscosity of the polymer, [η], is the limit, as the concentration approaches zero, of the reduced viscosity. The graphs of the reduced viscosity versus concentration data of Tables 3-4, 3-5, and 3-6 appear as Figure 3-3 for the PPF having M_w = 1497, Figure 3-4 for the PPF having M_w = 1904, and in Figure 3-5 for the PPF having M_w = 2714. The extrapolation of these least squares fit lines to zero concentration identifies the intrinsic viscosities of the three different molecular weight samples of PPF. The intrinsic viscosity of the M_w = 1497 polymer is 2.67 ml/g, that of the M_w = 1904 polymer is 2.97 ml/g, and that of the M_w = 2714 polymer is 5.27 ml/g.

Figure 3-6 is a graph of log M_w on the abscissa versus log [η] on the ordinate for the three molecular weights of PPF that had intrinsic viscosity determinations made. The data that were used to construct Figure 3-6 appear in Table 3-7, and the equation that describes a regression line fit to these data is:

$$\log [\eta] = \log K + a \times (\log M) \qquad \text{(Equation 3-1)}$$

which can be rearranged to give:

$$[\eta] = K \times (M^a) \qquad \text{(Equation 3-2)}$$

where **K** and **a** are the Mark-Houwink constants for PPF in THF at 25° C. These constants, calculated from a regression line fit to the data of Table 3-7, are:

$$\mathbf{K} = 3.3 \times 10^{-4} \text{ ml/g}$$

$$\mathbf{a} = 1.2$$

Table 3-4

Relative, Specific, and Reduced Viscosities for M_w = 1497 g/mole PPF

C (g/ml)	$\eta_r = t/t_0$	$\eta_{sp} = \eta_r - 1$	$\eta_{red} = \eta_{sp}/C$ (ml/g)
.01	1.03 ± .003	.03 ± .003	3.0 ± 0.3
.02	1.08 ± .004	.08 ± .004	4.0 ± 0.2
.03	1.12 ± .003	.12 ± .003	4.0 ± 0.1

Table 3-5

Relative, Specific, and Reduced Viscosities for M_w = 1904 g/mole PPF

C (g/ml)	$\eta_r = t/t_0$	$\eta_{sp} = \eta_r - 1$	$\eta_{red} = \eta_{sp}/C$ (ml/g)
.01	1.03 ± .002	.03 ± .002	3.0 ± 0.2
.02	1.07 ± .005	.07 ± .005	3.5 ± 0.3
.03	1.10 ± .004	.10 ± .004	3.3 ± 0.1

Table 3-6

Relative, Specific, and Reduced Viscosities for M_w = 2714 g/mole PPF

C (g/ml)	$\eta_r = t/t_0$	$\eta_{sp} = \eta_r - 1$	$\eta_{red} = \eta_{sp}/C$ (ml/g)
.01	1.05 ± .004	.05 ± .004	5.0 ± 0.4
.02	1.10 ± .004	.10 ± .004	5.0 ± 0.2
.03	1.14 ± .005	.14 ± .005	4.6 ± 0.2

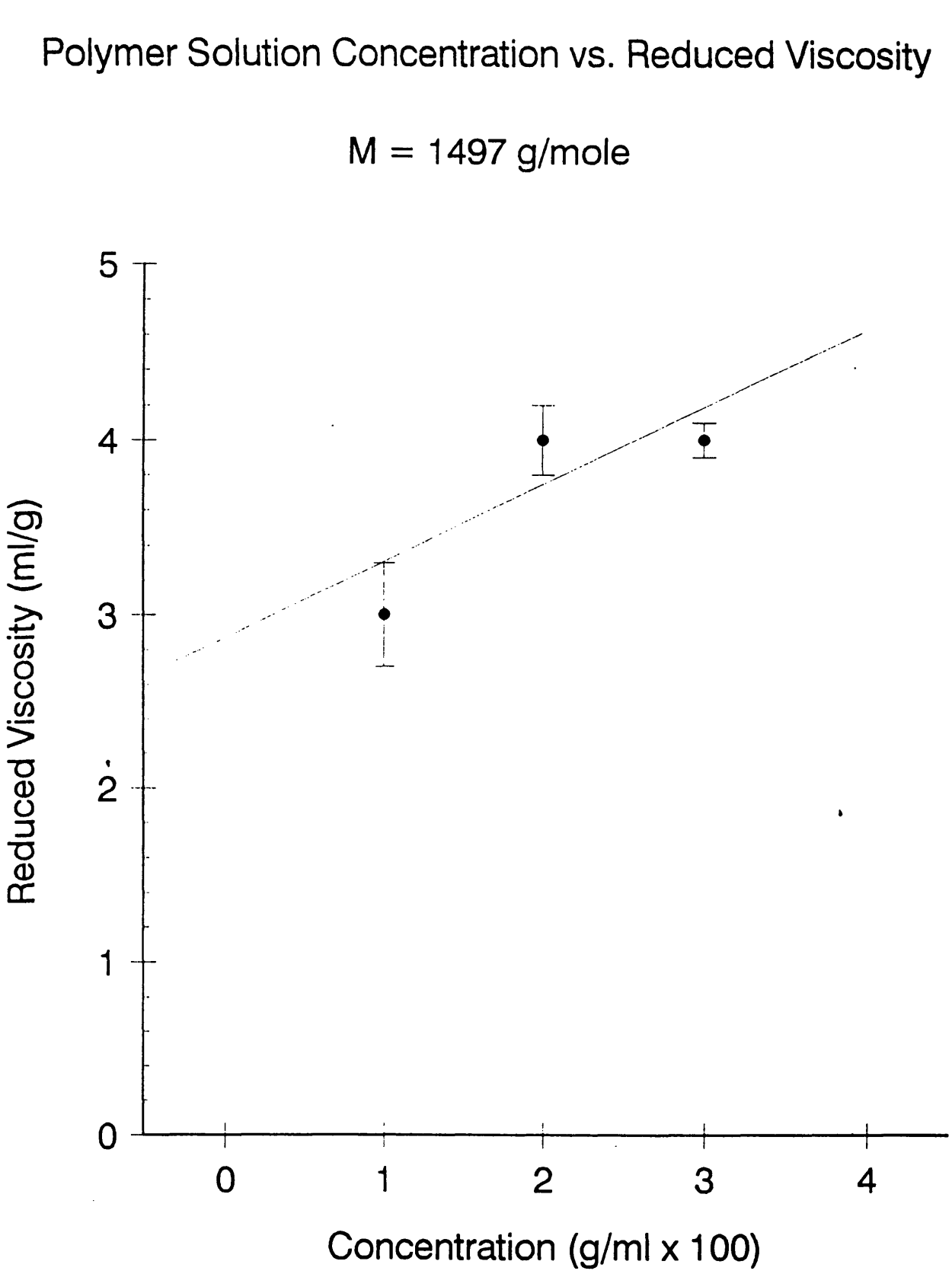

Dilute Polymer Solution Concentration vs. Reduced Viscosity, M_w=1497

Figure 3-3

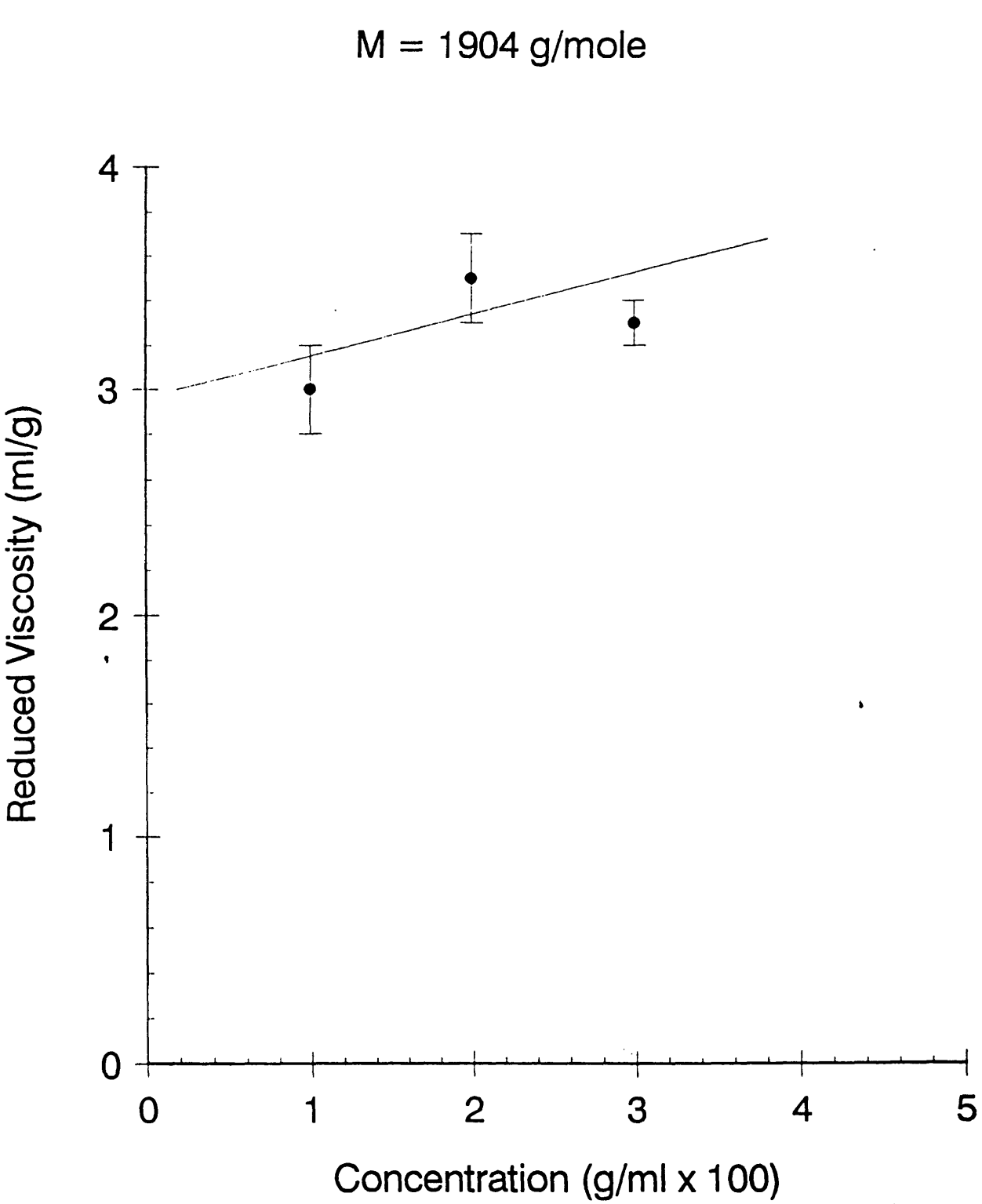

Dilute Polymer Solution Concentration vs. Reduced Viscosity, M_w=1904

Figure 3-4

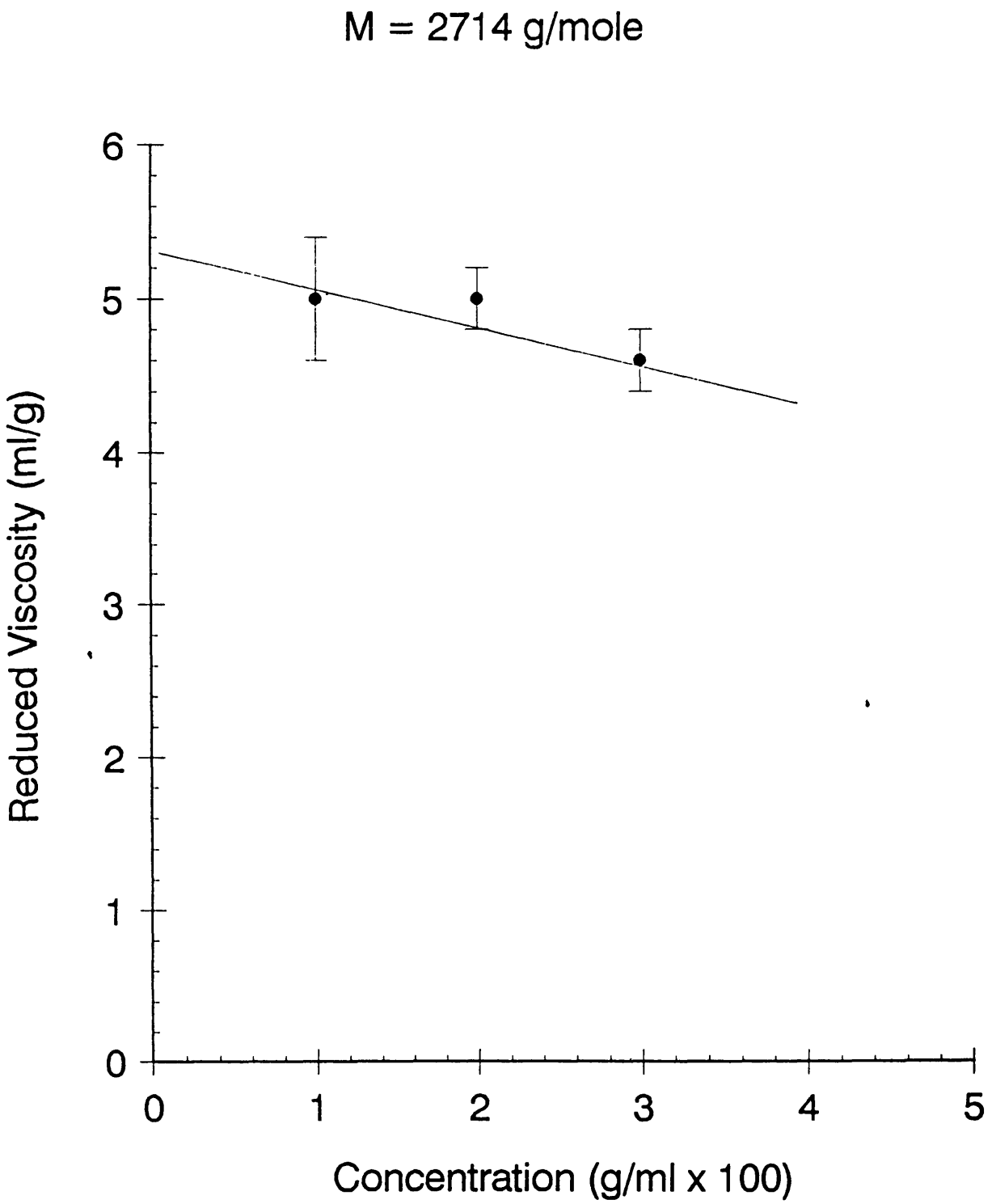

Dilute Polymer Solution Concentration vs. Reduced Viscosity, M_w=2714

Figure 3-5

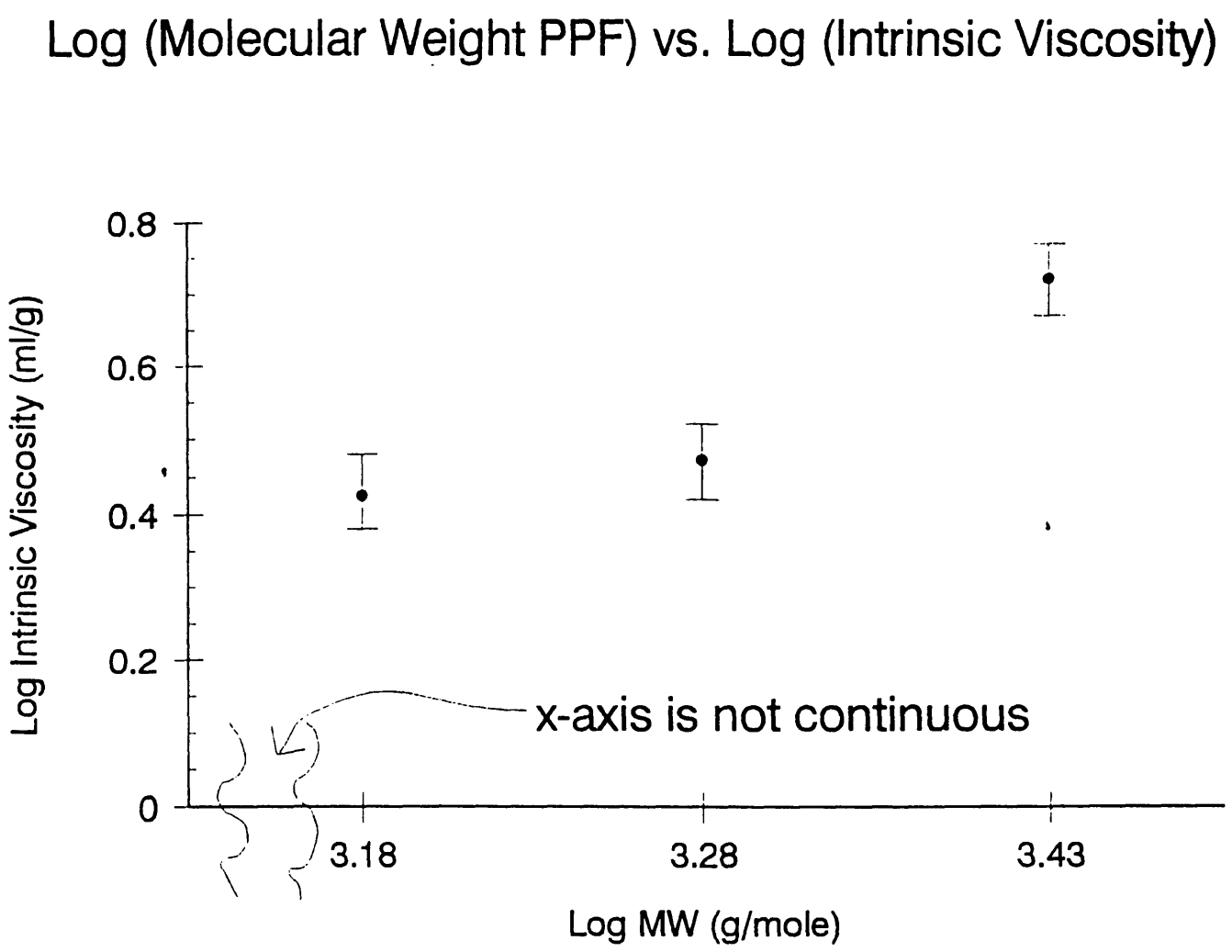

Graph of log M_w vs. log [η]

Figure 3-6

Table 3-7

Polymer Molecular Weight vs. Intrinsic Viscosity for PPF in THF at 25°C

M_w (g/mole)	log M_w	[η]	log [η]
1497	3.18	2.67	.43
1904	3.28	2.97	.47
2714	3.43	5.27	.72

Discussion

Poly (propylene fumarate) in the molecular weight range $1497 < M_w < 2714$ is a viscous semisolid at room temperature. It is readily soluble in methyl methacrylate monomer and N-vinyl pyrrolidone monomer. These two monomers are crosslinked by the fumarate double bonds of the PPF during the formation of a particulate filled composite material based on PPF. The Mark-Houwink exponent, **a**, is usually between 0.5 and 1.0[64]. The value calculated here for PPF in THF at 25°C, **a** = 1.2, may suggest that the PPF chains exist in THF solution in short, stiff, rodlike configurations.[65,66] Further work will include dilute solution viscometry of narrow molecular weight PPF fractions to refine the Mark-Houwink constant calculations.

CHAPTER 4

The In Vitro Strength and Degradation Characteristics of a Composite Material Based on Poly (Propylene Fumarate)

Introduction

This chapter focuses on the formulation of poly (propylene fumarate) into a particulate composite material, and the effect of several formula variations on that material's *in vitro* mechanical properties. The composite material must perform several functions in its intended role as a temporary bone substitute. It must pass through a low viscosity stage during which it can be molded to fit an arbitrarily shaped defect, harden over a time span of approximately ten to fifteen minutes, and attain a compressive strength and modulus on the order of magnitude of the trabecular bone that it will replace[22,23,24,25]. The need to have the material harden during a surgical procedure motivates the strategy of radical polymerization to crosslink a polymer through the fumarate double bonds of PPF. N-vinylpyrrolidone was chosen as the monomer for this function. Poly (vinylpyrrolidone) was used as a plasma expander during World War II, and has a long history of being biocompatible[67]. The radical initiation system chosen is the initiator benzoyl peroxide and the accelerator N,N-dimethyl paratoluidine. This is the same initiator-accelerator pair that is used in the clinical bone cement poly (methyl methacrylate).

Material properties that would be attractive in a bone replacement

composite, in addition to the strength criteria mentioned above, include porosity to allow ingrowth of vessels and new bone, and an appropriate scaffold structure upon which bone can grow. This work explores the use of β-tricalcium phosphate in the composite formulation as the osteoconductive scaffold to encourage bone growth and potentially provide increased strength to the composite. sodium chloride (NaCl) is used to function as a water soluble filler that will leach out upon exposure to the body's aqueous environment and provide the composite with initial porosity. Different molecular weights of PPF are used to assess whether polymer molecular weight affects composite strength and modulus[44]. The ratios of these various constituents to each other have been varied to assess the affect of composite's composition on it's handling properties, strength, and modulus. The handling properties are important because the composite, as it polymerizes, must remain a coherent mass. It should be neither fluid nor powdery. Either of these two extremes leads to loss of material from the intended site of application during polymerization.

The variables described above have been systematically investigated via a fractional factorial experimental design for their effect on composite strength, modulus, and handling properties. These experiments are described next.

Materials and Methods

The five variables for the composite material formulation were examined in a two level fractional factorial design. The material is a particulate filled composite. It consists of a linear polyester, poly (propylene-fumarate) (PPF), that is cross-linked through the fumarate double bond by a monomer, N-vinylpyrrolidone (N-VP) (Sigma, St. Louis, MO), and filled with sodium chloride (NaCl) (Sigma, St. Louis, MO) and β-tricalcium phosphate (β-TCP) (DePuy, Warsaw, IN). The variables in the experimental design were: 1) the molecular

weight of the PPF, 2) the ratio of the amount of sodium chloride (in grams) to the amount of PPF, 3) the particle size range of the sodium chloride, 4) the ratio of the amount of β-tricalcium phosphate (in grams) to the amount of PPF, and 5) the ratio of the amount of N-VP (in grams) to the amount of PPF. The low and high levels of the variables appear in Table 4-1. The fractional factorial design based on these variables appears in Table 4-2. There are a total of eight runs in this Resolution III design. A Resolution III experimental design will determine main effects of the variables, but will confound main effects with two-factor interactions[68]. Each run is a combination of the "high" and "low" levels of the variables listed in Table 4-1. These combinations of the variables are represented by a "+" sign for "high" and a "-" sign for "low" in Table 4-2. Each batch of the composite material was formulated on a basis of 4 grams of PPF. An example recipe, calculated from Run #4 of Table 4-2, appears in Figure 4-1. In addition to the variable components, each formulation also contains a radical polymerization initiator, benzoyl peroxide (Sigma, St. Louis, MO), and an accelerator, N,N-dimethyl paratoluidine (DMT) (Sigma, St. Louis, MO). Those formulations that contained the "high" amount of N-vinylpyrrolidone received 0.18 grams of benzoyl peroxide and 18 μl of DMT.

Table 4-1

High (+) and low (-) levels for the five variables in the fractional factorial design

	M.W. PPF	NaCl / PPF	Particle Size	β-TCP/ PPF	N-VP/ PPF
High Level	2350g/mole	0.25 / 1	250-425 μ	1.5 / 1	1.5 / 1
Low Level	1780g/mole	0 (no NaCl)	150-250 μ	0.75 / 1	0.75 / 1

Table 4-2

Combinations of the Experimental Variables for the 8 Runs

	M.W. PPF	NaCl / PPF	Particle Size	β-TCP/PPF	N-VP/PPF
Run #1	+	-	-	-	-
Run #2	-	+	-	+	-
Run #3	+	-	+	+	-
Run #4	-	+	+	-	-
Run #5	-	-	-	-	+
Run #6	+	+	-	+	+
Run #7	-	-	+	+	+
Run #8	+	+	+	-	+

Recipe for Composite Formulation Run #4

4 grams PPF

1.0 gram NaCl (250 - 425 μm size)

3 grams N-vinylpyrrolidone

3 grams β - Tricalcium Phosphate

0.12 grams Benzoyl Peroxide

12 μl Dimethyltoluidine

Figure 4-1

The formulations that contained the "low" amount of N-vinylpyrrolidone received 0.12 grams of benzoyl peroxide and 12 μl of DMT. Test specimens of the composite material formulated from the eight combinations of variables listed in Table 4-2 were made and analyzed in accordance with ASTM F451-86 for bone cements. The test specimens are 6mm diameter by 12 mm high cylinders, and are prepared by placing the polymerizing composite material into a 6 mm diameter by 12 mm high cylindrical Teflon mold. After hardening, and remaining in the mold for 12 hours, the specimens are removed from the mold and tested in compression on an Instron Model 1125 Materials Testing Machine. Prior to testing, the ends of the specimens were ground with #600 grit sandpaper on an electric polisher. This was done to produce plane parallel test specimens. The parallelism of the specimen ends was assessed visually with the aid of the parallel arms of a micrometer. Ten specimens of each of the eight formulations were tested for initial strength and modulus. The Instron was fitted with a 5 kN load cell, and the load measuring apparatus was zeroed, balanced, and calibrated. This was accomplished by the electronic calibration system built into the load cell. The specimens were compressed to failure at a crosshead speed of 1 mm/min, and the load vs. deformation curve was recorded. These data were reduced to calculate the Young's modulus (γ) and ultimate compressive stress (σ) for each formulation. The load-deformation curves had a toe region and an identifiable linear portion. A typical load-deformation curve appears as Figure 4-2. The Young's modulus was calculated as the slope of the load-deformation curve in its linear portion, and the ultimate compressive stress was calculated as the applied load at failure divided by the measured cross-sectional area of the test specimen.

The composite formulation shown in Figure 4-1 was chosen for *in vitro* assessment of degradation and the time course of material strength and modulus under simulated physiologic conditions. This composition had both acceptable initial strength and modulus for bone replacement, and good handling properties.

Test specimens of this formulation were made as described above. Ten specimens were made for testing at each of the following time points post-polymerization: 3 days, 1 week, 2 weeks, 4 weeks, 6 weeks, 8 weeks, and 12 weeks. The test specimens were removed from the Teflon mold after hardening, and were then placed in a phosphate buffered saline (PBS) bath. The bath was kept at 37°C and pH= 7.4. The saline solution was not changed during the experiment. At each of the scheduled time points, ten specimens were removed from the bath and tested on the Instron according to the above protocol.

Results

The results of initial compression testing for all eight combinations of variables appear in Table 4-3. The mechanical testing was done one day after placing the polymerizing composite material into the Teflon molds. Only Runs # 6 and 8 were too weak to be considered for further evaluation. We set a target minimum compressive strength of about 5 MPa, and a minimum compressive modulus of about 50 MPa as appropriate for a human trabecular bone replacement material[25]. The effects of the five variables in the fractional factorial design on the initial compressive strength and modulus of the resulting composite material appear in Table 4-4. A positive number indicates that the particular variable had an effect to increase the strength or modulus as it went from its "low" level to its "high" level, and a negative number indicates that the variable caused the strength or modulus to decrease as the variable went from its low level to its high level. The presence of NaCl as a filler, the lower molecular weight PPF, and the smaller amount of N-vinylpyrrolidone monomer had the strongest positive effects on

compressive strength and compressive modulus. The larger amount of β- TCP had a strong positive effect on the compressive modulus. The strengths of the

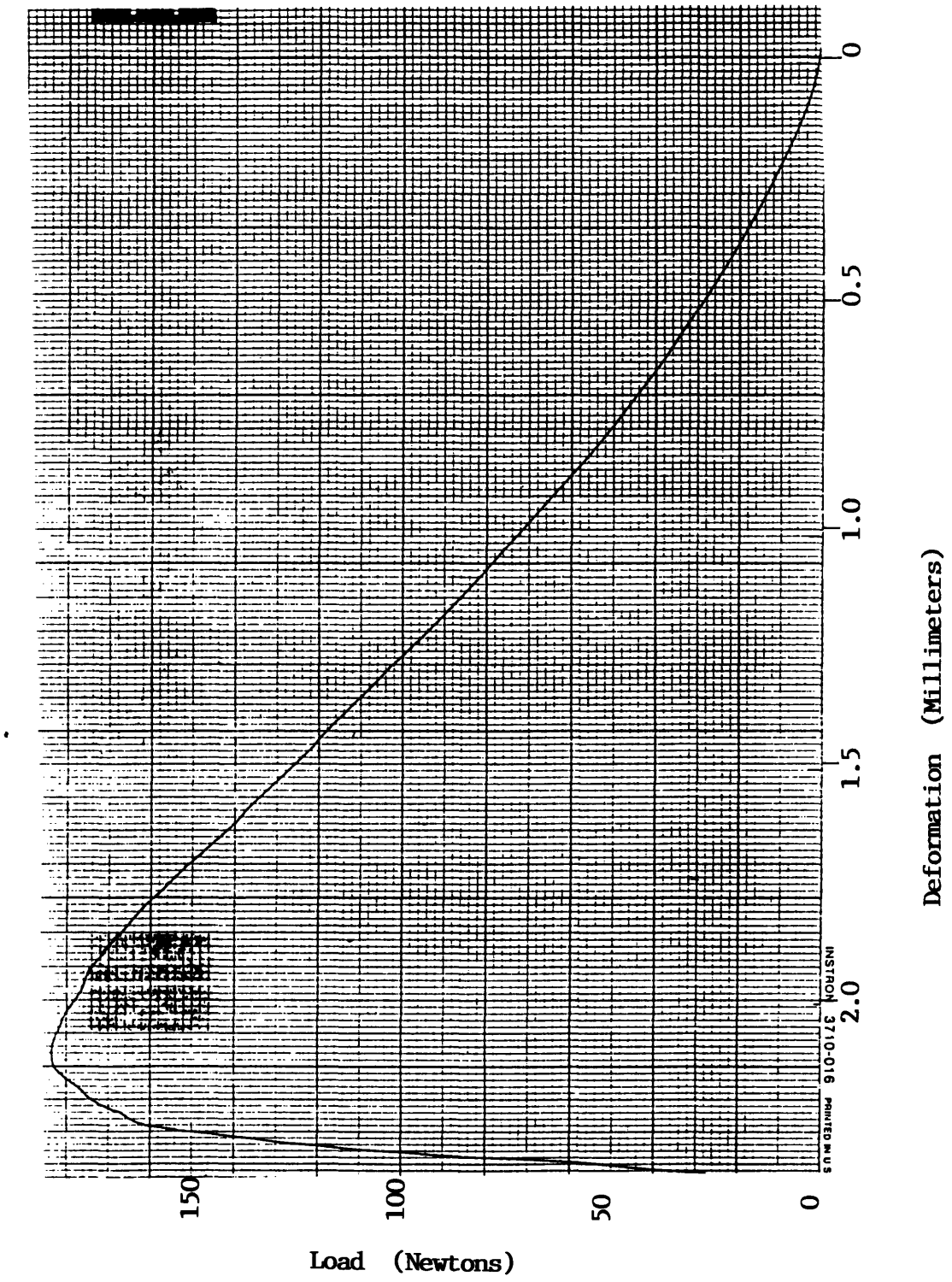

Typical Load-Deformation Curve from Compression Testing

Figure 4-2

Table 4-3

In Vitro Compressive Strengths and Moduli

Initial Values, Prior to Degradation

Experiment #	Strength, σ (MPa) ± s.d.	Modulus, γ (MPa) ± s.d.
Run #1	4.3 ± 0.9	38.6 ± 3.6
Run #2	10.6 ± 0.9	138.3 ± 5.4
Run #3	4.7 ± 1.1	58.0 ± 10.6
Run #4	14.2 ± 1.9	67.4 ± 7.5
Run #5	5.5 ± 0.9	25.3 ± 3.6
Run #6	1.5 ± 0.5	17.8 ± 5.3
Run #7	4.6 ± 0.4	25.8 ± 1.3
Run #8	1.3 ± 0.5	12.8 ± 2.8

Table 4-4

Main Effects of the Experimental Variables on Material Strength and Modulus

Initial Values, Prior to Degradation

Variable	Effect on Strength (MPa)	Effect on Modulus (MPa)
Presence of NaCl	+ 2.2	+ 22.1
Size of NaCl when present	+ 0.7	- 14.0
Amount of N-VP	- 5.2	- 55.2
Amount of β- TCP	- 1.0	+ 24.0
Molecular Weight of PPF	- 5.7	- 32.4

composites were on the order of 5 MegaPascals (MPa), a magnitude appropriate for consideration of the material as a temporary trabecular bone substitute.

The compressive strengths and moduli of the composite material after exposure to phosphate buffered saline solution at 37°C and pH = 7.4 for the six time periods studied appear in Table 4-5. The data appear graphically in Figure 4-3 for the strength vs. time relationship, and in Figure 4-4 for the modulus vs. time relationship. Figure 4-5 is a scanning electron micrograph of the surface of a specimen that had been in the phosphate buffered saline for one week. The irregularly shaped crevices are of the same magnitude as the sieved NaCl particles, and likely represent the sites from which the salt has leached out.

Table 4-5

Degradation Data for Composite in PBS over Twelve Weeks

Time in PBS	Strength (MPa)	Modulus, γ (MPa)	Diameter (mm)
3 days	9.1 ± 0.7	149 ± 21	5.6 ± .22
6 days	8.7 ± 2.4	156 ± 54	5.8 ± .14
2 weeks	11.1 ± 1.8	226 ± 46	5.6 ± .14
3 weeks	10.9 ± 1.8	241 ± 78	5.6 ± .10
4 weeks	20.9 ± 3.7	590 ± 150	5.6 ± .08
6 weeks	27.1 ± 4.1	690 ± 74	5.4 ± .09
8 weeks	17.3 ± 2.1	420 ± 82	5.6 ± .07
12 weeks	21.3 ± 0.4	696 ± 53	5.6 ± .08

Discussion

The in vitro mechanical strength results demonstrate that increasing the molecular weight of the PPF did not increase the compressive strength of the

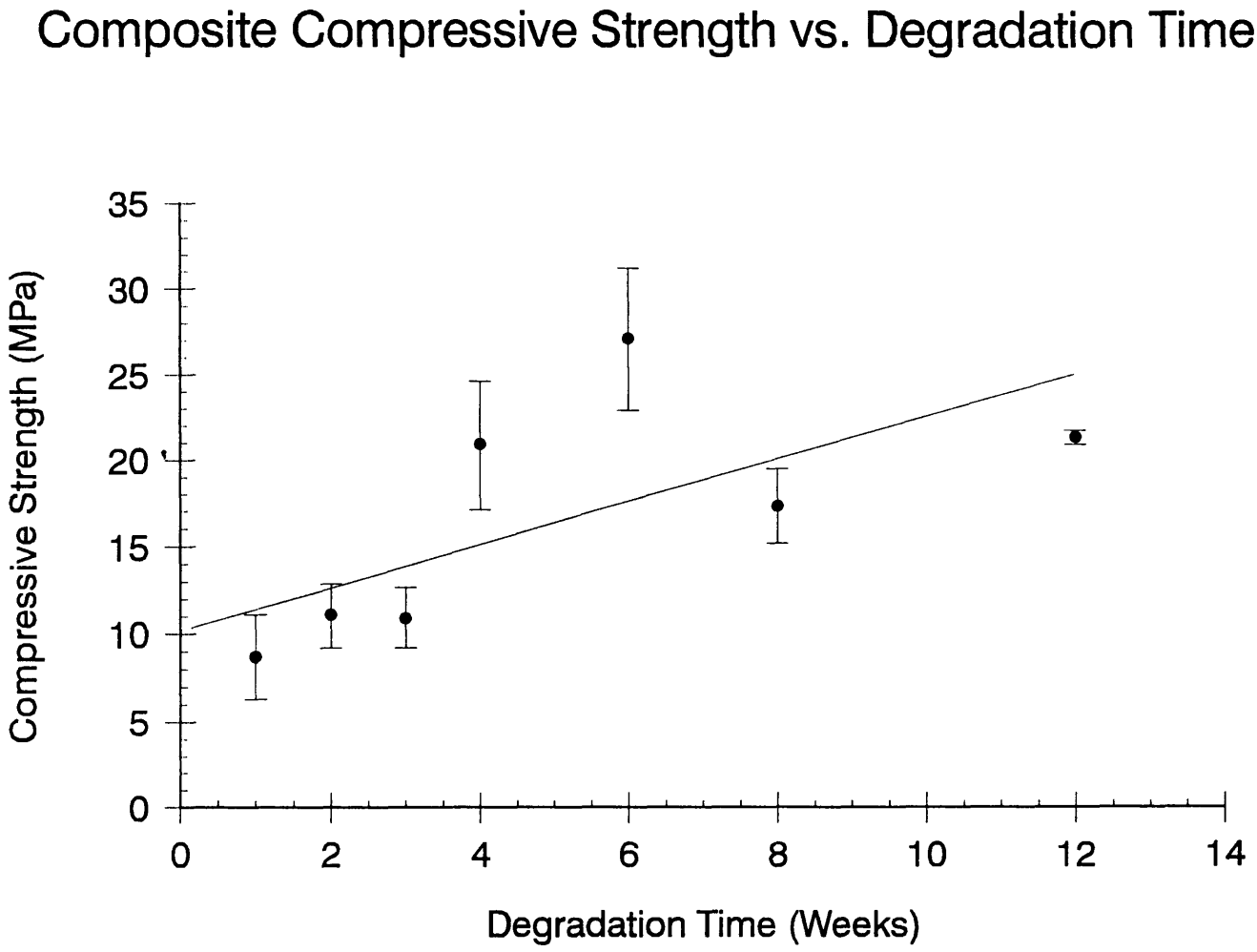

Graph of Composite Strength vs. Time for In Vitro Degradation

Figure 4-3

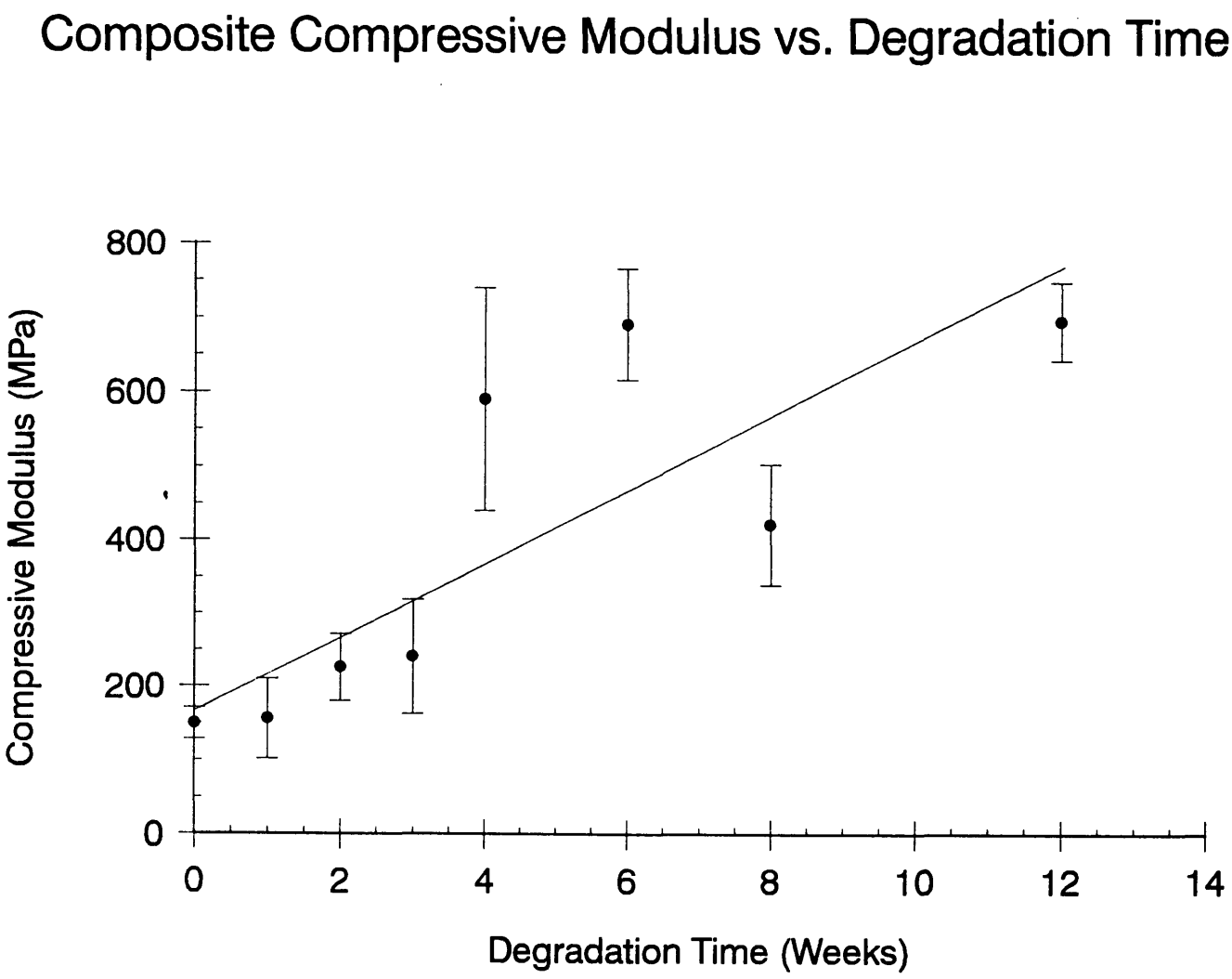

Graph of Composite Modulus vs. Time for In Vitro Degradation

Figure 4-4

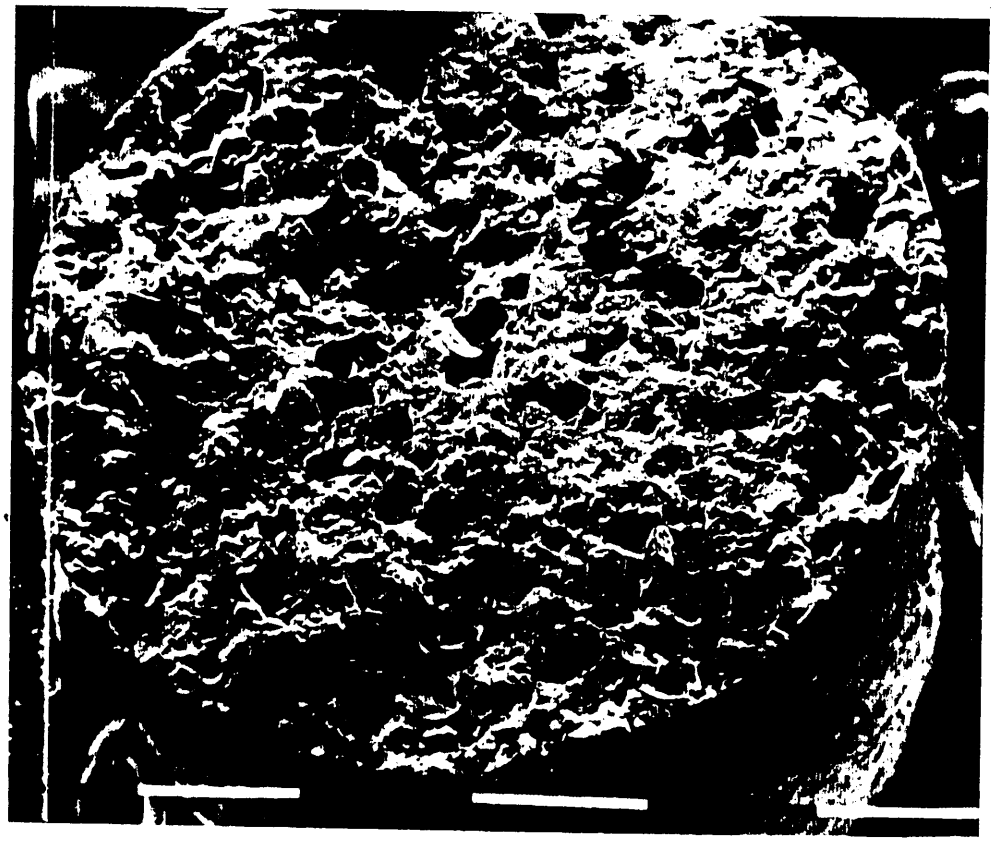

Scanning Electron Micrograph of In Vitro Degradation Specimen

Figure 4-5

composite material that is based upon the PPF. Since, in general, the mechanical properties of polymers improve with increasing molecular weight, this result is not obvious at first glance. However, the mechanical properties in question here are those of the composite material, not those of the base polymer. The compressive strength and modulus of the particulate composite are more likely to be affected by the nature and quantity of the cross links formed between the double bonds of the PPF and the N-vinylpyrrolidone, and less dependant upon the molecular weight of the PPF. One possible explanation for the inverse relationship between PPF molecular weight and composite strength is that the lower molecular weight polymer has a conformation such that its molecular size is smaller than that of the larger molecular weight polymer. Thus, a given weight of the lower molecular weight polymer would contain a larger number of molecules than an equal weight of the higher molecular weight polymer. The greater number of molecules per given weight would manifest itself as a larger surface area per mass. This could expose more potential crosslinking sites (i.e. fumarate double bonds) at the polymer surface in the case of the lower molecular weight PPF compared to the higher molecular weight PPF, and account for the observed strengths..

The NaCl was included in the composite formulation with the intent that it would leach out in the body's aqueous environment, and thus create an initial porosity into which granulation tissue and new bone could grow. Therefore, if the NaCl has the effect of acting as a filler to increase the initial mechanical strength, as demonstrated in this study, that increase may be short lived as the salt leaches out.

The specimen diameter decreased over the first several days in phosphate buffered saline, and then remained essentially constant for the remainder of the study. The scanning electron micrograph in Figure 4-5 shows crevices in the specimen, but there is no evidence that an interconnected porous network

develops. The maintenance of specimen diameter raises the question of whether the composite degrades in this *in vitro* simulated physiologic environment. As will be shown in the next chapter, there is clear evidence that the composite degrades *in vivo* in a rat model. The polymer may degrade *in vitro* over a longer time span than it does *in vivo*. Such a difference would suggest that enzymatic mechanisms *in vivo* supplement the hydrolytic degradation of the ester linkages.

The modulus increases steadily over the course of the twelve weeks. This phenomenon can be explained by postulating that ester linkages hydrolyze, PPF chains become shorter, and the shortened chains function as a filler that increases the composite modulus. The trend of strength increase over the twelve weeks may suggest that crosslinking continues to occur between PPF fumarate units and poly (vinylpyrrolidone) chains. This observation will be investigated by performing high performance liquid chromatography analysis of the phosphate buffered saline at intervals during composite degradation to determine the products of the degradation process. In addition, dynamic swelling experiments will be done to characterize the change of the crosslink density with time. The degradation will be allowed to continue longer than twelve weeks to assess whether, and over what time period, the specimens will decrease in size.

Conclusions

1. The composite material's initial compressive strength and modulus *in vitro* are of a magnitude appropriate for consideration as a temporary replacement for human trabecular bone.

2. The composite material's compressive strength and modulus maintain the above referenced appropriate magnitude in a simulated physiologic environment for twelve weeks.

CHAPTER 5

The Ingrowth of New Bone Tissue and Initial Mechanical Properties of a Degrading Polymeric Composite Scaffold.

Introduction

The motivation for temporary bone replacement is to exploit bone's inherent self healing ability by developing a material that can provide structural support to a region of the skeleton and be biocompatible, degrading in a controlled fashion into non-toxic substances that the body can eliminate via normal metabolic pathways. The data presented in Chapter 4 demonstrated that a particulate composite based on PPF attains a strength and modulus that are appropriate to perform the mechanical function of trabecular bone. The material's strength and modulus were maintained over twelve weeks in a simulated physiologic environment. The work presented in this chapter addresses two questions: will the composite material degrade in vivo, and will new bone occur in a skeletal defect that is reconstructed with the material? In addition, the histologic evaluation of the specimens will give information concerning the presence or absence of a local inflammatory response to the material, and thus an estimate of its short term biocompatibility. One of the concerns regarding the current nondegradable Orthopaedic bone cement, poly (methylmethacrylate), is that it lowers the infection threshold of the region into which it is placed[69,70]. The assessment of a new material's propensity to incite inflammation at an

implantation site is of significant interest to the clinician. A synthetic material, regardless of its level of biocompatibility, functions as a foreign body and excludes the host's infection fighting system from accessing the region in which it resides. The eventual disappearance of a temporary replacement material, and the reconstitution of the implantation site with normal host tissue is an attractive feature of biodegradable reconstruction materials.

Materials and Methods

The experimental design separates the *in vivo* work into two parts. In the first *in vivo* part of the study, five variables for the composite material formulation were examined in a two level fractional factorial design. This is the same design that was used for the assessment of *in vitro* mechanical properties in Chapter 4. The variables in the experimental design are: 1) the molecular weight of the PPF, 2) the ratio of the amount of sodium chloride (in grams) to the amount of PPF, 3) the particle size range of the sodium chloride, 4) the ratio of the amount of β-tricalcium phosphate (in grams) to the amount of PPF, and 5) the ratio of the amount of N-VP (in grams) to the amount of PPF. The low and high levels of the variables appear in Table 4-1. The fractional factorial design based on these variables appears in Table 4-2. Each batch of the composite material was formulated on a basis of 4 grams of PPF. In addition to the components which varied according to the experimental design, each formulation also contains a radical polymerization initiator, benzoyl peroxide (Sigma, St. Louis, MO), and an accelerator (N,N-dimethyl para-toluidine) (DMT) (Sigma, St. Louis, MO). Those formulations that contained the "high" amount of N-vinylpyrrolidone received 0.18 grams of benzoyl peroxide and 18 μl of DMT. The formulations that contained the "low" amount of N-vinylpyrrolidone received 0.12 grams of benzoyl peroxide and 12 μl of DMT. These are the same amounts of initiator and

accelerator that were used in the *in vitro* study of Chapter 4.

These material formulations were placed in a rat proximal tibial model, and were all harvested at four weeks post surgery. The rat surgery was reviewed and approved by the appropriate institutional animal use and care committee. Humane treatment of these experimental animals in accordance with NIH guidelines was observed at all times.

The model involves anesthetizing a 250-500 gram Sprague-Dawley rat via inhalational methoxyflurane (Metofane®, 100%, Pittman-Moore Co.), shaving the lower extremity, prepping it with Betadine, and draping it into a sterile surgical field. No preoperative antibiotics are given[71]. The surgeon then makes a medial surgical approach to the proximal tibia and exposes it subperiosteally. A 2 mm drill hole is made through the medial cortex and trabecular bone of the proximal tibia. The hole does not continue through the lateral cortex. The hole is made approximately 3-4 mm distal to the physeal scar of the proximal tibia and the long axis of the drill hole is perpendicular to the long axis of the tibia. This model has been used successfully to test bone replacement materials for Orthopaedic applications[72]. The specimen for implantation has either been prepolymerized in a Teflon mold, or is polymerized at surgery within the bony defect in the rat tibia. The prepolymerized specimens are right circular cylinders that have a diameter of 2 mm and a height of 4 mm. Each formulation was placed in rat tibiae two ways: previously polymerized cylinders and polymerization in situ within the bony defect. We added this in situ polymerization portion to the study in order to assess whether the handling properties and histologic characteristics of the composite material would be affected by employing an implantation technique that more closely approximates actual surgical conditions. The components of the composite material that were polymerized in situ were sterilized by exposure to ultraviolet radiation for 12 hours. Each preparation method (prepolymerized or in situ) of each formulation

was placed into two rats. Therefore, part one of the study used 32 rats. The different formulations were evaluated for handling properties at surgery, bone ingrowth on histologic cross-sections, and for the extent, if any, of an inflammatory response. Representative histologic sections from part one of this study appear in Figures 5-2 and 5-3.

The second *in vivo* part of the study used the best formulation from part one (based on handling properties during polymerization and ingrowth on histologic examination), and specimens made from this formulation were placed into rat proximal tibiae. The formulation appears in Figure 5-1. The specimens

Recipe for Part Two of Study: Ingrowth vs. Time

4 grams PPF
6 grams N-vinylpyrrolidone
6 grams β - Tricalcium Phosphate
0.18 grams Benzoyl Peroxide
6 μl Dimethyltoluidine

Figure 5-1

from part two of the study were harvested at 1 day, 3 days, 1 week, 2 weeks, 4 weeks, and 5 weeks post implantation. The histologic sections from the ingrowth vs. time implantations appear in Figures 5-4, 5-5, 5-6, and 5-7. There were 22 rats used in this part of the study. Nine rats had prepolymerized specimens implanted, and nine rats had the material polymerized in situ. We desired one rat per time period, and chose the quantity nine per group to mitigate against unexpected deaths as the longer time periods were approached. The observable quantities

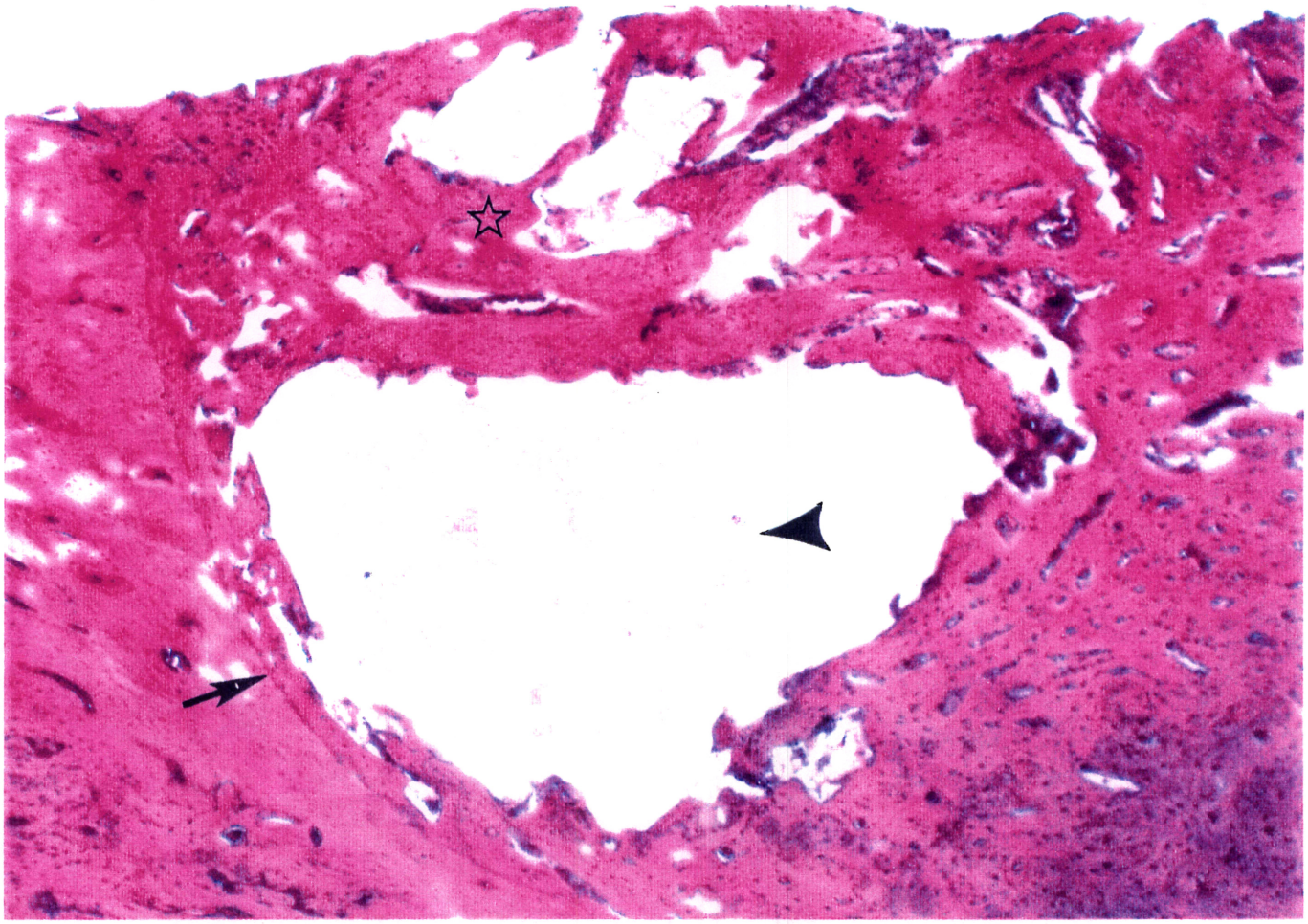

Low power hematoxylin and eosin stained specimen at four weeks from rat in part one of study, demonstrating bone ingrowth into tibial defect previously filled by composite material. Arrow points to junction between newly formed woven bone and previously existing host bone. Arrowhead points to degrading polymer. Star overlies region of new bone surrounding degrading polymer. Original magnification is 2.5

Figure 5-2

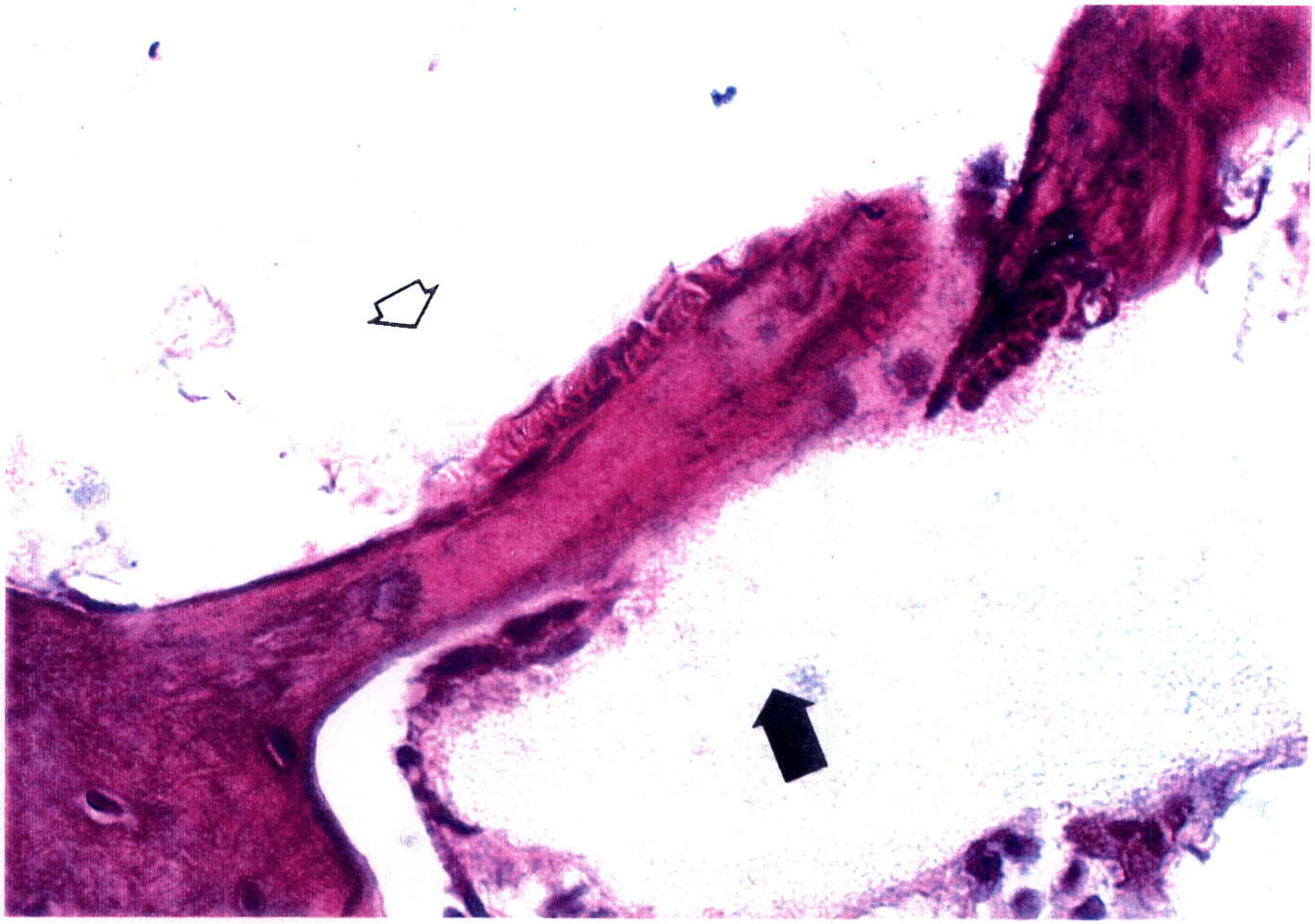

High power view of same section as Figure 5-2, demonstrating trabeculum of woven bone in close apposition to polymer (solid arrow) and β-TCP (open arrow). Original magnification is 10.

Figure 5-3

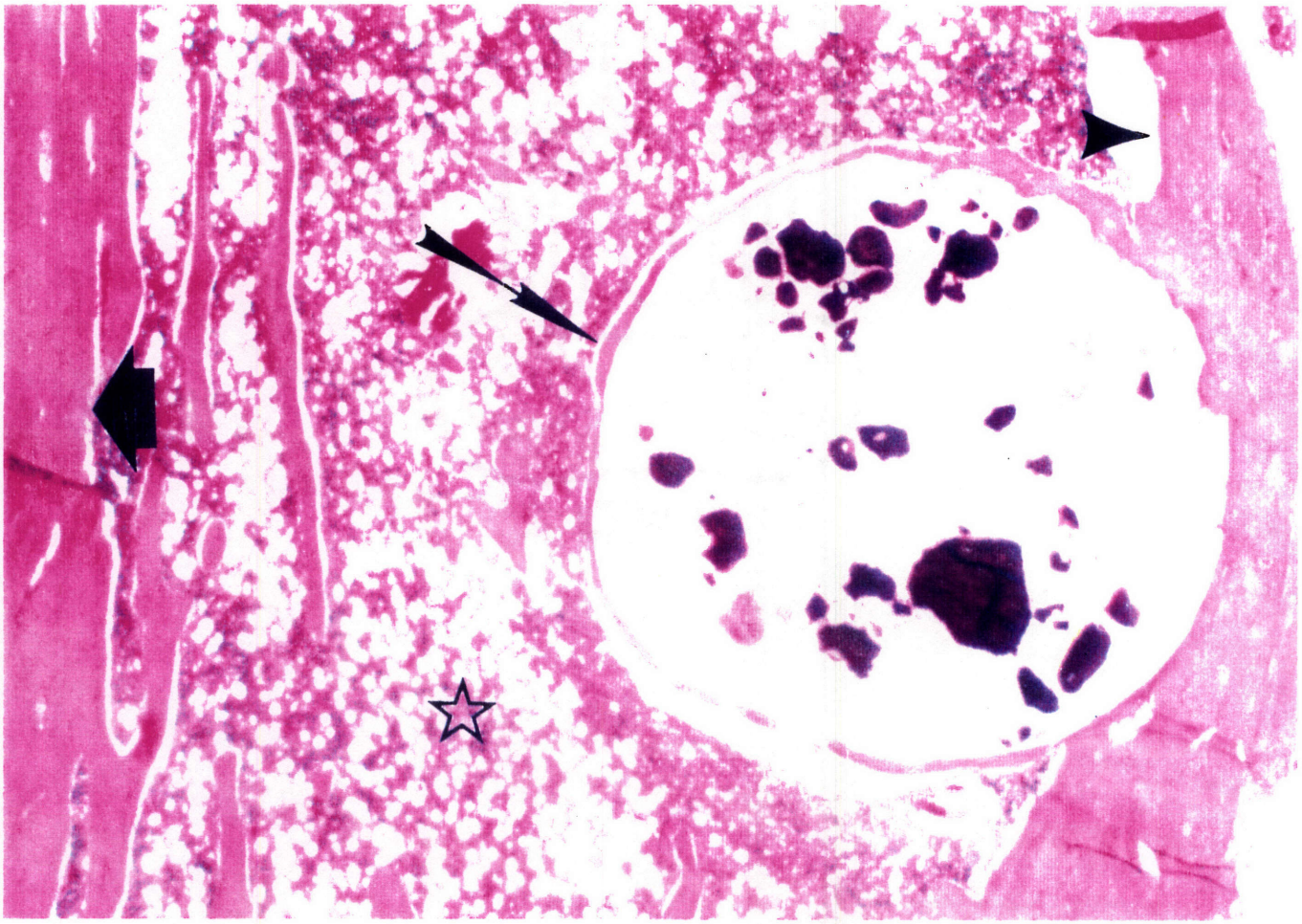

Hematoxylin and eosin stained section from rat in part two of the study to demonstrate surgical anatomy. Anterior tibial cortex (wide arrow), posterior tibial cortex (arrowhead), marrow elements (star), boundary of original 2mm diameter defect (narrow arrow). Plane of section is parallel to long axis of tibia. Original magnification is 1.6.

Figure 5-4

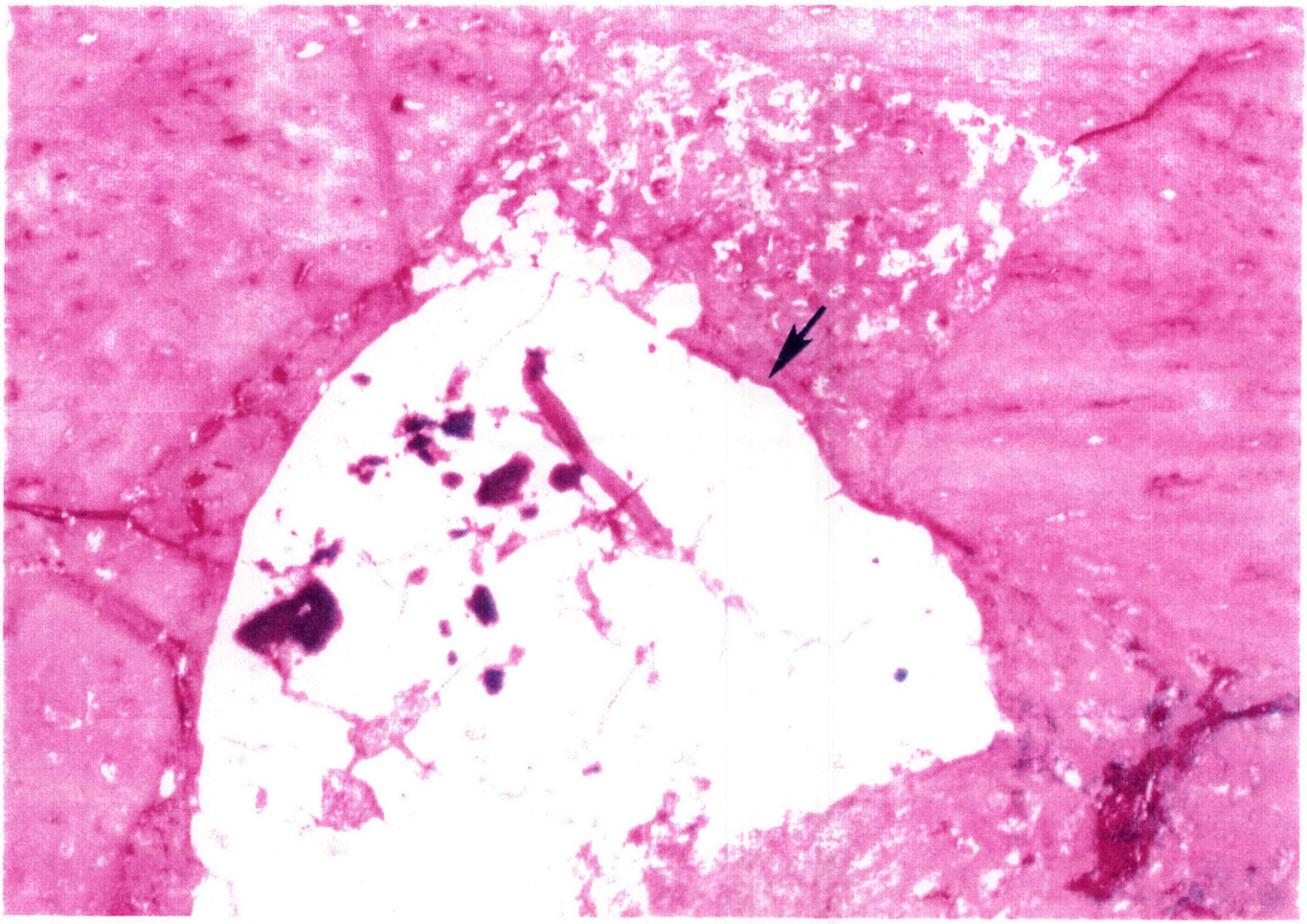

Hematoxylin and eosin stained section from part two of the study, 1 week post implantation. Arrow points to advancing edge of new bone. Original magnification is 4

Figure 5-5

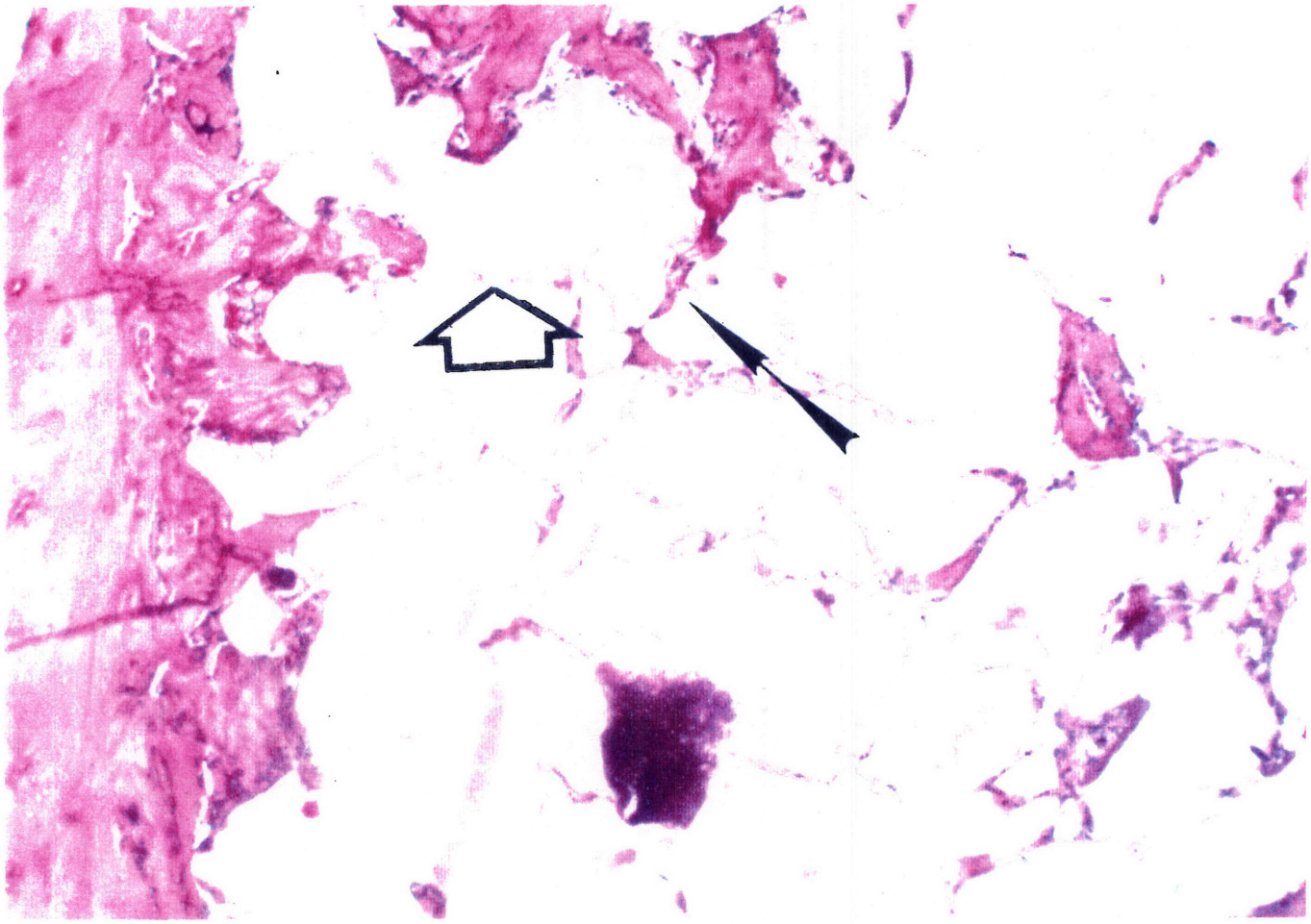

Same formulation and stain as Figure 5-5; specimen is 2 weeks post implantation. Original magnification is 10. Trabeculae of woven bone (solid arrow) have ingrown between degrading composite material (open arrow).

Figure 5-6

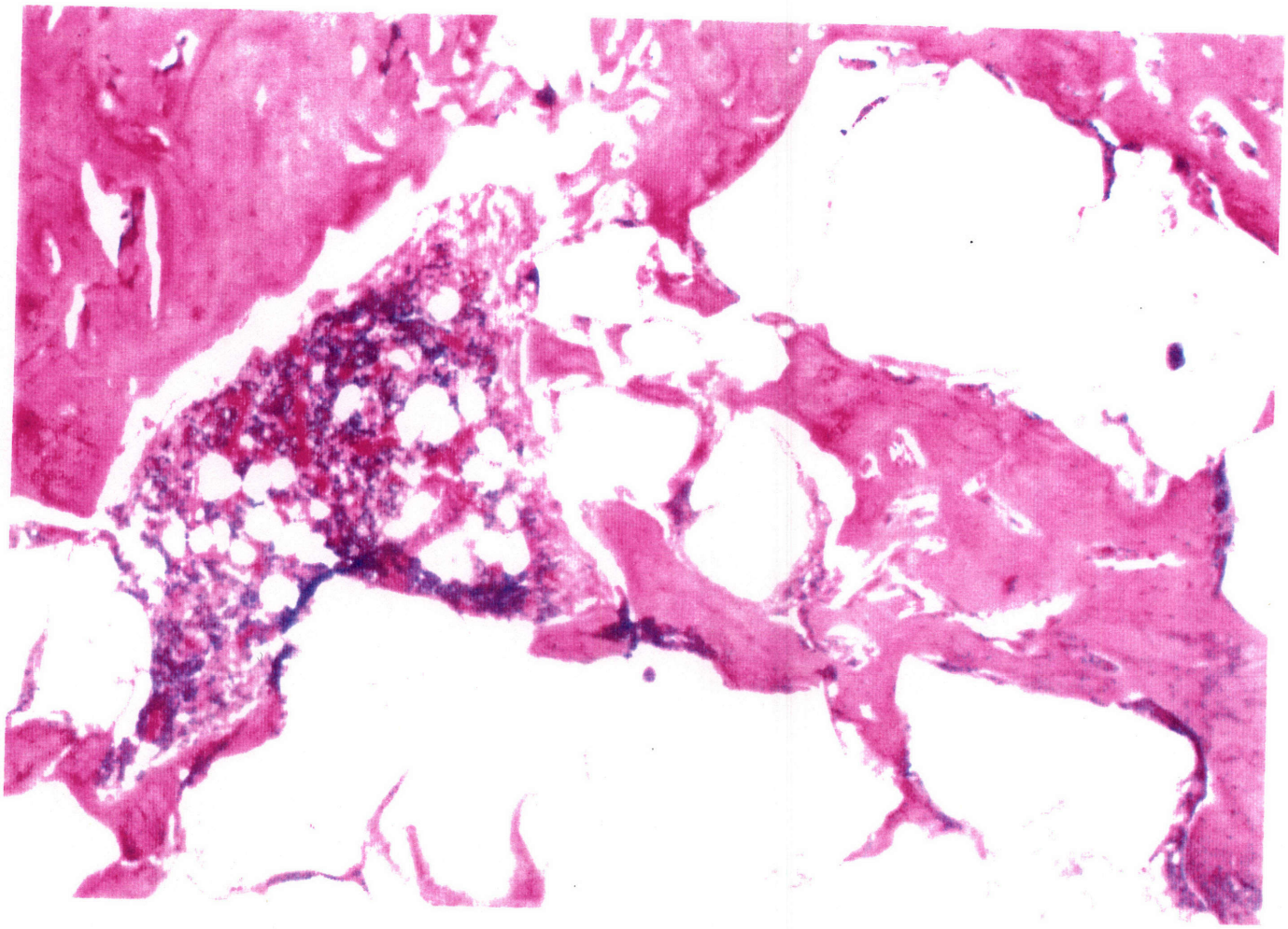

Same formulation and stain as Figure 5-5; specimen is 5 weeks post implantation. Original magnification is 10. New woven bone in intimate approximation to degrading material

Figure 5-7

were the same in this part of the study as they were in part one: material handling properties, histologic assessment of material degradation and bone ingrowth, and histologic evaluation of the composite's overall biocompatibility. One additional rat was added to the 3 day, 1 week, 2 week, and 4 week time groups to serve as a control for normal fracture healing of this bony defect. These rats had the same approach and 2 mm defect made in their proximal tibiae, but nothing was placed into the defect. There were 4 control rats.

The rats were euthanized at the appropriate time post surgery via administration of methoxyflurane inhalational anesthesia followed by guillotine decapitation. The entire tibia was harvested, cleaned of all soft tissues, and placed in 10% neutral buffered formalin. The tibiae were then placed in decalcification solution (TBD-2®, Shandon Instruments, Sewickley, PA) for 72 hours, dehydrated in a series of increasing concentrations of ethanol solution, embedded in paraffin, sectioned on a microtome parallel to the circular cross section of the cylindrical tibial defect, and stained with hematoxylin and eosin. Several sections were also prepared with a Von Kossa stain to assess the presence and distribution of residual calcific deposits within the experimental cross sectional area.

Results

The rats from part one of this study were all euthanized at four weeks post surgery. The different formulations of the material varied in their handling properties for the in situ polymerizations. Runs #2, 3, 6, and 7 handled well. That is, the components formed a homogeneous mass upon mixing, increased their viscosity with time such that the polymerizing mixture could be inserted into the bony defect, and hardened on the order of 5 - 10 minutes post mixing. The other formulations did not handle well. They either did not harden by 20 minutes, or they did not form a homogeneous mass that could be handled without crumbling

and loss of particulates.

Histologic analysis showed that the formulation with the most extensive bone ingrowth at 4 weeks was Run #7. Representative hematoxylin and eosin sections of this formulation appeared in Figures 5-2 and 5-3. Therefore, since this formulation also demonstrated good handling properties, and had an acceptable initial strength and modulus, we chose it as the formulation for the ingrowth vs. time experiment in part two of the *in vivo* study.

The histologic sections from the ingrowth vs. time implantations appeared in Figures 5-4, 5-5, 5-6, and 5-7. There is progressively more of the cross section occupied by bone as the implantation time increases from 1 day to 5 weeks post surgery. The new bone is woven bone histologically, and the junction between the woven bone and older lamellar bone can be seen at the margins of the circular cross section originally occupied by the implant material. There is intimate incorporation of the implant into the host bone defect created at surgery. The light staining irregularly shaped areas in the hematoxlyn and eosin sections demonstrate strong staining affinity with the Von Kossa preparation. This indicates that they contain calcium, and likely represent the β- TCP. There is an absence of acute inflammatory cells in the vicinity of the implant. Osteoblasts, osteoid, and new woven bone are in close apposition to the degrading material without evidence of an acute or other adverse pathologic inflammatory response. This situation existed in all the specimens retrieved, and suggests that the material's biocompatibility is good in the short term.

The general nature of the new bone formation bears mentioning. The areas of the implant closest to its outer circumference appear to be replaced before there is bone in the interior of the implant, and the interior areas of the implant become progressively more infiltrated with trabeculae of woven bone as time progresses. The replacement of the material by bone appears to progress from the peripheral surface towards the center of the circular cross section. The control rats had an

organizing hematoma in the cylindrical defect by three days, a combination of cartilage and woven bone at 1 week, and had essentially filled the defect with new bone by 2 -3 weeks.

Discussion

The control rats had the entire cross section of the tibial defect filled with an organizing hematoma at three days post surgery, and by the end of 2 - 3 weeks the defects were completely filled with new bone. This model, therefore, is not a model to determine whether or not a defect will heal in the presence of this material, but a model to assess the interplay between degrading material and host in a weight bearing location. The rats all appeared to demonstrate normal use of their operated leg. They walked and climbed in their cages without preference to operated vs. nonoperated hindlimb. We would have expected no change in the appearance of the defect if it were filled with the non-degradable bone cement poly (methylmethacrylate). The defects in this study, however, did change over the four weeks of the first part of the study, and over the five weeks of the second part of the study. The outer margins of the composite gradually receded, and new bone appeared in their place. The material throughout the cross section of the defect became infiltrated with fingerlike trabeculae of new woven bone as time passed. The material was not responsible for the bone formation, but it degraded in vivo, and it produced no foreign body inflammatory response to hinder the normal process of fracture repair. In the future, delivery of bioactive molecules from the material or delivery of osteoblasts and osteoid cultured on the material may enhance bone growth in a surgical site where it would otherwise not occur.

The relatively greater degradation from the surface region compared to the interior of the specimen is encouraging for the following reason. In its intended use, this material will need to provide a reconstructed skeletal region with

adequate mechanical properties from the time of surgery, through the time that the material degrades and the region reconstitutes itself with new bone, and until the new bone provides the required mechanical strength. A material that degrades uniformly throughout its volume may be more likely to exhibit a decrease in mechanical properties since new bone must work its way into the interior from cellular elements near the surface, leaving part of the interior degraded but not yet filled with new bone. In addition, this would initially be mechanically weaker woven bone as opposed to lamellar bone. Alternatively, a material that recedes from its surface and has bone continually advance against that surface may allow the remaining bulk of non-degraded material farther from the surface to retain its mechanical properties and provide strength to the reconstructed region. An alternative to this scenario would be osteoblast transplantation and culture throughout the replacement material prior to insertion of that material into the surgical site[58].

The in vivo studies in a rat proximal tibia model demonstrated progressive growth of new bone against the receding surface of the degrading material, and ingrowth of new bone trabeculae into the interior of the degrading specimen. The specimen was also well integrated with the surrounding bone, with no internal fibrosis. There was an absence of a foreign body inflammatory response to the presence of this material over a five week time span. This material may thus be an attractive candidate for temporary replacement of trabecular bone, facilitating both osteoconduction and osteoinduction

Conclusions

1. This composite material, based on the linear polyester poly (propylene-fumarate), has handling properties at surgery that are similar in quality and in hardening time to the widely used nondegradable Orthopaedic bone cement poly (methylmethacrylate).

2. The short term biocompatibility of this composite material appears to be good, as evidenced by the absence of an acute foreign body inflammatory response to its presence in these experimental animals.

3. The composite material, placed in the rat proximal tibial model, demonstrates progressive replacement of the degrading material with woven bone from the periphery towards the center over five weeks.

CHAPTER 6

Future Work on Synthetic Strategies Toward Autologous Bone Regeneration.

The currently ongoing aspects of this work involve refinement of the polymer synthesis reaction. The monomer ratios, monomer addition rates, and reaction times are being investigated with the goal of removing all residual chlorine. The addition of evolved gas analysis capability to our laboratory's FTIR instrument will permit the identification of gaseous state reaction products in real time. Thus, the IR gas cell will be placed in front of the condenser for future synthesis runs, and the nature of the reaction products will be compared to the expected species as the polymerization proceeds.

The product polymer, PPF, will undergo further characterization. The trimer and polymer have been analyzed by light scattering, elemental analysis, FTIR, size exclusion chromatography, and dilute solution viscometry. In addition, the trimer has been characterized by gas chromatography/mass spectrometry (GC/MS), and by both carbon and proton nuclear magnetic resonance spectroscopy (^{13}C-NMR and ^{1}H-NMR). The GC/MS, ^{13}C-NMR, and ^{1}H-NMR evaluations of the polymer are underway.

The PPF has several features that are attractive for its intended biologic use. These have been mentioned previously, and include the biocompatible nature of its component monomers, the fumarate double bond that permits subsequent cross linking, and the ester linkage that forms the basis of its biodegradation. We have been investigating several other polymers that either have been used biologically or show promise for such use. Examples of these polymers include

poly (L-lactic acid) (PLLA), poly (glycolic acid) (PGA), poly (lactic-co-glycolic acid) (PLGA), poly (ethylene oxide) (PEO), polydioxanone (PDS), and various polyimides. The PLLA, PGA, PLGA, and PDS polymers have been used successfully for many years as degradable surgical sutures. The PEO class has found use in blood circulation applications[73,74]. The polyimides have a double ring structure that confers rigidity to them. Experiments are currently in progress to copolymerize PPF with these classes of polymers, and to determine both the chemical and physical properties of the resulting materials. The goal is to produce materials that possess the attractive qualities of each polymer that is part of the copolymer. Preliminary results with PPF-PEO and PPF-PLGA are encouraging[63]. The target application for PPF-PEO is prophylaxis against post-angioplasty re-stenosis of coronary arterial disease. The copolymerization will attempt to exploit the anti-thrombotic properties of PEO with the ability of PPF to cross link in situ. This will be explored as a polymerizable, degradable stent for temporary stabilization of dilated arteries. The PPF-PLGA will be used for osteoblast attachment and migration studies. The PLGA has good osteoblast attachment properties, but does not possess mechanical properties consistent with temporary bone replacement applications[36,58]. The copolymerization of PLGA with PPF will attempt to exploit the good osteoblast attachment and migration characteristics of PLGA with the good mechanical property characteristics of PPF. Currently, our group uses rat calvarial osteoblasts for cell growth and attachment studies. Work is currently underway to use human osteoblasts for these studies. The proposed source of the human osteoblasts will be the femoral head of patients who undergo total hip arthroplasty. The femoral head is a source of abundant trabecular bone, and is discarded after the procedure that replaces its worn cartilage surface with a prosthesis. This proposal is currently working its way through the appropriate institutional review committees. It will need to pass critical review of issues related to informed consent and the removal of human tissue from the hospital to

the research laboratory. This is an important step, however, since the goal of our osteoblast transplantation program is to eliminate the immunologic problems associated with allograft. The strategy will be to harvest autograft osteoblasts, culture them on degradable polymer scaffolds in the laboratory, and implant the cell-polymer constructs back into the host.

The in vivo rat experiments that were completed in this work need to be scaled up to a larger animal model. The rat proximal tibial model is a good model to assess initial biocompatibility and ingrowth in a weight bearing location, but it is not a critical size defect. The rat proximal tibial 2 mm defect will repair itself in approximately two weeks time when left untreated. A critical size defect is one that will not heal without treatment in the lifetime of the animal. Work is in progress to evaluate our composite material in a goat model. The protocol has been reviewed and approved by the institutional animal use and care committee. The composite material will be placed in a cylindrical defect in the distal lateral metaphysis of a goat knee. The specimen will be inserted in a defect created with a jig attached to the lateral femur. The jig is a hole saw guide that has a metal extension which contains screw holes. The jig is attached to the lateral femur with screws, and a one centimeter diameter hole saw passes through the guide to remove bone and create the trabecular defect. The screws that attach the jig to the lateral femur are replaced in the femur after the jig is removed. They can then be used at necropsy to reposition the jig in the same location, and harvest the bony region that was reconstructed with the temporary composite material. This specimen will be analyzed by bone histomorphometry for number of bone trabeculae, width of bone trabeculae, and principal directionality of trabeculae[75]. The reconstructed region will be tested mechanically for compressive strength and modulus using the protocol described in Chapter 4.

The delivery of both drugs and bioactive molecules from this material will be explored. The sustained local delivery of antibiotics to a skeletal site would

represent an advantage over the current practice of formulating these antibiotics into nondegradable poly (methylmethacrylate) (PMMA) beads. The beads deliver the antibiotics from only the outer regions of the spherical bead, and must then be removed at a second operation. Experiments are now underway to evaluate the in vitro elution of several antibiotics from PPF and PPF-PEO polymers. The same PPF-PEO copolymers will be evaluated as delivery vehicles for both retroviruses and genetically engineered cells in an arterial stenosis model. In addition, plans are being made to assess the loading and delivery characteristics of bone morphogenetic protein-2 (BMP-2) from PPF and a composite material that contains PPF. The biologic activity of BMP-2 under conditions of loading into a degradable polymer and sustained delivery from that polymer will need to be assessed. If the BMP-2 retains its activity, then it may serve to direct bone formation in locations where the composite material degrades and exposes the BMP.

There is one further area of planned future studies that should be discussed here. The intended use of the degradable composite material described in this thesis will be to provide temporary mechanical strength and conditions for new bone growth into a skeletal region deficient in trabecular bone. This use will require compressive strength and modulus similar to trabecular bone. This material will not be required to resist tensile or shear forces. The extension of this work to include temporary replacement of compact bone will require the consideration of both tensile and shear forces. In addition, structures of various shapes will need to be fabricated to replace various anatomic parts of the skeleton that contain compact bone. Copolymerization experiments are underway to form poly (ester-co-imides), with the expectation of exploiting the rigid planar imide linkage as a source of increased strength. The in vitro growth of osteoblasts onto these new polymers is being explored. The goal will be a composite material with a desired shape that contains viable autologous osteoblasts, so that the cell-

polymer construct can be implanted in the deficient location. The desired end result, as it is in this work, will be to replace the degrading implant with new host bone that can then remodel along lines of local stress. The synthetic parts of the construct should degrade and be excreted or metabolized by the body.

References

1. Senn N: "On the Healing of Aseptic Cavities by Implantation of Antiseptic Decalcified Bone." Am J Med Sci, 219, 1889.
2. Meek'ren JJV: " Observations Medico-Chirurgicae. Amsterdam: H & T Boon; p.6, 1632.
3. Bertram JE, Swartz SM: "The 'Law of Bone Transformation': A Case of Crying Wolff?" Biol Review 66:245-73, 1991.
4. Lane JM, Sandhu HS: "Current Approaches to Experimental Bone Grafting." Orthop Clin North Am 18:213-25, 1987.
5. Chase SW, Herndon CH: "The Fate of Autogenous and Homogenous Bone Grafts, a historical review." J Bone Joint Surg 37-A:809-41, 1955.
6. Gross TP, Cox QGN, Jinnah RH: "History and Current Application of Bone Transplantation." Orthopedics 16:895-900, 1993.
7. Prolo DJ, Rodrigo JJ: "Contemporary Bone Graft Physiology and Surgery." Clin Orthop Rel Res 200:322-42, 1985.
8. Barth A: "Die Entstehung und das Wachstum der freien Gelenkkorper. Eine histologisch-klinische Studie." (The formation and growth of free joints. A histological-clinical study.) Arch f Klin Chir 56:507-73, 1898.
9. Phemister DB: "The Fate of Transplanted Bone and Regenerative Power of its Various Constituents." Surg Gynec Obstet 19:303-33, 1914.
10. Levander G: "A Study of Bone Regeneration." Surg Gynec Obstet 67:705-14, 1938.
11. Urist MR: "Bone: Formation by Autoinduction." Science 150:893-9, 1965.
12. Wozney JM: "Bone Morphogenetic Proteins." Prog Growth Factor Res 1:267-80, 1989.

13. Wang EA, Rosen V, D'Alessandro JS, et al.: "Recombinant Human Bone Morphogenetic Protein Induces Bone Formation." Proc Nat Acad Sci USA 87:2220-4, 1990.
14. Hollinger J: "Strategies for Regenerating Bone of the Craniofacial Complex." Bone 14:575-80, 1993.
15. Vacanti JP: "Beyond Transplantation." Archives of Surgery 123:545-9, 1988.
16. Gibson LJ: "The Mechanical Behavior of Cancellous Bone." J Biomech 18:317-28, 1985.
17. Burchardt H: "Biology of Bone Transplantation." Orthop Clin North Am 18:187-96, 1987.
18. Buckwalter JA, Cruess RL: *in* Fractures in Adults. Rockwood CA, Green DP, and Bucholz RW, editors, 3rd ed. Philadelphia: J.B. Lippincott, 1991; pp. 181-222.
19. White III AA, Panjabi MM, Southwick WO: "The Four Biomechanical Stages of Fracture Repair." J Bone Joint Surg 59-A:188-92, 1977.
20. Ogden JA: *in* Skeletal Injury in the Child. JA Ogden, editor, Philadelphia: W.B. Saunders, 1990; pp. 23-64.
21. Heiple KG, Goldberg VM, Powell AE, Bos GD, Zika JM: "Biology of Cancellous Bone Grafts." Orthop Clin North Am 18:179-85, 1987.
22. Hayes WC: *in* Basic Orthopaedic Biomechanics. VC Mow, WC Hayes, editors, New York: Raven Press, 1991; pp. 93-142.
23. Cowin SC: *in* Bone Mechanics. Cowin SC, editor, Boca Raton: CRC Press, 1989; pp. 97-127.
24. Cowin SC: *in* Bone Mechanics. Cowin SC, editor, Boca Raton: CRC Press, 1989; pp. 129-57.
25. Goldstein SA, Wilson DL, Sonstegard DA, Matthews LS: "The Mechanical Properties of Human Tibial Trabecular Bone as a Function of Metaphyseal Location." J Biomech 16:965, 1983.

26. Gerhart TN, Renshaw AA, Miller RL, Noecker RJ, Hayes WC: "In Vivo Histologic and Biomechanical Characterization of a Biodegradable Particulate Composite Bone Cement." J Biomed Mat Res 23:1-16, 1989.
27. Uchida A, Nade S, McCartney E, Ching W: "Bone Ingrowth into Three Different Porous Ceramics Implanted into the Tibia of Rats and Rabbits." J Orthop Res 3:65-77, 1985.
28. Iyoda K, Miura T, Nogami H: "Repair of Bone Defect with Cultured Chondrocytes Bound to Hydroxyapatite." Clin Orthop Rel Res 288:287-93, 1993.
29. Miyamoto S, Takaoka K: "Bone Induction and Bone Repair by Composites of Bone Morphogenetic Protein and Biodegradable Synthetic Polymers." Annales Chirurgiae et Gynaecologiae 82:69-75, 1993.
30. Holmes RE, Bucholz RW, Mooney V: "Porous Hydroxyapatite as a Bone Graft Substitute in Diaphyseal Defects: A Histometric Study." J Orthop Res 5:114-21, 1987.
31. Ripamonti U, Ma S, Cunningham NS, Yeates L, Reddi AH: "Initiation of Bone Regeneration in Adult Baboons by Osteogenin, a Bone Morphogenetic Protein." Matrix 12:369-80, 1992.
32. Ripamonti U: "Delivery System for Bone Morphogenetic Proteins. A Summary of Experimental Studies in Primate Models." Annales Chirurgiae et Gynaecologiae 82:13-24, 1993.
33. Hollinger JO, Kleinschmidt JC: "The Critical Size Defect as an Experimental Model to Test Bone Repair Materials." J Craniofacial Surg 1:60-8, 1990.
34. Thomson RC, Yaszemski MJ, Powers JM, Mikos AG: "Fabrication of Biodegradable Polymer Scaffolds to Engineer Trabecular Bone." J Biomat Sci, Polymer Ed, *in press.*

35. Thomson RC, Yaszemski MJ, Powers JM, and Mikos, AG: "A Novel Biodegradable Poly (Lactic-co-Glycolic Acid) Foam for Bone Regeneration." *in* Biomaterials for Drug and Cell Delivery. Mikos AG, Murphy RM, Bernstein H, and Peppas NA, editors, Pittsburgh: Materials Research Society, 1994; pp. 33-40.

36. Thomson RC, Wake MC, Yaszemski MJ, Mikos AG: "Biodegradable Polymer Scaffolds to Regenerate Organs." Advances in Polymer Science. Peppas NA, and Langer RS, eds., *in press.*

37. Nichter LS, Yazdi M, Kosari K, Sridjaja R, Ebramzadeh E, Nimni ME: Demineralized Bone Matrix/Polydioxanone Composite as a Substitute for Bone Graft: A Comparative Study in Rats." J Craniofacial Surg 3:63-9, 1992.

38. Solheim E, Pinholt EM, Bang G, Sudmann E: "Regeneration of Calvarial Defects by a Composite of Bioerodible Polyorthoester and Demineralized Bone in Rats." J Neurosurg 76:275-9, 1992.

39. Mathiowitz E, Amato C, Langer R: "Polyanhydride Microspheres: 3. Morphology and Characterization of Systems Made by Solvent Removal." Polymer 31:547-55, 1990.

40. Nielsen FF, Karring T, Gogolewski S: "Biodegradable Guide for Bone Regeneration: Polyurethane Membranes Tested in Rabbit Radius Defects." Acta Orthop Scand 63:66-9, 1992.

41. Pajamaki KJJ, Andersson OH, Lindholm TS, Karlsson KH, Yli-Urpo A: "Induction of New Bone by Allogeneic Demineralized Bone Matrix Combined to Bioactive Glass Composite in the Rat." Annales Chirurgiae et Gynaecologiae 82:137-44, 1993.

42. Gerhart TN, Miller RL, Kleshinski SJ, Hayes WC: "In Vitro Characterization and Biomechanical Optimization of a Biodegradable Particulate Composite Bone Cement." J Biomed Mat Res 22:1071-82, 1988.

43. Gerhart TN, Roux RD, Horowitz G, Miller RL, Hanff P, Hayes WC: "Antibiotic Release From an Experimental Biodegradable Bone Cement." J Orthop Res 6:585-92, 1988.

44. Yaszemski MJ, Mikos AG, Payne RG, and Hayes WC: "Biodegradable Polymer Composites for Temporary Replacement of Trabecular Bone: The Effect of Polymer Molecular Weight on Composite Strength and Modulus." *in* Biomaterials for Drug and Cell Delivery. Mikos AG, Murphy RM, Bernstein H, and Peppas NA, editors, Pittsburgh: Materials Research Society, 1993; pp. 251-6.

45. Yaszemski MJ, Payne RG, Hayes WC, Langer RS, Aufdemorte TB, Mikos AG: "The Ingrowth of New Bone Tissue and Initial Mechanical Properties of a Degrading Polymeric Composite Scaffold." Tissue Engineering, *in press*.

46. LeGeros RZ: "Biological and Synthetic Apatites." *in* Hydroxyapatite and Related Materials . Brown PW and Constantz B, editors, Boca Raton: CRC Press, 1994; pp. 3-28.

47. Klawitter JJ, Hulbert SF: "Application of Porous Ceramics for the Attachment of Load Bearing Orthopedic Applications." J Biomed Mat Res 2:161, 1971.

48. Metsger DS, Driskell TD, Paulsrud JR: "Tricalcium Phosphate Ceramic--a Resorbable Bone Implant: Review and Current Status." JADA 105:1035-8, 1982.

49. Eggli PS, Muller W, Schenk RK: "Porous Hydroxyapatite and Tricalcium Phosphate Cylinders with Two Different Pore Size Ranges Implanted in the Cancellous Bone of Rabbits." Clin Orthop Rel Res 232:127-38, 1988.

50. Herr G, Wahl D, Kusswetter W: "Osteogenic Activity of Bone Morphogenetic Protein and Hydroxyapatite Composite Implants." Annales Chirurgiae et Gynaecologiae 82:99-107, 1993.

51. Doll BA, Towle HJ, Hollinger JO, Reddi AH, Mellonig JT: "The Osteogenic Potential of Two Composite Graft Systems Using Osteogenin." J Periodontol 61:745-50, 1990.

52. Yasko AW, Lane JM, Fellinger EJ, Rosen V, Wozney JM, Wang EA: "The Healing of Segmental Bone Defects Induced by Recombinant Human Bone Morphogenetic Protein (rhBMP-2): A Radiographic, Histological, and Biomechanical Study in Rats." J Bone Joint Surg 74A:659-70, 1992.

53. Desilets CP, Marden LJ, Patterson AL, Hollinger JO: "Development of Synthetic Bone-Repair Materials for Craniofacial Reconstruction." J Craniofacial Surg 1:150-3, 1990.

54. Gao TJ, Lindholm TS, Marttinen A, Puolakka T: "Bone Inductive Potential and Dose-Dependent Response of Bovine Bone Morphogenetic Protein Combined with Type IV Collagen Carrier." Annales Chirurgiae et Gynaecologiae 82:77-84, 1993.

55. Yamazaki Y, Oida S, Akimoto Y, Shioda S: "Response of the Mouse Femoral Muscle to an Implant of a Composite of Bone Morphogenetic Protein and Plaster of Paris." Clin Orthop Rel Res 234:240-9, 1988.

56. Takaoka K, Nakahara H, Yoshikawa H, Masuhara K, Tsuda T, Ono K: "Ectopic Bone Induction on and in Porous Hydroxyapatite Combined With Collagen and Bone Morphogenetic Protein." Clin Orthop Rel Res 234:250-4, 1988.

57. Johnson EE, Urist MR, Finerman G: "Distal Metaphyseal Tibial Nonunion: Deformity and Bone Loss treated by Open Reduction, Internal Fixation, and Human Bone Morphogenetic Protein (hBMP)." Clin Orthop Rel Res 250:234-40, 1990.

58. Ishaug SL, Yaszemski MJ, Bizios R, Mikos AG: "Osteoblast Function on Synthetic Biodegradable Polymers." J Biomed Mat Res 28:1445-53, 1994.

59. Laurencin CT, Norman ME, Elgendy HM, El-Amin SF, Allcock HR, Pucher SR, Ambrosio AA: "Use of Polyphosphazenes for Skeletal Tissue Regeneration." J Biomed Mat Res 27:963-73, 1993.

60. Domb AJ, Laurencin CT, Israeli O, Gerhart TN, Langer R: "The Formation of Propylene Fumarate Oligomers for use in Bioerodible Bone Cement Composites." J Polymer Science: Part A: Polymer Chemistry; Vol. 28:973-85, 1990.

61. Suggs LJ, Payne RG, Yaszemski MJ, Wu KK, Mikos AG: "The Synthesis and Characterization of a Novel Block Copolymer consisting of Poly (propylene fumarate) and poly (ethylene oxide). *in* Polymers in Medicine and Pharmacy, AG Mikos, KW Leong, ML Radomsky, JA Tamada, and MJ Yaszemski, editors, Materials Research Society, Pittsburgh, PA, 1995.

62. Gerhart TN, Hayes WC, Stern SH: "Biomechanical Optimization of a Model Particulate Composite for Orthopaedic Applications." J Orthop Res 4:76-85, 1986.

63. Gerhart TN, Renshaw AA, Miller RL, Noecker RJ, Hayes WC: "In Vivo Histologic and Biomechanical Characterization of a Biodegradable Particulate Composite Bone Cement." J Biomed Mat Res 23:1-16, 1989.

64. Allcock, HR, and Lampe, FW: "Secondary Methods for Molecular Weight Determination." *in* Contemporary Polymer Chemistry, 2nd edition, Prentice-Hall, Englewood Cliffs, 1990, p. 388.

65. Rabek, JF: "Viscosimetric Methods." *in* Experimental Methods in Polymer Chemistry, Wiley-Interscience, New York, 1980, p.129.

66. Personal Communication, E.W. Merrill, October 1994.

67. Sandler, SR, and Karo, W: "Poly(N-Vinylpyrrolidone)" *in* Polymer Synthesis, Volume II, Academic Press, New York, 1977, pp. 232-263.

68. Box, GEP, Hunter, WG, and Hunter, JS: "Fractional Factorial Designs at Two Levels." *in* Statistics for Experimenters, J. Wiley and Sons, New York, 1978, pp. 385-398.

69. Petty, W, Spanier, S, and Shuster, J: "The Influence of Skeletal Implants on the Incidence of Infection. Experiments in a Canine Model.", J Bone Joint Surg, 67A, 1236, 1985.

70. Petty, W, Spanier, S, Shuster, J: "Prevention of Infection after Total Joint Replacement.", J Bone Joint Surg, 70A, 536, 1988.

71. Hollinger, JO, and Kleinschmidt, JC: "Animal Models in Bone Research.", *in* Habal, MB, Reddi, AH, Editors, Bone Grafts and Bone Substitutes, Philadelphia, W.B. Saunders, 1992, pp. 133-146.

72. Gerhart, TN, Renshaw, AA, Miller, RL, Noecker, RJ, and Hayes, WC: "In Vivo Histologic and Biomechanical Characterization of a Biodegradable Particulate Composite Bone Cement.", J Biomed Mat Res, 23: 1, 1989.

73. Kim, WG, Park, KD, Mohammad, SF, and Kim, SW: "SPUU-PEO-Heparin Graft Copolymer Surfaces. Patency and Platelet Deposition in Canine Small Diameter Arterial Grafts." American Society of Artificial Internal Organs Transactions, 37(3): M148-9, July-September 1991.

74. Desai, NP, and Hubbel, JA: "Biological Responses to Polyethylene Oxide Modified Polyethylene Terephthalate Surfaces." J Biomed Mater Res, 25: 829-843, 1991.

75. Eriksen, EF, Axelrod, DW, and Melsen, F: "Histomorphometric Indices." *in* Bone Histomorphometry, Raven Press, New York, 1994, pp. 39-48.

APPENDIX 1

ACKNOWLEDGEMENTS

There are several individuals and institutions that have made significant contributions to the completion of this work. Their help has included conceptual discussions among colleagues, technical assistance in the collection of data, administrative assistance at the Institute, and financial assistance. It gives me great pleasure at this time to acknowledge their help and thank them for it. I offer my apologies to anyone whose help I have overlooked here. Such an oversight is certainly unintentional, and their assistance is appreciated just as much as those whom I have remembered.

My colleagues Mr. Richard Payne and Professor Antonios Mikos have both spent significant amounts of time working with me during this project. Dr. Mikos and I were co-principal investigators on the Orthopaedic Research and Education Foundation Grant (OREF) which funded much of our work. Mr. Payne served as my research associate, and he performed diligent, meticulous work in addition to making many practical contributions during our discussions. I am grateful to them both, and look forward to our continued collaboration as this project continues.

I acknowledge and appreciate the time, guidance, and support of my thesis committee: Professors Robert Langer, Wilson Hayes, Augustus White III, Myron Spector, and Edward Merrill. Professor Langer and Professor Hayes were instrumental in helping me with grant preparation to obtain funding for my research and tuition.

I thank my colleagues Professor Thomas Aufdemorte and Ms. Karen Buffum for their expertise in the preparation and interpretation of the histopathology material. This help was invaluable to me. I look forward to a continuing productive collaboration with them.

Marilyn Unroe at the Nonmetallic Materials Directorate, Polymer Division, Wright Laboratories, Wright-Patterson Air Force Base, Ohio, provided me with friendly, accurate, and very useful collaboration in polymer characterization. I appreciate her help and hope for similar academic interchanges in the future.

I thank my colleagues and the staff at the Orthopaedic Biomechanics Laboratory (OBL), Beth Israel Hospital, Harvard Medical School, Boston, Massachusetts for their many academic discussions and necessary administrative support during my biomechanics fellowship there. Adam Singer assisted me in the early stages of the polymer synthesis as an Undergraduate Research Opportunities (UROP) student from MIT working at the Harvard OBL.

I likewise appreciate the help of colleagues and administrative staff in

Langer laboratories and the Department of Chemical Engineering at MIT. The productive scientific discussions with colleagues occurred more easily as a result of the administrative help of Ms. Pam Brown, Ms. Janet Fischer, and Ms. Elaine Aufiero-Peters. Dr. Mark Prausnitz helped me frequently as critic and friend when I visited Cambridge to give reports and seminars on this work.

Professor Robert Lenz of Amherst College provided many useful discussions and answers to my frequent questions. I thank Colonel Thomas Shepler, M.D., United States Air Force, Retired, who conceived the need for an M.D.-Ph.D. position in our Orthopaedic Surgery Residency program at Wilford Hall Medical Center, Lackland Air Force Base, Texas. He successfully completed the many administrative steps which were necessary to obtain Air Force funding for this educational program. The staff of the Clinical Investigations Directorate, Wilford Hall Medical Center, Lackland Air Force Base, Texas, were invaluable to me for help with protocol management, laboratory support, grant management, animal surgery, testing equipment, and academic discussions. Colonel Arthur Kennedy, United States Army, Retired, organized and entered into my database over six hundred references during the course of this work. I thank him for the order that exists in my files.

Professors Robert Brown and William Deen of the Chemical Engineering Department at MIT were very kind and flexible in their roles as Department Chair and Graduate Committee Chair during my attempts to arrange the resident and non-resident portions of my studies. I thank them for their help.

Professor Frank Perkins, Dean of the Graduate School at MIT, helped solve several administrative problems that I created by being in Texas for the non resident portion of my studies. His timely and fair decisions were a great solace to me, and I appreciate his help.

Professor Leonard A. Wenzel, Professor and Chairman Emeritus, Department of Chemical Engineering, Lehigh University, Bethlehem,PA, has provided me with sound advice and guidance in Chemical Engineering for over twenty years. I thank him for this and for his long term friendship.

I am thankful to the institutional funding sources that made my doctoral program possible. The United States Air Force paid my salary and most of the tuition. I received tuition support from Professor Langer's Kenneth Germeshausen Chair in Chemical and Biochemical Engineering at MIT, and from the Orthopaedic Research and Education Foundation of the American Academy of Orthopaedic Surgeons. Project support came from two grants on which I served as co-principal investigator. First, the Swiss Association for the Study of Internal Fixation (Arbeitsgemeinschaft fur Osteosynthesefragen) supported Professor Hayes and me during the 1991-1992 academic year. Second, the Orthopaedic Research and Education Foundation supported Professors Mikos (co-PI), Hayes, Langer, and me during the 1993-1994 and 1994-1995 years. Finally, Professor Mikos and I received support from his T.N. Law Professorship at Rice University.

APPENDIX 2

BIOGRAPHICAL SKETCH

Michael J. Yaszemski was born on 13 December 1955 in Nanticoke, Pennsylvania to Chester B. Yaszczemski and Pearl A. (Ascani) Yaszczemski. He was reared in Harrison, New Jersey. He attended Saint Peter's Preparatory School in Jersey City, New Jersey, and graduated in 1973. He attended Lehigh University, Bethlehem, Pennsylvania, where he received a Bachelor of Science degree in Chemical Engineering in 1977 and a Master of Science degree in Chemical Engineering in 1978. His Master's thesis was entitled "The Preparation And Characterization Of A Vinyl Acetate- Diallylamine Copolymer Latex To Be Used As An Immunological Reagant." He then worked for GAF Corporation as a research engineer in their latex polymers group before matriculating at Georgetown University School of Medicine, Washington, D.C., where he received his M.D. in 1983. He entered active duty in the US Air Force in 1983. He then completed a residency in Orthopaedic surgery at Wilford Hall Medical Center, San Antonio, Texas, and a fellowship in spine surgery at Harvard Medical School, Boston, Massachusetts. He matriculated at M.I.T. as a doctoral student in 1989. He completed two years in residence at M.I.T., and completed his thesis work as a non-resident student in San Antonio, Texas. He serves there on active duty in the Air Force as an Orthopaedic Surgeon at Wilford Hall Medical Center, Lackland Air Force Base.

He married Karen L. (Adamec) Yaszemski on 21 July 1979. They reside in San Antonio, Texas, with their two children, Andrew John and Alexandra Katherine.